UNIQUE REGULATORY MECHANISMS FOR DNA REPLICATION AND GENOME MAINTENANCE IN MAMMALS

A Dissertation

Presented to the Faculty of the Graduate School

of Cornell University

In Partial Fulfillment of the Requirements for the Degree of

Doctor of Philosophy

by

Chen-Hua Chuang

January 2012

UNIQUE REGULATORY MECHANISMS FOR DNA REPLICATION AND GENOME MAINTENANCE IN MAMMALS

Chen-Hua Chuang, Ph. D.

Cornell University 2012

DNA replication is a fundamental process in all organisms. Using single stranded DNA (ssDNA) as a template, DNA polymerase synthesizes new DNA to produce an exact copy of the genome. However, most DNA polymerases lack the ability to unwind the double stranded DNA (dsDNA) necessary to expose ssDNA [1]. Therefore, an additional DNA helicase is required to initiate DNA replication by unwinding dsDNA and exposure of ssDNA as a template. In eukaryotes, genetic and biochemical assays have shown the MCM (minichromosome maintenance) family of proteins functions in a hexameric complex as the genomic DNA replication helicase [2]. MCMs have been well studied through *in vitro* biochemistry, cells in culture, and simple model organisms including *S. cerevisiea* and *Xenopus laevis*. These experimentally tractable systems have shown that misrelated or dysfunctional MCMs have deleterious consequences, especially genomic instability (GIN). However, there are still several major unresolved issues that need to be addressed. (1) The "MCM paradox" described that the MCMs are in excess of the number of origins. What is the function of these excess MCMs, and how does it relate to cells and animals? (2) The "MCM puzzle" indicates that mini-MCM complexes exist, but their functions are still unclear (3) Very little is known about the function of the MCM helicase with respect to the health of whole animals.

To accomplish these issues and explore the relationship between MCMs and disease, I generated mice deficient in MCMs as a model of *in vivo* disease in this thesis. The mice which carry 50% reduction of *Mcm2, 3, 4, 6,* and *7* is phenotypically

identical to wild-type at least through 1 year of age. Further reduction of *Mcms* to 70% causes several detrimental phenotypes, including embryonic lethality, growth retardation, genomic instability, and cancer susceptibility. Most importantly, the reduction of MCM3 rescues most of the detrimental phenotypes in other MCM deficient mice, suggesting a unique function of MCM3. Highly similar to *in vitro* results, I showed that the MCM3/5 dimer inhibits the MCM2-7 complex from binding chromatin and hinders cell cycle. I also discovered that the $Mcm4^{Chaos3}$ mutation induces a pan-downregulation of *Mcm2-7* post-transcriptionally. The pan-down regulation of *Mcm2-7* is a self-preservation mechanism because it reduces MCM3 levels that block the recruitment of chromatin bound MCM2-7. Finally, I identified that *Mcm* hypomorphic mice possess a unique gender bias phenotype. The male animals are more resistant to MCM insufficiency due to a testosterone protective effect.

In summary, this dissertation explores the function of the excess MCMs in aspects of cell cycle and in whole animals. It builds understanding about the regulation of MCMs with emphasis upon cancer formation as a result of MCM deficiency. The MCM hypomorphic mice also reveal a post-transcriptional regulation of *Mcms* that responded to helicase complex instability or insufficiency. The unique negative function of the MCM3/5 dimer overturns the current theory that the MCM2-7 heterohexamer is the only type of replication helicase that forms.

BIOGRAPHICAL SKETCH

Chen-Hua Chuang was born in Taipei City, Taiwan in 1977. His family provided him a wealth of love and concern, and in the course of his study, he could afford to pursue his interests and dreams. In 2001, he obtained his bachelor's degree at National Yang-Ming University. During his undergraduate studies, the Department of Life Sciences helped him to build up a solid background in molecular biology, biochemistry, and physics. Due to his excellent performance in participating in the undergraduate student research program, he was recommended with honors into the Institute of Microbiology & Immunology at Yang-Ming and obtained his Master's degree in 2003.

As a passionate young person in Taiwan, Chen-Hua Chuang joined the Army to fulfill his patriotic duty. He was appointed Second Lieutenant Medical Officer in Kinmen Island, the front line of defending the country. In his period of military service, he learned that he had a great passion for helping people and a commitment to biomedical research. By actively pursuing of his dream, he was recruited by Cornell University and started his Ph.D. in the field of Molecular and Integrative Physiology.

During Chen-Hua Chuang's Ph.D. study, he has enjoyed building the connections between research and life. He spends most of time in the lab conducting research, studying, learning, and communicating with others. After five years of productive and delightful life at Cornell, he has now decided to devote his career to the field of academia and answer fundamental biological questions in the hope of benefiting human.

I dedicate my thesis to my parents, my family, and the people who love me.

ACKNOWLEDGMENTS

I am especially grateful to my Ph.D. advisors, Dr. John Schimenti for his commendable guidance throughout my research and life. His excellent mentorship and personality accomplishment light up my path to be success. I thank my committee members, Dr. Robert Weiss, Dr. Paula Cohen, Dr. Bik Tye, and Dr. Natasza Kurpios for their help, advice and expertise. I thank the current and former members of the Schimenti lab including Dr. Ewelina Bolcun-Filas, Dr, Yung-Hao Ching, Dr. Weipeng Mu, Dr. Xin Li, Robert Munroe, Suzanne Hartford, Christian Abratte, Marsha Wallace, Edward Strong, Kerry Schimenti, Shrivatsav Pattabiraman, Gongshi Bai, Yunhai Luo, and Lauren Schnabel. I want to thank Dian Yang, my undergraduate student, who is now a Ph.D. student at Stanford. I would like to thank Dr. Mark Roberson, Dr. Robin Davisson, Dr. Yi Zhou, Dr. Jenn-Wei Chen, Dr. Chang-il Hwang, Boram Kim. Casey Isham, Janna S. Lamey, and Charlotte Williams. They are generous people and encourage and help me for everything. Finally, I want to especially thank Dr. Chia-Hsin Ju who supported and encouraged me throughout my years as a graduate student.

TABLE OF CONTENTS

LIST OF FIGURES

LIST OF TABLES

CHAPTER I

INTRODUCTION

1. The discovery of MCMs

The *MCM* series of genes was identified through mutation screens for genes required to maintain a minichromosome or cell cycle control in *Saccharomyces cerevisiae* and *Schizosaccharomyces pombe* [1-4]. The MCM series of proteins includes MCM1, MCM2, MCM3, MCM4, MCM 5, MCM6, MCM7 and MCM10. Only MCM2 through 7, as known as "MCM family", function as the DNA helicase in DNA replication [1-4]. MCM1 does not function in the hexameric helicase and has been shown to be a transcription factor [5]. MCM10 plays a role in stabilizing the replication fork but does not belong to canonical MCM2-7 complex [6-8]. Subsequently, MCM8 and MCM9 were identified on the basis of sequence similarity to the MCM2-7[9, 10]. However, MCM8 and MCM9 are not present in all eukaryotes and their functions are yet to be elucidated fully [11-13]. To simplify and standardize the nomenclature in this thesis, I will focus upon MCM2-7, hereafter known as the "MCMs".

2. The Role of MCMs in DNA replication

During the late M and early G1 phase of the cell cycle, the DNA origins of replication are bound by origin recognition complex (ORC1-6) (Fig. 1.1A) [14, 15]. The binding of ORC1-6 in DNA is competent to recruit CDC6 [16]. When CDC6 binds ATP, it recruits CDT1 bound to MCMs to form pre-replication complex (pre-RC) (Fig. 1.1B). ATP hydrolysis by CDC6 leads to the loading of MCM2-7 at origins and the release of CDT1. After MCMs are loaded, ORC1-6 and CDC6 will dissociate from DNA [17, 18]. As the cell enters S phase, the cyclin-dependent kinases (CDKs) and the Dbf4-dependent kinase (DDK) CDC7 activate the replication forks [15, 19]. This helps recruit additional replication factors such as CDC45 [20], the GINS complex [21], and MCM10 [22]. After the complete assembly of the replication complex, the DNA can unwind and begin to replicate (Fig. 1.1C).

A. Late M/Early G1: Recruit Pre-RC

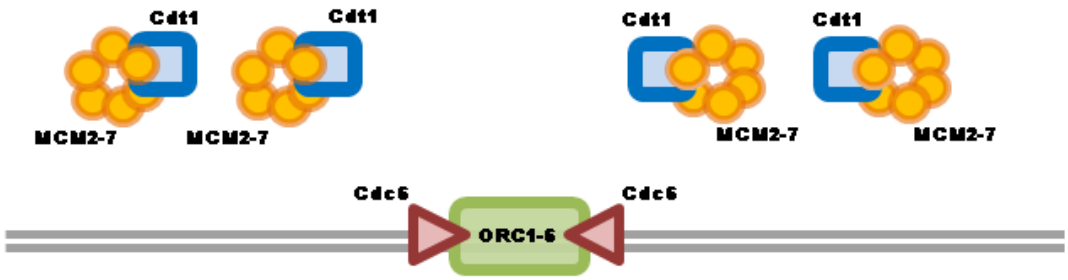

B. G1/Early S: Initiation

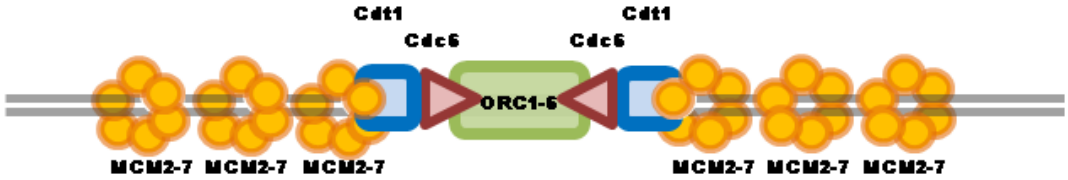

CDKs and DDK

C. S phase: Elongation

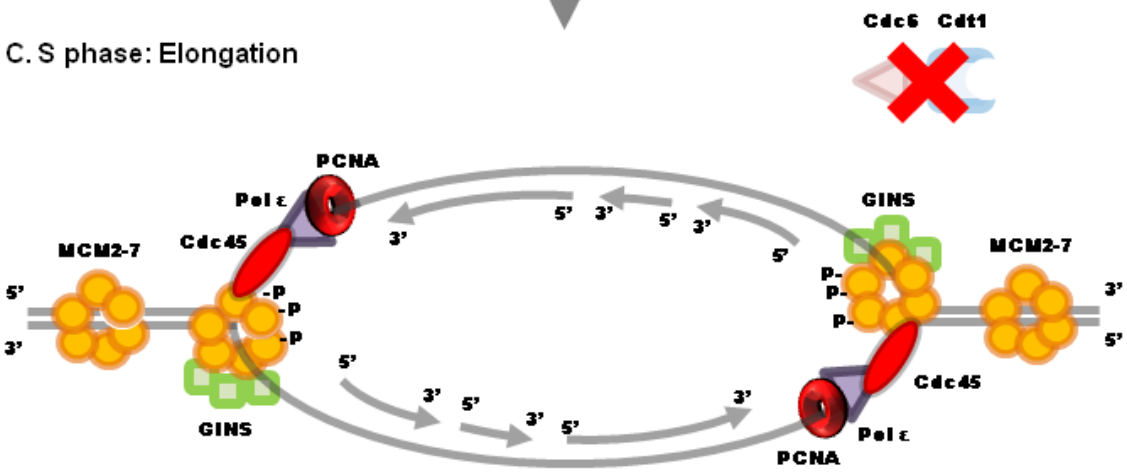

Figure 1.1. Model for MCM proteins function in replication initiation and elongation. (A) During the late M/early G1 phase, origin recognition complexes (ORC1-6) bind to the DNA origins of replication. (B) In the G1 phase, ORC1-6 and CDC6 recruit CDT1 and load MCM2-7 to origins of replication to form pre-RC. (C) In the S phase, CDKs and DDK activate pre-RC and facilitates the loading of additional replication factors such as CDC45, GINS, DNA polymerase ε, and PCNA. MCMs start to unwind the dsDNA at the origin. During the S phase, CDC6 and CDT1 are degraded or inactivated to block additional pre-RC formation on the newly synthesized DNA.

Replication fork integrity is highly critical. The abnormal dissociation of the replication fork can cause DNA double-strand breaks and trigger the S phase checkpoint. The checkpoint will stop DNA replication and stimulate DNA damage responses [23-25]. The physical stabilization of the replication fork requires multiple proteins including Mrc1, Tof1, and Csm3 (M/T/C complex) in yeast. In the absence of these proteins, the MCM helicase activity will continually unwind DNA, but the DNA polymerase dissociates from the replication fork. This is a typical type of replisome collapse [26-28].

DNA re-replication can have serious genomic instability (GIN) outcomes such as DNA double-strand breaks and chromosome rearrangements, or aneuploidy [24, 29-32]. The re-loading of the replication complex may initiate a new replication fork on the newly synthesized DNA, leading to DNA aneuploidy and damage. Therefore, the excess or free MCMs must be inactive to prevent the re-loading after entering S phase. This is accomplished by following means [33]. Firstly, in addition to the loss of Orc1-6 and Cdc6 from chromosomes as mentioned previously, Cdc6 is also transported out of nuclei by CDK activity in yeast [34-37]. Secondly, another protein, GEMININ, interacts with CDT1 and blocks the function of CDT1 to bind ORCs or MCMs [38, 39]. Thirdly, in yeast, excess Mcms are also transported out of the nuclei immediately after passage into S phase [40]. It bears mentioning that results suggest that nuclear membrane integrity may play a role in the regulation of MCMs and their ability to bind to chromatin. In *Xenopus* extracts, adding complete nuclear membrane was sufficient to block MCMs loading onto DNA and stopping replication while broken nuclear membrane showed no effect [41]. Also, MCMs physically associate with nuclear pore proteins ELYS/MEL-28, suggesting that nuclear membrane integrity is required to shut down licensing prior to entry into S phase [42].

3. **The transcription and expression of MCMs**

Based on their function in DNA replication, *Mcms* are predicted to be transcribed during the G1/S phase in actively dividing cells. However, only *Mcm5, 6, 7* have E2F

binding sites located on the promoter regions [33]. Although *Mcm7* was predicted to be up-regulated by E2F, evidence for increased transcription of *Mcm7* was shown in G2/M phase, suggesting that E2F is not the only regulating factor [34]. *Mcm3* was also proven to be transcribed after entering S phase without any known regulation sites on the promoter [35]. Interestingly, although MCMs function in DNA replication, the MCM protein levels do not fluctuate during the cell cycle, even though the mRNA expression levels differ in different phases of cell cycle [36-41].

MCMs are highly abundant proteins, and several experiments suggest that the protein levels of MCMs exceed the requirements of the pre-RC. Results of cytological studies have shown that MCMs are liberally distributed in the nucleus and not concentrated on the chromatin, suggesting that only a fraction of the MCMs are bound to the chromatin [42-44]. The chromatin bound MCMs are in excess of the number of origins. Using a *Xenopus* egg extract system, the number of MCMs bound to ORC at the origin was examined and found to be approximately 20 to 40 molecules (varies by different MCMs) per ORC. Additionally, only 10% to 20 % of chromatin-associated MCMs are bound by CDC45 which is required for replication fork activity [45]. These data indicate an important issue. Not all MCMs function as a component of the replication fork. This suggests that certain amounts of MCMs functions are distinct from the origin (termed the MCM paradox [46, 47]).

4. The protein structure of MCMs

Each of the MCM2-7 proteins are essential. They share significant sequence similarity; however, they cannot be substituted by each other. The "MCM box" is a nearly 250 amino acid region which encodes an ATPase domain (AAA+ domain) in the center of each protein (Fig. 1.2)[48]. MCMs oligomerize into a ring-shaped hexamer to create a central pore for holding DNA, and the AAA+ domain hydrolyzes ATP to unwind the substrate DNA within the pore [49, 50]. Most of the MCM AAA+ domains include two sub-domains, a series of parallel beta-strands loops (P loop) and a lid P loop C-terminal to the beta-strand loops [51]. The first P loop contains a

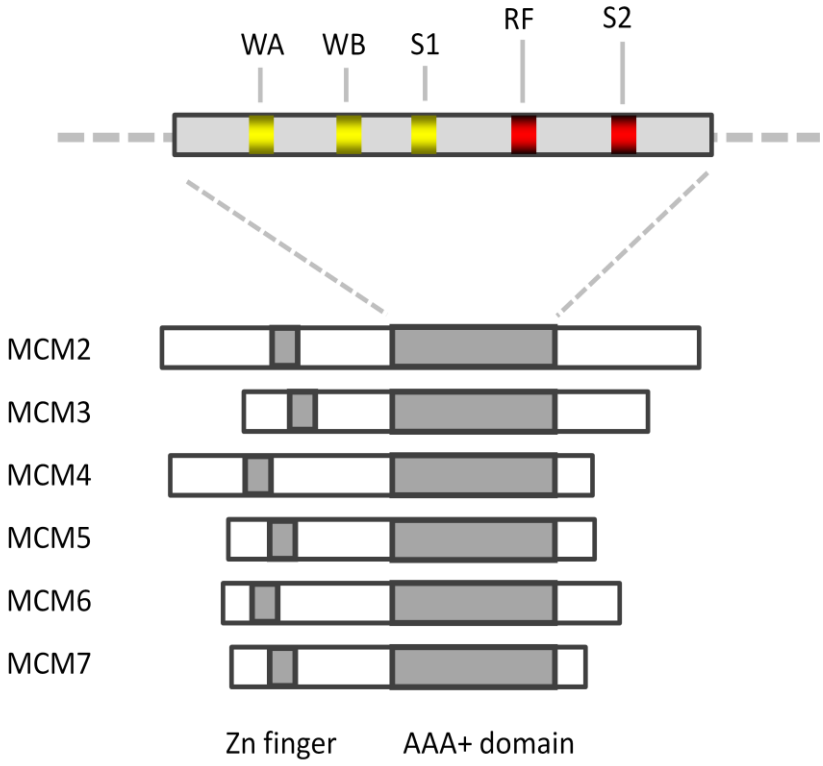

Figure 1.2. Conserved protein motifs in MCMs. MCM2-7 share significant sequence similarity. Each MCM contains zinc finger motif at the N terminus and an ATPase domain in the center of each protein.The MCM AAA+ domain, which is a nearly 250 amino acid region, includes two sub-domains. “WA” represents Walker A box; “WB” represents Walker B box; “S1” represents sensor 1 motif; “RF” represents arginine finger; and ”S2” represents sensor 2 motif.

Walker A box (WA), Walker B box (WB) and a sensor 1 motif (S1); the lid P loop contains an arginine finger (RF) and a sensor 2 motif (S2) (Fig. 1.2). Commonly for proteins with AAA+ domain, a complex is formed to hydrolyze ATP. In this complex, the P loop (cis motif) tends to form an active ATP hydrolysis site with the lid P loop (trans motif) from a partner protein within the same complex. Additional to the AAA+ domain, MCMs contain zinc finger motifs in the N termini. Those zinc finger motifs do not directly bind to DNA (Fig. 1.2), however, mutation analysis in yeast has shown they are required for viability [37, 52]. Biochemical analysis suggests that the zinc finger motif contributes to MCM complex stability and ATPase activity [53-55].

In both yeast and metazoans, only Mcm2 and Mcm3 have identifiable nuclear localization sequences (NLS) and these NLS signals have been functionally verified [56-58]. Besides, Mcm3 contains a putative nuclear export sequences (NES) that has been molecularly characterized in *S. cerevisiae* [59]. The homologous MCM3 NES has been identified in mouse and human but the function and importance is yet unknown in these disease-relevant higher eukaryotes [60]. The function of the MCM3 NES remains a topic of much controversy due to the observation that the bulk of MCM proteins, including MCM3, are constitutively located in the nucleus regardless of cell cycle stage.

5. The formation of MCM2-7 hexamers

The formations of yeast Mcms have been well characterized by different means. Genetic evidence, such as co-suppression and synthetic lethal interactions, suggest Mcms form a protein complex [37, 53, 61-63]. Cell extract fractions yield a variety of Mcm sub-complexes: dimer, trimer, tetrameric [22, 35, 64-75], and the intact Mcm hexamer [64-66, 68, 70, 71, 73, 74]. By coimmunoprecipitation assays in yeast [65], it was demonstrated that any Mcm subunit can associate physically with other Mcms. Gel filtration analyses have shown the size of the Mcm heterohexamer to be about 600 kDa and contains each Mcm subunit in a 1:1:1:1:1:1 stoichiometry [65,

66, 71, 74, 76]. Furthermore, electron microscopy studies indicate that eukaryotic Mcm2-7 forms a ring-shaped toroidal complex similar to archaeal MCM proteins and other AAA+ proteins [49, 65], however, the architecture of the heterohexameric complex is still unknown. Systematic studies of the pairwise interactions to individual Mcm subunits utilizing the yeast two-hybrid system and co-immunoprecipitation have identified five dimeric subunit pairs: Mcm5/3, Mcm3/7, Mcm7/4, Mcm4/6, and Mcm6/2 [66, 77, 78]. These interaction results suggest the hexameric arrangement for Mcms is: Mcm5-3-7-4-6-2 (Fig. 1.3). Although Mcm2 and Mcm5 are predicted to physically interact in the toroidal Mcm2-7 structures observed in electron micrographs, a direct interaction between them has never been demonstrated. *In vitro* MCM complex reconstitution assays have shown that the Mcm2/5 interaction is highly unstable [66, 77], suggesting a structural discontinuity between Mcm2 and Mcm5. It has been suggested that a "switch or shut off" mechanism exists between Mcm2/5 on the toroidal hexamer [79].

Interestingly, the situation is different in mammalian cells. Using various purification methods, MCM4, MCM6, and MCM7 subunits bind most tightly together to form a trimeric complex commonly called the "MCM core". The MCM4/6/7 core will then dimerize to form a dimertrimer $(MCM4/6/7)_2$. MCM3/5 interacts together and weakly binds to the MCM4/6/7 core, probably through Mcm7 (Fig. 1.3). MCM2 also binds to the core with low affinity, however the binding of MCM2 disrupts the dimertrimer of $(MCM4/6/7)_2$ [67, 73, 80]. The observation of MCM sub-complexes has proven very important, because instead of MCM heterohexamer only $(MCM4/6/7)_2$ has been shown to possess helicase activity *in vitro* [67, 81]. This "MCM puzzle", which point out an obvious conflict between *in vivo* and *in vitro*, is an unresolved issue. Further studies are required to understand the role of MCMs and their assembly *in vivo*.

6. The function of MCMs

In order to ensure that genomic DNA is only replicated once per cell cycle,

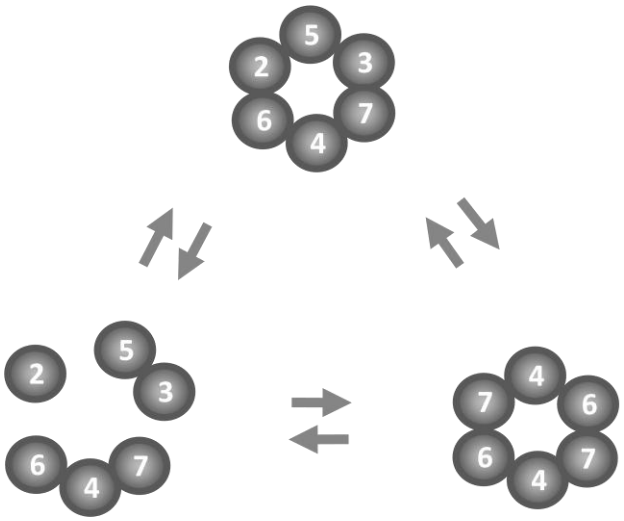

Figure 1.3. MCM2-7 hexamers and sub-complex assembly. The MCM hexameric arrangement is: Mcm5-3-7-4-6-2. MCM heterohexamer can break into two major sub-complex, MCM4/6/7 and MCM3/5. The MCM4/6/7 core will then dimerize to form a dimertrimer $(MCM4/6/7)_2$.

DNA replication is strictly regulated at every stage. DNA replication can be divided into two steps, initiation and elongation. The individual MCM2-7 proteins are essential for viability in every model that has been tested [29, 53]. All MCMs colocalize to origins of replication during pre-RC formation that including ORC1-6, CDT1, and CDC6 [54-57].

A yeast temperature-sensitive allele of *MCM4* was used to show that Mcms are involved in DNA synthesis [4]. In the *Xenopus* extract system, depletion of MCMs from the reaction resulted in failing to initiate DNA replication [58-60]. MCMs also have been proven to be involved in the step of elongation. As shown in chromatin immune-precipitation experiments, all MCMs co-localize with the DNA polymerases during elongation. Inactivation of MCMs also inhibits elongation during S phase [54-57].

Based on previous results and protein structure, MCMs were predicted as a DNA helicase which unwinds DNA during replication. The helicase includes three essential activities: ATP hydrolysis, DNA binding, and DNA unwinding. However, *in vitro* studies showed that this Mcm hexamer lacked helicase activity [36, 37, 45, 47]. Instead, the dimeric heterotrimer $(Mcm4/6/7)_2$ (only contained two copies each of the Mcm4, Mcm6, and Mcm7) which exists in most systems, possessed an ATP-dependent, 3` to 5` DNA unwinding activity [37, 41, 61, 62]. The helicase activity remains in the absence of Mcm6 [39], suggesting helicase activity only requires the Mcm7/4 sub-complex. Furthermore, the addition of Mcm2 or the Mcm5/3 dimer inhibits Mcm4/6/7 helicase activity [63]. These results predict a model in which the Mcm2-7 helicase activity is contributed by Mcm4, Mcm6, and Mcm7, while Mcm2, Mcm3, and Mcm5 function as negative regulators [45].

Both Mcm2-7 and Mcm4/6/7 complexes from *S. cerevisiae* possess ATP-dependent DNA binding activity. Additionally, the binding affinity for ssDNA is 100-fold-greater than dsDNA [17], suggesting ssDNA is the major substrate. Although

both Mcm2-7 and Mcm4/6/7 bind ssDNA with similar affinities, however, the abilities to bind circular ssDNA are different. The binding of Mcm4/6/7 to circular ssDNA is 20 times lower than that of Mcm2-7 [39, 64]. Interestingly, if Mcm2-7 is mixed with ATP prior to the DNA, then the binding becomes poor [64]. These results suggest a simple hypothesis, that Mcm2-7 has the ATP-dependent ability to transiently open and then clamp the circular ssDNA to its central channel.

7. MCMs mouse model

Little is known about MCMs in relation to the health of whole animals. Mcms are essential genes so homozygous knock-out animals are not viable. Therefore, only heterozygous knock-out or hypomorphic mice exist. One Mcm hypomorphic mouse model is the *Mcm4*^{Chaos3} mouse, which was generated by ethylnitrosourea (ENU). The *Mcm4 Chaos3* point mutation changed PHE to ILE at residue 345 (Phe345Ile). This amino acid is conserved across diverse eukaryotes and is important for interaction with other MCMs [54]. In previous work, *Shima et al* found that the *Mcm4*^{Chaos3} allele caused high levels of GIN and extreme mammary cancer susceptibility in the C3HeB/FeJ background [82]. This provided the first concrete evidence that endogenous mutations in replication licensing machinery may have a causative role in cancer development. Surprisingly, MEFs from *Mcm4*^{Chaos3} mice not only had reduced levels of MCM4, but also MCM7 [82], suggesting that the point mutation might destabilize the MCM2-7 complex.

The first *Mcm2* hypomorphic mouse model was generated by integration of a Cre recombinase into the *Mcm2* coding sequence that decreases the amount of *Mcm2* mRNA [83]. The heterozygous *Mcm2* ^{CreERT2} mouse expresses 70% of *Mcm2* mRNA and is phenotypically identical to wild-type at least through 1 year of age. The homozygous *Mcm2*$^{(IRES\text{-}CreERT2)}$ mouse only expresses 30% *Mcm2* mRNA and develops early onset lymphomas. These studies demonstrate that deficiencies in the MCMs result in a chronic phenotype leading to cancer, and also points out an

important concept that the 30% to 60% loss of MCMs might be tolerable to animals and consistent with good health.

8. **Brief outline of dissertation research**

The function of MCMs in DNA replication has been extensively investigated by yeast genetic and *Xenopus* extracts models. However, very little is known about MCMs related to health of the whole animal. MCMs deregulation has been reported in many clinical cases, especially in tumor samples, suggesting that MCMs are highly relevant to cancer formation. In this dissertation, the overall goal is to generate the animal models to test the hypothesize that insufficient MCMs result in failure to completely replicate genomic DNA and hinder cell cycle, which causes serious physiological problems.

Chapter II reports phenotypic studies of MCMs insufficient mice. In this chapter, I generated *Mcm2, 3, 4, 6,* and *7* hypomorphic mice from gene trap-containing ES cells. The gene trap alleles are disrupted by a beta-geo DNA fragment and lead to truncated hybrid MCM proteins. Therefore, each gene trap mouse has only half the amount of the corresponding normal MCM level. I also crossed *Mcm2, 3, 4, 6,* and *7* gene trap mice to *Mcm4*^{Chaos3} mice to generate further reduced MCMs levels. These studies showed that MCMs insufficiency causes several detrimental phenotypes, including embryo lethality, growth retardation, genomic instability, and cancer susceptibility. Most importantly, I found that the reduction of MCM3 rescues most of detrimental phenotypes in other MCMs insufficient mice, suggesting a unique function of MCM3. In chapter III, I examined how *Chaos3* mutation affects MCM2-7 complex stability. I found that MCM6 cannot interact with MCM4^{Chaos3}. Furthermore, the *Chaos3* mutation induces a pan-downregulation of *Mcm2-7* from post-transcriptional events. The pan-down regulation of *Mcm2-7* is a self-preservation mechanism because it reduces MCM3 levels that block the recruitment of chromatin bound MCM2-7. In chapter IV, the analysis of genetic data from MCMs hypomorphic mice indicates a unique gender bias phenotype. I found that male animals are more resistant to MCMs

insufficiency due to testosterone protection. Finally, Chapter V summarizes my data, discusses the significance of results and point out future directions for this research area.

References

1. Maine, G.T., P. Sinha, and B.K. Tye, *Mutants of S. cerevisiae defective in the maintenance of minichromosomes.* Genetics, 1984. **106**(3): p. 365-85.
2. Hennessy, K.M., et al., *A group of interacting yeast DNA replication genes.* Genes Dev, 1991. **5**(6): p. 958-69.
3. Moir, D., et al., *Cold-sensitive cell-division-cycle mutants of yeast: isolation, properties, and pseudoreversion studies.* Genetics, 1982. **100**(4): p. 547-63.
4. Takahashi, K., H. Yamada, and M. Yanagida, *Fission yeast minichromosome loss mutants mis cause lethal aneuploidy and replication abnormality.* Mol Biol Cell, 1994. **5**(10): p. 1145-58.
5. Treisman, R. and G. Ammerer, *The SRF and MCM1 transcription factors.* Curr Opin Genet Dev, 1992. **2**(2): p. 221-6.
6. Gregan, J., et al., *Fission yeast Cdc23/Mcm10 functions after pre-replicative complex formation to promote Cdc45 chromatin binding.* Mol Biol Cell, 2003. **14**(9): p. 3876-87.
7. Izumi, M., et al., *The human homolog of Saccharomyces cerevisiae Mcm10 interacts with replication factors and dissociates from nuclease-resistant nuclear structures in G(2) phase.* Nucleic Acids Res, 2000. **28**(23): p. 4769-77.
8. Wohlschlegel, J.A., et al., *Xenopus Mcm10 binds to origins of DNA replication after Mcm2-7 and stimulates origin binding of Cdc45.* Mol Cell, 2002. **9**(2): p. 233-40.
9. Gozuacik, D., et al., *Identification and functional characterization of a new member of the human Mcm protein family: hMcm8.* Nucleic Acids Res, 2003. **31**(2): p. 570-9.
10. Yoshida, K., *Identification of a novel cell-cycle-induced MCM family protein MCM9.* Biochem Biophys Res Commun, 2005. **331**(2): p. 669-74.
11. Liu, Y., T.A. Richards, and S.J. Aves, *Ancient diversification of eukaryotic MCM DNA replication proteins.* BMC Evol Biol, 2009. **9**: p. 60.
12. Lutzmann, M. and M. Mechali, *MCM9 binds Cdt1 and is required for the assembly of prereplication complexes.* Mol Cell, 2008. **31**(2): p. 190-200.
13. Maiorano, D., et al., *MCM8 is an MCM2-7-related protein that functions as a DNA helicase during replication elongation and not initiation.* Cell, 2005. **120**(3): p. 315-28.
14. Aparicio, O.M., D.M. Weinstein, and S.P. Bell, *Components and dynamics of DNA replication complexes in S. cerevisiae: redistribution of MCM proteins and Cdc45p during S phase.* Cell, 1997. **91**(1): p. 59-69.
15. Bell, S.P. and A. Dutta, *DNA replication in eukaryotic cells.* Annu Rev Biochem, 2002. **71**: p. 333-74.
16. Randell, J.C., et al., *Sequential ATP hydrolysis by Cdc6 and ORC directs loading of the Mcm2-7 helicase.* Mol Cell, 2006. **21**(1): p. 29-39.
17. Hua, X.H. and J. Newport, *Identification of a preinitiation step in DNA replication that is independent of origin recognition complex and cdc6, but dependent on cdk2.* J Cell Biol, 1998. **140**(2): p. 271-81.

18. Rowles, A., S. Tada, and J.J. Blow, *Changes in association of the Xenopus origin recognition complex with chromatin on licensing of replication origins.* J Cell Sci, 1999. **112 (Pt 12)**: p. 2011-8.
19. Nougarede, R., et al., *Hierarchy of S-phase-promoting factors: yeast Dbf4-Cdc7 kinase requires prior S-phase cyclin-dependent kinase activation.* Mol Cell Biol, 2000. **20**(11): p. 3795-806.
20. Kamimura, Y., et al., *Sld3, which interacts with Cdc45 (Sld4), functions for chromosomal DNA replication in Saccharomyces cerevisiae.* EMBO J, 2001. **20**(8): p. 2097-107.
21. Takayama, Y., et al., *GINS, a novel multiprotein complex required for chromosomal DNA replication in budding yeast.* Genes Dev, 2003. **17**(9): p. 1153-65.
22. Ricke, R.M. and A.K. Bielinsky, *Mcm10 regulates the stability and chromatin association of DNA polymerase-alpha.* Mol Cell, 2004. **16**(2): p. 173-85.
23. Branzei, D. and M. Foiani, *Interplay of replication checkpoints and repair proteins at stalled replication forks.* DNA Repair (Amst), 2007. **6**(7): p. 994-1003.
24. Lopes, M., et al., *The DNA replication checkpoint response stabilizes stalled replication forks.* Nature, 2001. **412**(6846): p. 557-61.
25. Tercero, J.A. and J.F. Diffley, *Regulation of DNA replication fork progression through damaged DNA by the Mec1/Rad53 checkpoint.* Nature, 2001. **412**(6846): p. 553-7.
26. Bailis, J.M., et al., *Minichromosome maintenance proteins interact with checkpoint and recombination proteins to promote s-phase genome stability.* Mol Cell Biol, 2008. **28**(5): p. 1724-38.
27. Gambus, A., et al., *GINS maintains association of Cdc45 with MCM in replisome progression complexes at eukaryotic DNA replication forks.* Nat Cell Biol, 2006. **8**(4): p. 358-66.
28. Katou, Y., et al., *S-phase checkpoint proteins Tof1 and Mrc1 form a stable replication-pausing complex.* Nature, 2003. **424**(6952): p. 1078-83.
29. Marchetti, M.A., et al., *A single unbranched S-phase DNA damage and replication fork blockage checkpoint pathway.* Proc Natl Acad Sci U S A, 2002. **99**(11): p. 7472-7.
30. Pasero, P., K. Shimada, and B.P. Duncker, *Multiple roles of replication forks in S phase checkpoints: sensors, effectors and targets.* Cell Cycle, 2003. **2**(6): p. 568-72.
31. Sogo, J.M., M. Lopes, and M. Foiani, *Fork reversal and ssDNA accumulation at stalled replication forks owing to checkpoint defects.* Science, 2002. **297**(5581): p. 599-602.
32. Tercero, J.A., M.P. Longhese, and J.F. Diffley, *A central role for DNA replication forks in checkpoint activation and response.* Mol Cell, 2003. **11**(5): p. 1323-36.
33. Ohtani, K., et al., *Cell growth-regulated expression of mammalian MCM5 and MCM6 genes mediated by the transcription factor E2F.* Oncogene, 1999. **18**(14): p. 2299-309.

34. Fitch, M.J., J.J. Donato, and B.K. Tye, *Mcm7, a subunit of the presumptive MCM helicase, modulates its own expression in conjunction with Mcm1.* J Biol Chem, 2003. **278**(28): p. 25408-16.
35. Schulte, D., et al., *Properties of the human nuclear protein p85Mcm. Expression, nuclear localization and interaction with other Mcm proteins.* Eur J Biochem, 1996. **235**(1-2): p. 144-51.
36. Dalton, S. and L. Whitbread, *Cell cycle-regulated nuclear import and export of Cdc47, a protein essential for initiation of DNA replication in budding yeast.* Proc Natl Acad Sci U S A, 1995. **92**(7): p. 2514-8.
37. Forsburg, S.L., et al., *Mutational analysis of Cdc19p, a Schizosaccharomyces pombe MCM protein.* Genetics, 1997. **147**(3): p. 1025-41.
38. Kimura, H., et al., *Molecular cloning of cDNA encoding mouse Cdc21 and CDC46 homologs and characterization of the products: physical interaction between P1(MCM3) and CDC46 proteins.* Nucleic Acids Res, 1995. **23**(12): p. 2097-104.
39. Schulte, D., et al., *Expression, phosphorylation and nuclear localization of the human P1 protein, a homologue of the yeast Mcm 3 replication protein.* J Cell Sci, 1995. **108 (Pt 4)**: p. 1381-9.
40. Tsuruga, H., et al., *Expression, nuclear localization and interactions of human MCM/P1 proteins.* Biochem Biophys Res Commun, 1997. **236**(1): p. 118-25.
41. Young, M.R. and B.K. Tye, *Mcm2 and Mcm3 are constitutive nuclear proteins that exhibit distinct isoforms and bind chromatin during specific cell cycle stages of Saccharomyces cerevisiae.* Mol Biol Cell, 1997. **8**(8): p. 1587-601.
42. Dimitrova, D.S., et al., *Mcm2, but not RPA, is a component of the mammalian early G1-phase prereplication complex.* J Cell Biol, 1999. **146**(4): p. 709-22.
43. Krude, T., et al., *Human replication proteins hCdc21, hCdc46 and P1Mcm3 bind chromatin uniformly before S-phase and are displaced locally during DNA replication.* J Cell Sci, 1996. **109 (Pt 2)**: p. 309-18.
44. Madine, M.A., et al., *The nuclear envelope prevents reinitiation of replication by regulating the binding of MCM3 to chromatin in Xenopus egg extracts.* Curr Biol, 1995. **5**(11): p. 1270-9.
45. Edwards, M.C., et al., *MCM2-7 complexes bind chromatin in a distributed pattern surrounding the origin recognition complex in Xenopus egg extracts.* J Biol Chem, 2002. **277**(36): p. 33049-57.
46. Hyrien, O., K. Marheineke, and A. Goldar, *Paradoxes of eukaryotic DNA replication: MCM proteins and the random completion problem.* Bioessays, 2003. **25**(2): p. 116-25.
47. Laskey, R.A. and M.A. Madine, *A rotary pumping model for helicase function of MCM proteins at a distance from replication forks.* EMBO Rep, 2003. **4**(1): p. 26-30.
48. Koonin, E.V., *A common set of conserved motifs in a vast variety of putative nucleic acid-dependent ATPases including MCM proteins involved in the initiation of eukaryotic DNA replication.* Nucleic Acids Res, 1993. **21**(11): p. 2541-7.

49. Bochman, M.L. and A. Schwacha, *Differences in the single-stranded DNA binding activities of MCM2-7 and MCM467: MCM2 and MCM5 define a slow ATP-dependent step.* J Biol Chem, 2007. **282**(46): p. 33795-804.
50. Pape, T., et al., *Hexameric ring structure of the full-length archaeal MCM protein complex.* EMBO Rep, 2003. **4**(11): p. 1079-83.
51. Erzberger, J.P. and J.M. Berger, *Evolutionary relationships and structural mechanisms of AAA+ proteins.* Annu Rev Biophys Biomol Struct, 2006. **35**: p. 93-114.
52. Yan, H., A.M. Merchant, and B.K. Tye, *Cell cycle-regulated nuclear localization of MCM2 and MCM3, which are required for the initiation of DNA synthesis at chromosomal replication origins in yeast.* Genes Dev, 1993. **7**(11): p. 2149-60.
53. Yan, H., S. Gibson, and B.K. Tye, *Mcm2 and Mcm3, two proteins important for ARS activity, are related in structure and function.* Genes Dev, 1991. **5**(6): p. 944-57.
54. Fletcher, R.J., et al., *The structure and function of MCM from archaeal M. Thermoautotrophicum.* Nat Struct Biol, 2003. **10**(3): p. 160-7.
55. Fletcher, R.J., et al., *Double hexamer disruption and biochemical activities of Methanobacterium thermoautotrophicum MCM.* J Biol Chem, 2005. **280**(51): p. 42405-10.
56. Ishimi, Y., et al., *Biochemical activities associated with mouse Mcm2 protein.* J Biol Chem, 2001. **276**(46): p. 42744-52.
57. Nguyen, V.Q., C. Co, and J.J. Li, *Cyclin-dependent kinases prevent DNA re-replication through multiple mechanisms.* Nature, 2001. **411**(6841): p. 1068-73.
58. Pasion, S.G. and S.L. Forsburg, *Nuclear localization of Schizosaccharomyces pombe Mcm2/Cdc19p requires MCM complex assembly.* Mol Biol Cell, 1999. **10**(12): p. 4043-57.
59. Liku, M.E., et al., *CDK phosphorylation of a novel NLS-NES module distributed between two subunits of the Mcm2-7 complex prevents chromosomal rereplication.* Mol Biol Cell, 2005. **16**(10): p. 5026-39.
60. Chuang, C.H., et al., *Incremental genetic perturbations to MCM2-7 expression and subcellular distribution reveal exquisite sensitivity of mice to DNA replication stress.* PLoS Genet, 2010. **6**(9).
61. Coxon, A., K. Maundrell, and S.E. Kearsey, *Fission yeast cdc21+ belongs to a family of proteins involved in an early step of chromosome replication.* Nucleic Acids Res, 1992. **20**(21): p. 5571-7.
62. Hennessy, K.M., C.D. Clark, and D. Botstein, *Subcellular localization of yeast CDC46 varies with the cell cycle.* Genes Dev, 1990. **4**(12B): p. 2252-63.
63. Miyake, S., et al., *Fission yeast genes nda1+ and nda4+, mutations of which lead to S-phase block, chromatin alteration and Ca2+ suppression, are members of the CDC46/MCM2 family.* Mol Biol Cell, 1993. **4**(10): p. 1003-15.
64. Madine, M.A., et al., *MCM3 complex required for cell cycle regulation of DNA replication in vertebrate cells.* Nature, 1995. **375**(6530): p. 421-4.

65. Adachi, Y., J. Usukura, and M. Yanagida, *A globular complex formation by Nda1 and the other five members of the MCM protein family in fission yeast.* Genes Cells, 1997. **2**(7): p. 467-79.
66. Davey, M.J., C. Indiani, and M. O'Donnell, *Reconstitution of the Mcm2-7p heterohexamer, subunit arrangement, and ATP site architecture.* J Biol Chem, 2003. **278**(7): p. 4491-9.
67. Ishimi, Y., *A DNA helicase activity is associated with an MCM4, -6, and -7 protein complex.* J Biol Chem, 1997. **272**(39): p. 24508-13.
68. Ishimi, Y., et al., *Binding of human minichromosome maintenance proteins with histone H3.* J Biol Chem, 1996. **271**(39): p. 24115-22.
69. Kanter, D.M., I. Bruck, and D.L. Kaplan, *Mcm subunits can assemble into two different active unwinding complexes.* J Biol Chem, 2008. **283**(45): p. 31172-82.
70. Kubota, Y., et al., *A novel ring-like complex of Xenopus proteins essential for the initiation of DNA replication.* Genes Dev, 2003. **17**(9): p. 1141-52.
71. Lee, J.K. and J. Hurwitz, *Isolation and characterization of various complexes of the minichromosome maintenance proteins of Schizosaccharomyces pombe.* J Biol Chem, 2000. **275**(25): p. 18871-8.
72. Musahl, C., et al., *A human homologue of the yeast replication protein Cdc21. Interactions with other Mcm proteins.* Eur J Biochem, 1995. **230**(3): p. 1096-101.
73. Prokhorova, T.A. and J.J. Blow, *Sequential MCM/P1 subcomplex assembly is required to form a heterohexamer with replication licensing activity.* J Biol Chem, 2000. **275**(4): p. 2491-8.
74. Schwacha, A. and S.P. Bell, *Interactions between two catalytically distinct MCM subgroups are essential for coordinated ATP hydrolysis and DNA replication.* Mol Cell, 2001. **8**(5): p. 1093-104.
75. Yabuta, N., et al., *Mammalian Mcm2/4/6/7 complex forms a toroidal structure.* Genes Cells, 2003. **8**(5): p. 413-21.
76. Ying, C.Y. and J. Gautier, *The ATPase activity of MCM2-7 is dispensable for pre-RC assembly but is required for DNA unwinding.* EMBO J, 2005. **24**(24): p. 4334-44.
77. Bochman, M.L., S.P. Bell, and A. Schwacha, *Subunit organization of Mcm2-7 and the unequal role of active sites in ATP hydrolysis and viability.* Mol Cell Biol, 2008. **28**(19): p. 5865-73.
78. Yu, Z., D. Feng, and C. Liang, *Pairwise interactions of the six human MCM protein subunits.* J Mol Biol, 2004. **340**(5): p. 1197-206.
79. Bochman, M.L. and A. Schwacha, *The Saccharomyces cerevisiae Mcm6/2 and Mcm5/3 ATPase active sites contribute to the function of the putative Mcm2-7 'gate'.* Nucleic Acids Res, 2010. **38**(18): p. 6078-88.
80. Mendez, J. and B. Stillman, *Chromatin association of human origin recognition complex, cdc6, and minichromosome maintenance proteins during the cell cycle: assembly of prereplication complexes in late mitosis.* Mol Cell Biol, 2000. **20**(22): p. 8602-12.

81. Lee, J.K. and J. Hurwitz, *Processive DNA helicase activity of the minichromosome maintenance proteins 4, 6, and 7 complex requires forked DNA structures.* Proc Natl Acad Sci U S A, 2001. **98**(1): p. 54-9.
82. Shima, N., et al., *A viable allele of Mcm4 causes chromosome instability and mammary adenocarcinomas in mice.* Nat Genet, 2007. **39**(1): p. 93-8.
83. Pruitt, S.C., K.J. Bailey, and A. Freeland, *Reduced Mcm2 expression results in severe stem/progenitor cell deficiency and cancer.* Stem Cells, 2007. **25**(12): p. 3121-32.

CHAPTER II
INCREMENTAL GENETIC PERTURBATIONS TO MCM2-7 EXPRESSION AND SUBCELLULAR DISTRIBUTION REVEAL EXQUISITE SENSITIVITY OF MICE TO DNA REPLICATION STRESS

* Reprinted from Chen-Hua Chuang, Marsha D. Wallace, Christian Abratte, Teresa Southard, and John C. Schimenti. Incremental genetic perturbations to MCM2-7 expression and subcellular distribution reveal exquisite sensitivity of mice to DNA replication stress. *PLoS Genet*. September 2010, Volume 6, Issue 9. *Copyright. 2010 Chuang et al.*

Abstract

Mutations causing replication stress can lead to genomic instability (GIN). *In vitro* studies have shown that drastic depletion of the MCM2-7 DNA replication licensing factors, which form the replicative helicase, can cause GIN and cell proliferation defects that are exacerbated under conditions of replication stress. To explore the effects of incrementally attenuated replication licensing in whole animals, we generated and analyzed the phenotypes of mice that were hemizygous for *Mcm2*, *3*, *4*, *6*, and *7* null alleles, combinations thereof, and also in conjunction with the hypomorphic $Mcm4^{Chaos3}$ cancer susceptibility allele. $Mcm4^{Chaos3/Chaos3}$ embryonic fibroblasts have ~40% reduction in all MCM proteins, coincident with reduced *Mcm2-7* mRNA. Further genetic reductions of *Mcm2*, *6*, or *7* in this background caused various phenotypes including synthetic lethality, growth retardation, decreased cellular proliferation, GIN, and early onset cancer. Remarkably, heterozygosity for *Mcm3* rescued many of these defects. Consistent with a role in MCM nuclear export possessed by the yeast Mcm3 ortholog, the phenotypic rescues correlated with increased chromatin-bound MCMs, and also higher levels of nuclear MCM2 during S phase. The genetic, molecular and phenotypic data demonstrate that relatively minor quantitative alterations of MCM expression, homeostasis or subcellular distribution can have diverse and serious consequences upon development and confer cancer susceptibility. The results support the notion that the normally high levels of MCMs in cells are needed not only for activating the basal set of replication origins, but also "backup" origins that are recruited in times of replication stress to ensure complete replication of the genome.

Author Summary

Proper replication of the genome is essential for maintenance of the genetic material and normal cell proliferation. DNA replication can be compromised by exogenous factors and genetic disruptions. Such compromise can lead to disease such as cancer, which is characterized by genomic instability (an elevated mutation rate). Because the DNA replication apparatus is essential, relatively little is known about how genetic variants impact the health of whole animals. In this report, we studied mice bearing combinatorial mutations in a component of the replication apparatus, the MCM2-7 helicase. MCM2-7 is a complex of 6 proteins that are essential for initiating DNA replication along chromosomes, and to unwind the DNA during DNA replication. We find that although cells have excess amounts of MCM2-7 to support proliferation under normal circumstances, that incremental MCM depletions have multiple drastic effects upon the whole animal, including embryonic lethality, stem cells defects, and severe cancer susceptibility. Additionally, we report that mouse cells regulate and coordinate the levels of usable MCM proteins, both at the level of synthesis and also by regulating access to chromatin. The implication is that genetic variants that impact MCM levels, even to a minor degree, can translate into disease.

Introduction

In late mitosis to early G1 phase of the cell cycle, DNA replication origins are selected and bound by the hexameric origin recognition complex (ORC; [1]). ORC then recruits the initiation factors CDC6 and CDT1, which are required for loading MCM2-7, thereby forming the "pre-replicative complex" (pre-RC). The formation of pre-RCs is termed origin "licensing" and this gives origins competency to initiate a single round of DNA synthesis before entering S phase. MCM2-7 is a hexamer of six distinct but structurally-related minichromosome maintenance (MCM) proteins (reviewed in [2-5]). *In vivo* and *in vitro* evidence indicates that the MCM2-7 complex is the replicative helicase [6-8].

MCM2-7 proteins are abundant in proliferating cells [9], and are bound to chromatin in amounts exceeding that which is present at active replication origins or required for complete DNA replication [10-14]. Although these and other studies showed that drastic decreases in MCMs are tolerated by dividing cells, there are certain deleterious consequences. In *Xenopus* extracts and mammalian cells, excess chromatin-bound MCM2-7 complexes occupy dormant or "backup" origins that are activated under conditions of replication stress, compensating for stalled or disrupted primary replication forks [11, 15, 16]. The depletion of these backup licensed origins was associated with elevated chromosomal instability and susceptibility to replication stress, factors that might predispose to cancer.

In previous work, Shima *et al* found that a hypomorphic allele of mouse *Mcm4* (*Mcm4*^{Chaos3}) caused high levels of GIN and extreme mammary cancer susceptibility in the C3HeB/FeJ background [17]. This provided the first concrete evidence that endogenous mutations in replication licensing machinery may have a causative role in cancer development. The ethylnitrosourea (ENU)-induced *Mcm4*^{Chaos3} point mutation changed PHE to ILE at residue 345 (Phe345Ile). This amino acid is conserved across diverse eukaryotes and is important for interaction with other MCMs [18]. Budding yeast engineered to bear the orthologous mutation exhibit DNA replication defects and

GIN [17, 19]. Surprisingly, MEFs from *Mcm4*^{Chaos3} mice not only had reduced levels of MCM4, but also MCM7 [17], suggesting that the point mutation might destabilize the MCM2-7 complex. Subsequently, it was reported that mice containing 1/3 the normal level of MCM2 succumbed to lymphomas at a very young age, and had diverse stem cell proliferation defects [20]. These mice also had 27% reduced levels of MCM7 protein, and their cells exhibited decreased replication origin usage when under replication stress (treatment with hydroxyurea) conditions [21]. These studies imply that relatively modest decreases in any of the MCMs may be sufficient to cause cancer susceptibility, developmental defects, and GIN [20].

Here, we report that genetically-induced reductions of MCM levels in mice, achieved by breeding combinations of MCM2-7 alleles, caused several health-related defects including increased embryonic lethality, GIN, cancer susceptibility, growth retardation, defective cell proliferation, and hematopoiesis defects. Remarkably, genetic reduction of MCM3, which mediates nuclear export of excess MCM2-7 complexes in yeast [22], rescued many of these defects, presumably attributable to observed increases in chromatin-bound MCM levels. These data suggest that relatively minor misregulation or destabilization of MCM homeostasis can have serious consequences for health, viability and cancer susceptibility of animals.

Results

Mcm4$^{Chaos3/Chaos3}$ cells exhibit pan-reduction of total and chromatin-bound MCM2-7 due to decreased mRNA levels

To extend previous findings that *Mcm4*^{Chaos3Chaos3} cells exhibited decreases in MCM4 and MCM7 protein, and to determine if the decreased levels were differentially compartmentalized in the cell, we quantified soluble and chromatin-bound MCM2-7 levels in mouse embryonic fibroblasts (MEFs) by Western blot analysis. As shown in Figure 1A, all MCMs were decreased in both compartments by at least 40% compared to WT cells. Because *Mcm4*$^{Chaos3/Chaos3}$ MEF cultures have slightly decreased proliferation and G2/M delay (Fig. 2.1A and [17]), it is possible

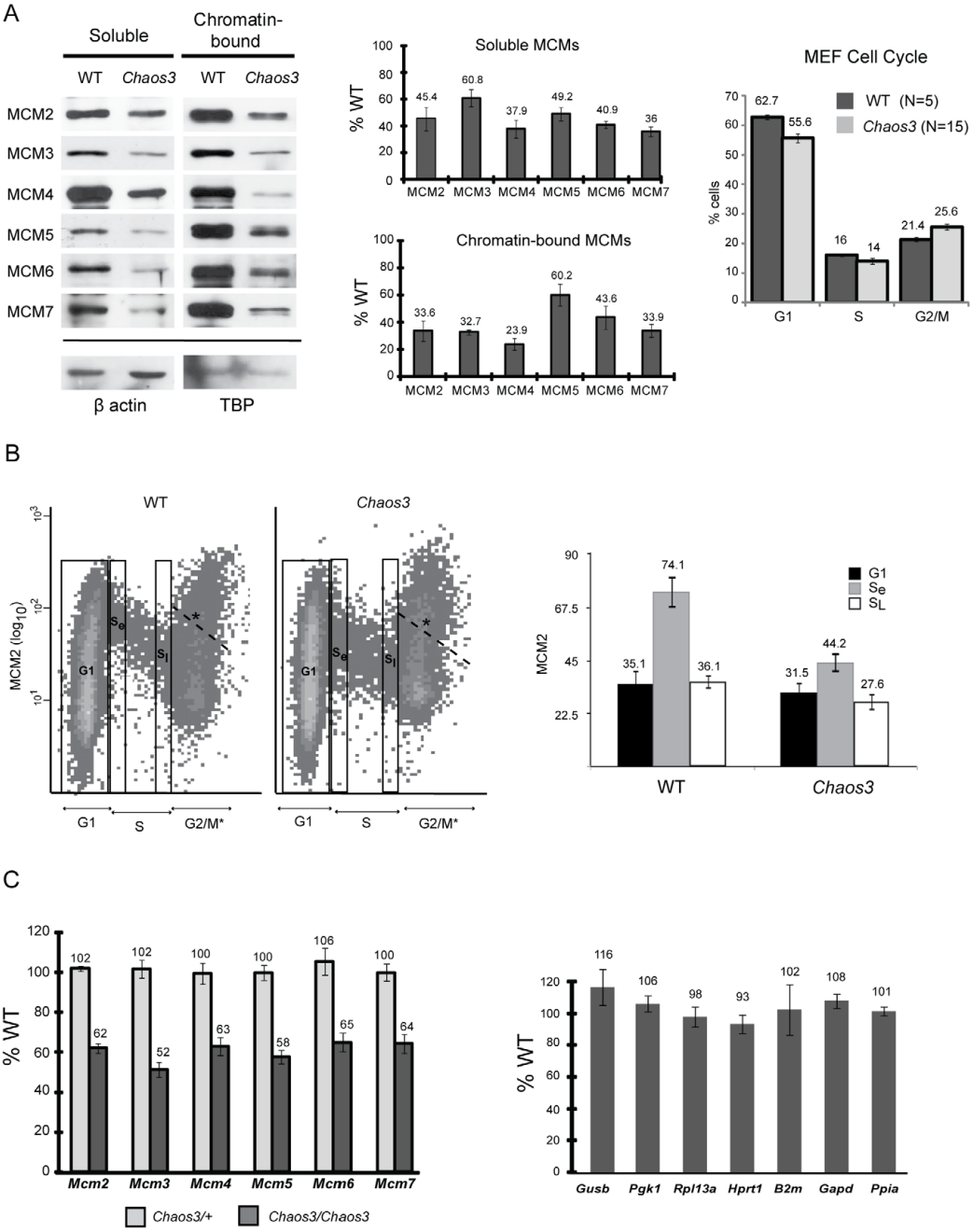

Figure 2.1. MCM2-7 proteins and mRNA are reduced in *Mcm4*$^{Chaos3/Chaos3}$ MEFs, particularly in early S phase (A) Western blot analysis of MCM2-7 (left panel). Soluble or chromatin-bound protein was electrophoresced on PAGE gels, electrotransferred, and the blots were immunolabeled with the indicated antibodies.

The bands correspond to the predicted molecular weights of these proteins, and for MCM2, the identity of the band was verifed by RNAi knockdown and transient overexpression in NIH 3T3 cells. TBP = TATA box binding protein. Quantification of Western blot data by densitometry is shown in the center panel. The amounts relative to WT cells (after normalization to the controls) are plotted. Error bars represent SEM, derived from 4 replicate experiments. The rightmost panel graphs the results of flow cytometric analysis of unsynchronized MEF culture cell cycle profiles, based on DNA content. (B) Flow cytometric quantification of MCM2 content (fluorescence intensity of antibody staining) is plotted on the Y axis, vs DNA content on the X axis. Plotted at the right is the mean fluorescent intensity of the 3 gated (boxed) regions from the flow data. S_e = early S phase; S_L = late S phase. The labeled cell cycle stages are based on DNA content. However, because light scatter was inadequate to distinguish individual nuclei from clumped nuclei or artifactual structures, the 4c category (denoted G2/M*) contains events other than G2/M nuclei. *We drew a dashed line representing an arbitrary cutoff above which contains such undefined events. (C) qRT-PCR analysis of Mcm mRNAs (left panel) and control genes (right panel), in the three indicated genotypes of MEFs. Relative transcript levels were normalized to β-actin. Charted are the percent levels of the indicated RNAs in mutant compared to WT (considered to be 100%). At least 3 replicate cultures were analyzed for each genotype. Error bars are SEM. In all panels, the raw data shown are from MEFs established from littermates. Furthermore, the replicates involved MEFs from pairs of littermates. Chaos3 = $Mcm4^{Chaos3/Chaos3}$; WT = +/+.

that the lower MCM levels in mutant MEFs are entirely attributable to growth defects. To test this, we assessed the levels of nuclear MCM2 in S-phase cells by flow cytometry (Fig. 2.1B). Although MCM2 levels in WT and *Mcm4*$^{Chaos3/Chaos3}$ G1 nuclei were essentially the same (P=.65; t-test), mutant cells transitioned from G1 to S with 40% less nuclear MCM2 content than in WT (P<.02; t-test). The levels of nuclear MCM2 in WT decreased through S phase more sharply than in mutants, which transitioned to G2 with only ~23% less than controls (Fig. 2.1B). This differential decline is apparent in the flow plots, where WT cells exhibit a greater downward slope in the S compartment (Fig. 2.1B). The decreases in MCM2 from early to late S were 51% in WT and 38% in mutants. The MCM2 intra-S modulation phenomenon is also addressed in subsequent experiments. The marked differences in nuclear MCM2 concentration between actively proliferating (S-phase) WT and mutant cells indicates that a biochemical or regulatory basis, rather than a population skewing, underlies the differences in protein levels.

Another possible explanation for the coordinated decrease in MCMs is that the mutant MCM4^{Chaos3} protein destabilizes the MCM2-7 hexamer and causes subsequent degradation of uncomplexed MCMs. Other groups reported that knockdown of *Mcm2, Mcm3, or Mcm5* in human cells decreased the amount of other chromatin-bound MCMs [15, 16], leading to a similar proposition that the cause was MCM2-7 hexamer destabilization [16]. If true, then we would expect mRNA levels to be unchanged in mutant cells. To test this, we performed quantitative RT-PCR (qRT-PCR) analysis of *Mcm2-7*, and several control housekeeping genes in *Mcm4*$^{Chaos3/Chaos3}$ MEFs. Analysis of 5 littermate pairs of primary MEF cultures revealed that transcript levels for each of these genes in mutant cells was 51-65% of WT, similar to the protein decreases (Fig. 2.1C). Levels of mRNA in the 7 housekeeping genes analyzed were not altered significantly (Fig. 2.1C, right panel). This data suggest that either reduced MCM4 levels *per se*, or defects resulting from the *Mcm4*^{Chaos3} allele, cause a decrease in the levels of all Mcm mRNAs. Interestingly, the mRNA reduction appears to occur post-

transcriptionally, a phenomenon that is currently under investigation (Chuang and Schimenti, unpublished observations).

Decreased Mcm gene dosages cause elevated chromosomal instability and *Mcm2*-specific pan-decreases in Mcm mRNAs.

The *Mcm4*^{Chaos3} allele was identified in a forward genetic screen for mutations causing elevated micronuclei (MN) in red blood cells, an indicator of GIN [17]. While the altered MCM4^{Chaos3} protein may cause DNA replication errors as does a yeast allele engineered to contain the same amino acid change [19], it is also possible that the decrease in overall MCM levels in *Mcm4*^{Chaos3} mutants contributes to, or is primarily responsible for, elevated S-phase DNA damage and GIN as is seen in various cell culture models (see Introduction). To test this possibility, we generated mice from ES cells bearing gene trap insertions in *Mcm2*, *Mcm3*, *Mcm6*, and *Mcm7* (Fig. 2.2A; alleles are designated as *Mcm#*^{Gt}). These gene traps are designed to disrupt gene expression by fusing the 5' end of the endogenous mRNA (*via* use of a splice acceptor) to a vector-encoded reporter, resulting in a fusion protein lacking the C-terminal portion of the endogenous (MCM) protein. As with a previously-reported *Mcm4* gene trap [17], each of these alleles proved to be recessive embryonic lethal. Furthermore, each allele appeared to be a null, since mRNA levels in heterozygous MEF cultures were ~50% lower than WT controls (Fig. 2.2B). To determine if heterozygosity for various Mcms caused pan-decreases in Mcm mRNA levels as does homozygosity for *Mcm4*^{Chaos3}, mRNA levels for each of the Mcm2-7 genes were also quantified. Whereas *Mcm2*$^{Gt/+}$ cells did show ~20% decreases in the other Mcms, the *Mcm3*, *Mcm4*, *Mcm6* and *Mcm7* gene trap alleles did not (Fig. 2.2B). Thus, it appears that the marked Mcm pan-decreases in *Mcm4*$^{Chaos3/Chaos3}$ cells are not due to decreased *Mcm4* RNA *per se*, but rather a response to replication defects cause by the mutant protein. Notably, the pan Mcm2-7 downregulation in *Mcm2*$^{Gt/+}$ cells is consistent with the observation that MCM7 is decreased in *Mcm2*$^{IRES\text{-}CreERT2/\ IRES\text{-}CreERT2}$ mice, although mRNA levels were not evaluated in that study [20].

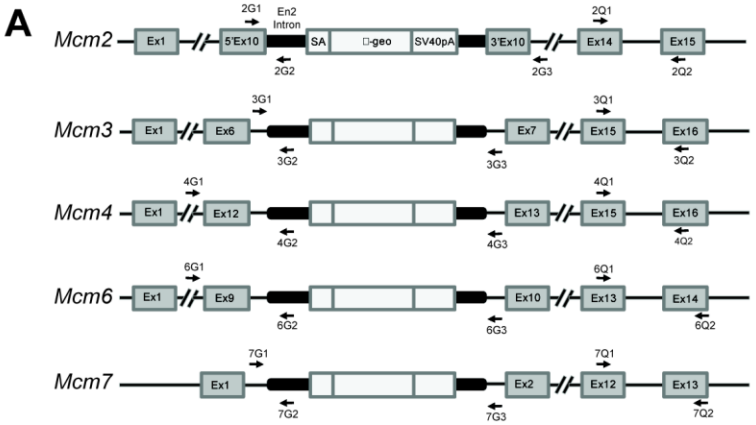
A
Mcm2
Ex1
2G1
En2 Intron
5'Ex10
SA
□-geo
SV40pA
3'Ex10
2Q1
Ex14
Ex15
2G2
2G3
2Q2
Mcm3
3G1
Ex6
Ex7
3Q1
Ex15
Ex16
3G2
3G3
3Q2
Mcm4
4G1
Ex12
Ex13
4Q1
Ex15
Ex16
4G2
4G3
4Q2
Mcm6
6G1
Ex9
Ex10
6Q1
Ex13
Ex14
6G2
6G3
6Q2
Mcm7
7G1
Ex2
7Q1
Ex12
Ex13
7G2
7G3
7Q2

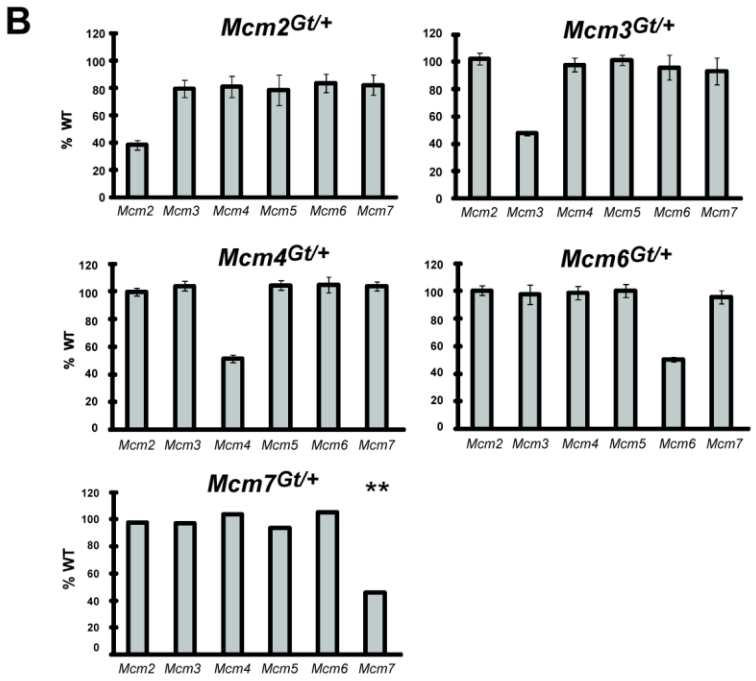
B
Mcm2Gt/+
Mcm3Gt/+
Mcm4Gt/+
Mcm6Gt/+
Mcm7Gt/+
**
% WT
0
20
40
60
80
100
120
Mcm2 Mcm3 Mcm4 Mcm5 Mcm6 Mcm7

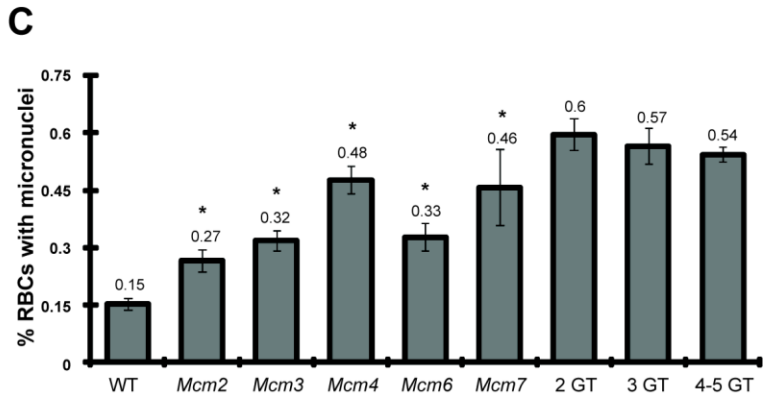
C
% RBCs with micronuclei
0
0.15
0.3
0.45
0.6
0.75
0.15
0.27
0.32
0.48
0.33
0.46
0.6
0.57
0.54
*
WT
Mcm2
Mcm3
Mcm4
Mcm6
Mcm7
2 GT
3 GT
4-5 GT

Figure 2.2. Mcm gene trap alleles, associated mRNA levels, and peripheral blood micronuclei (A) Genomic structures of mutated Mcm genes. Indicated is the intron/exon structure of each gene (not to scale), the locations of the gene trap insertions, and qPCR primer locations. (B) qRT-PCR analyses of MEF mRNA from gene trap heterozygotes. Charted are the percent levels of the indicated RNAs in mutant compared to WT (considered to be 100%). For all but *Mcm7*, the data were obtained from at least 3 MEF cultures from different embryos. The *Mcm7* data represents the average of three replicates from 1 MEF culture, hence there are no error bars. Otherwise, error bars show SEM. (C) Micronucleus levels in Mcm gene trap-bearing male mice. At least 5 animals were analyzed for each single gene trap mutant allele. The "2GT" (two gene trap) group contains: 4 mice doubly heterozygous for $Mcm2^{Gt}$ and $Mcm3^{Gt}$ ("Mcm2/3"), 4 Mcm2/4 mice, and 4 Mcm3/4 mice. The 3GT group contains: 4 Mcm2/3/4 mice, 1 Mcm2/3/6 mouse, 1 Mcm2/4/6 mouse, and 3 Mcm3/4/6 mice. The 4-5GT group contains: 3 Mcm2/3/4/6 mice, 1 Mcm2/3/6/7 mouse, and 2 Mcm2/3/4/6/7 mouse. SEM bars are shown.

After breeding the gene trap alleles into the C3HeB/FeJ genetic background for at least 2 generations (*Mcm4*$^{Chaos3/Chaos3}$ females get mammary tumors in this background), blood MN levels were measured. Heterozygosity for each allele caused an increase in the fraction of cells with MN (Fig. 2.2C). Compound heterozygosity further increased MN on average, as did heterozygosity for 3 or more gene traps (Fig. 2.2C), indicating that genetically-based decreases in any of the MCMs precipitate GIN.

Genetic reductions of *Mcm2*, *Mcm6* or *Mcm7* in an *Mcm4*$^{Chaos3/Chaos3}$ background causes partial synthetic lethality, severe growth defects and (for *Mcm2*) dramatically accelerated cancer onset.

As outlined above, previous studies showed that reductions of particular MCMs in cells or mice reduces the levels of other MCMs, causing GIN, cancer, and developmental defects. However, the reduction in MCM levels required to precipitate these consequences, and whether there is a threshold effect, is unclear. To explore the consequences of incremental MCM reductions on viability and cancer in mice, we crossed the *Mcm4*^{Chaos3} and gene trap alleles into the same genome. In the case of *Mcm2*, there was a striking and highly significant shortfall of *Mcm4*$^{Chaos3/Chaos3}$ *Mcm2*$^{Gt/+}$ offspring at birth (Fig. 2.3A). Heterozygosity for *Mcm2*^{Gt} itself was not haploinsufficient, as indicated by Mendelian transmission of *Mcm2*^{Gt} in crosses of heterozygotes to WT (119/250; $\chi^2 = 0.448$). These results demonstrate that there is a synthetic lethal interaction between *Mcm4*^{Chaos3} and *Mcm2*^{Gt} that is related to MCM2 levels. Additionally, the surviving *Mcm4*$^{Chaos3/Chaos3}$ *Mcm2*$^{Gt/+}$ offspring were severely growth retarded; males weighed ~50% less than *Mcm4*$^{Chaos3/Chaos3}$ siblings (Figure 3B; this genotype causes disproportionate female lethality). Another indication of a quantitative MCM threshold effect is that C3H-*Mcm4*$^{Chaos3/Chaos3}$ mice are developmentally normal, but *Mcm4*$^{Chaos3/Gt}$ animals die *in utero* or neonatally (Fig. 2.3A)[23].

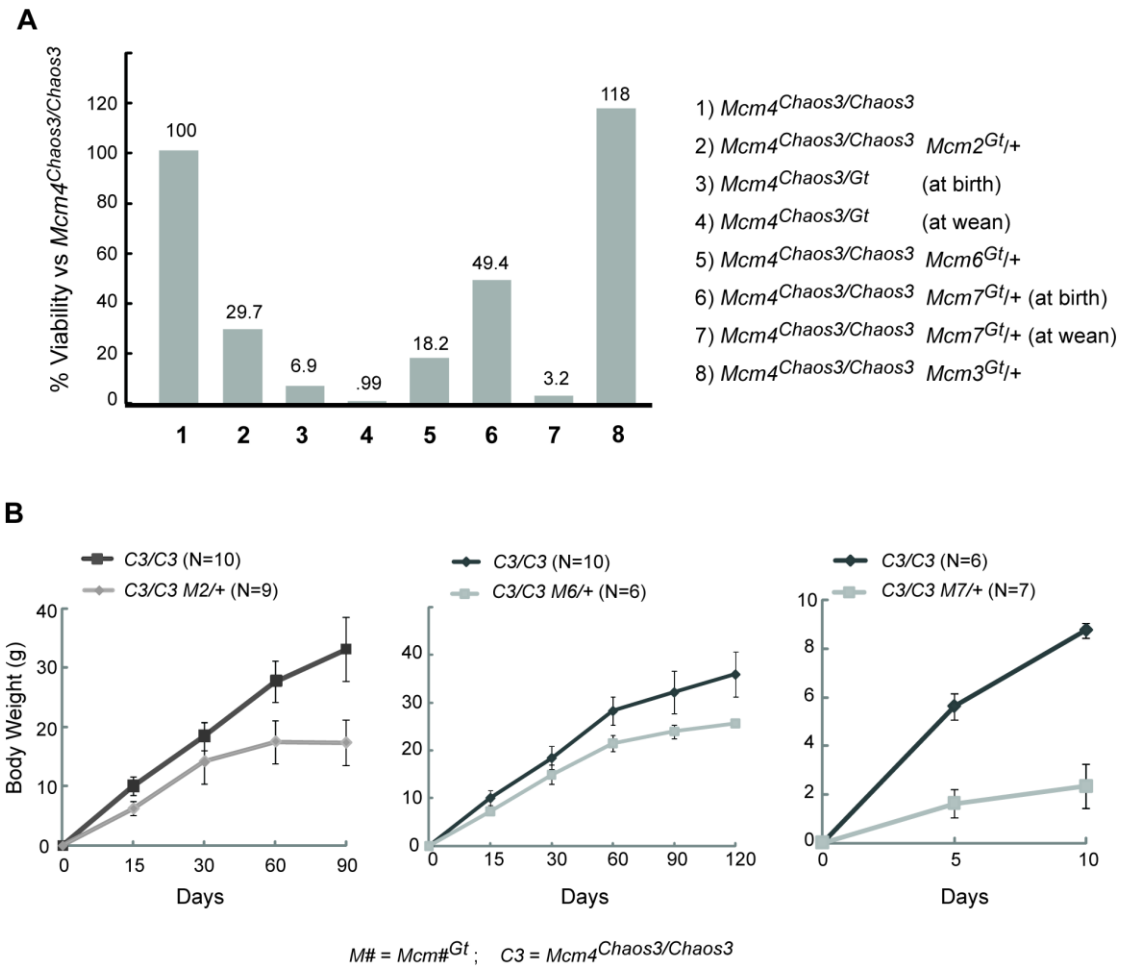

Figure 2.3. Synthetic lethality and growth retardation between *Mcm4*^{Chaos3} and *Mcm2, Mcm6* and *Mcm7* (A) Graphed are viability data from genotype presented in the right, which includes statistics. Unless otherwise indicated, the values represent expected proportions of indicated genotypes that were present at wean. (B) Weights of surviving animals are graphed over time. SEM bars are shown

The synthetic interaction between *Mcm4*^{Chaos3} and *Mcm2*^{Gt} might be specific, or it may reflect a general consequence of reduced replication licensing (and consequent elevated replication stress). We therefore tested whether hemizygosity for *Mcm3*, *Mcm6* or *Mcm7* would also cause synthetic phenotypes in the *Mcm4*$^{Chaos3/Chaos3}$ background. The *Mcm4*$^{Chaos3/Chaos3}$ *Mcm6*$^{Gt/+}$ genotype caused highly penetrant embryonic lethality; only 10% of the expected number of such animals survived to birth (Fig. 2.3A). The *Mcm4*$^{Chaos3/Chaos3}$ *Mcm7*$^{Gt/+}$ genotype caused both embryonic and postnatal lethality. The number of liveborns was ~50% of the expected value, and only 8% of those (5/62) survived to weaning (Fig. 2.3A). Additionally, as with *Mcm2*, hemizygosity for *Mcm6*^{Gt} *and Mcm7*^{Gt} in the *Mcm4*$^{Chaos3/Chaos3}$ background caused growth retardation (Fig. 2.3B). The decrease in male weight was ~20% and ~80% respectively, compared to *Mcm4*$^{Chaos3/Chaos3}$ siblings at the oldest age measured (*Mcm4*$^{Chaos3/Chaos3}$ *Mcm7*$^{Gt/+}$ animals died before wean, so the oldest weights were taken at 10 dpp). In contrast to the synthetic phenotypes with *Mcm2*, *4*, *6* and *7*, there was no significant decrease in viability (Fig. 2.3A) or weight (not shown) in *Mcm4*$^{Chaos3/Chaos3}$ *Mcm3*$^{Gt/+}$ mice. This seeming inconsistency is addressed in the following section.

As mentioned earlier, mice with ~35% of WT MCM2 protein, but not 62%, showed early latency (10-12 week) lymphoma susceptibility [20]. To identify if there is a critical MCM threshold for cancer susceptibility, we aged a cohort of *Mcm2*$^{Gt/+}$ mice, representing approximately intermediate MCM2 levels. As shown in Figure 4A, these animals did not show a dramatic cancer-related mortality in the first 12 months of life. However, we did find that ~3/4 of these animals had tumors at death or necropsy by 18 months of age (data not shown). These combined data are suggestive of a potential gradient of susceptibility, but that there is a critical minimum threshold of MCM levels, between ~35 and 50% in the case of MCM2, required to avoid early cancer and other developmental defects.

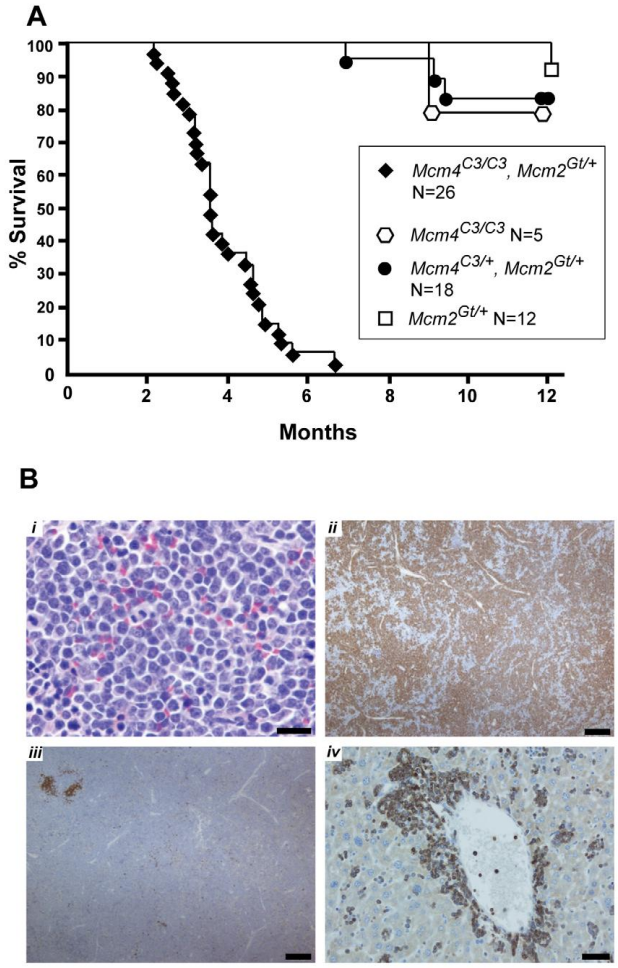

Figure 2.4. Premature morbidity and cancer susceptibility in *Mcm4*$^{Chaos3/Chaos3}$ *Mcm2*$^{Gt/+}$ mice (A) Kaplan-Meier survival plot of the indicated genotypes. Animals of both sexes are combined. "C3" = *Chaos3*. (B) Spleen and liver histopathology of a *Mcm4*$^{C3/C3}$ *Mcm2*$^{Gt/+}$ male diagnosed with T cell leukemic lymphoma. ***i.*** H&E stained spleen. Neoplastic cells have abundant cytoplasm, 1-2 nucleoli and a high mitotic rate, consistent with lymphoblastic lymphoma. Bar = 20 µm. ***ii.*** Neoplastic cells in spleen demonstrate immunoreactivity with anti-CD3 (brown; immunoperoxidase staining with DAB chromogen & hematoxalin counterstain), indicating T lymphocytes. Bar = 200µm. ***iii.*** In spleen, immunoreactivity (brown) with anti-PAX-5 (a B cell marker) is limited to follicular remnants and scattered individual cells. Bar = 200 µm. ***iv.*** In liver, neoplastic cells surround central veins and expand sinusoids and demonstrate immunoreactivity (brown) with the anti-CD3 T lymphocyte marker. Bar = 50 µm.

To further resolve this phenomenon, surviving *Mcm4*$^{Chaos3/Chaos3}$ *Mcm2*$^{Gt/+}$ mice were aged and monitored. They began dying at 2 months of age, and all were dead (or sacrificed when they appeared moribund) by 7 months (Fig. 2.4A). Gross necropsy and histopathological analyses revealed or suggested lymphomas/leukemias in 20 of these animals (detailed histopathology analysis of a T cell leukemic lymphoma is presented in (Fig. 2.4B). Six of these had chest tumors that were likely thymic lymphomas. The cause of death for the remaining 7 animals was undetermined. Consistent with previous studies [17], most *Mcm4*$^{Chaos3/Chaos3}$ mice hadn't yet succumbed from tumors or other causes by 12 months of age. Additional animals of these genotypes are incorporated in Figure 6, but histopathological analyses weren't conducted. These data show clearly that removing a half dose of MCM2 from *Mcm4*$^{Chaos3/Chaos3}$ cells is sufficient to produce greatly elevated cancer predisposition to the already-underrepresented survivors at wean. *Mcm4*$^{Chaos3/Chaos3}$ *Mcm2*$^{Gt/+}$ MEFs had 45% the amount of *Mcm2* mRNA as *Mcm4*$^{Chaos3/Chaos3}$ cells (Fig. 2.7C), which already had a 38% reduction compared to WT (Fig. 1). Thus, *Mcm2* RNA was reduced to ~17% of WT. To determine if elevated GIN might be responsible for the cancer susceptibility phenotype, we measured erythrocyte MN. Whereas the percentage of micronucleated RBCs in *Mcm4*$^{Chaos3/Chaos3}$ mice was 4.18 $\pm$ 0.26 (mean$\pm$ SEM, N=12), *Mcm4*$^{Chaos3/Chaos3}$ *Mcm2*$^{Gt/+}$ mice averaged 5.85 $\pm$ 0.47 (N=16), indicating a synergistic increase ($P< 0.01$). Overall, the data support the notion that in whole animals, reduction of MCMs to under 50% of WT causes severe developmental and physiological problems.

Rescue of phenotypic defects in *Mcm4*$^{Chaos3/Chaos3}$ and *Mcm4*$^{Chaos3/Chaos3}$ *Mcm2*$^{Gt/+}$ mice by reducing *Mcm3* genetic dosage.

The data reported here and elsewhere [17, 20] support a model where phenotypic severity is proportionally related to MCM concentrations. However, our genetic experiments uncovered one notable exception: hemizygosity for *Mcm3* did not cause any severe haploinsufficiency phenotypes (increased lethality and decreased weight) as did *Mcm2/6/7* in the *Mcm4*$^{Chaos3/Chaos3}$ background, or *Mcm4*^{Gt} in *trans* to

Mcm4^{Chaos3} (Fig. 2.3A). Since extreme reductions of MCM3 in cultured human cells caused GIN and cell cycle arrest [16], the absence of synthetic effects with *Mcm*^{Chaos3} led us to hypothesize that either mice are more tolerant to lower levels of this particular MCM, or that MCM3 is present in a stoichiometric excess compared to the other MCMs, at least in a subset of cell types. To explore these issues we performed additional phenotype analyses, and also sought to uncover potential effects of MCM3 reduction by reducing other MCMs simultaneously.

Strikingly, rather than exacerbating the synthetic lethality in *Mcm4*$^{Chaos3/Chaos3}$ *Mcm2*$^{Gt/+}$ mice, *Mcm3*^{Gt} heterozygosity significantly *rescued* their viability to 72.5% from 29.7% (Fig. 2.5A). Not only was viability rescued, but also growth (weight) of *Mcm4*$^{Chaos3/Chaos3}$ *Mcm2*$^{Gt/+}$ *Mcm3*$^{Gt/+}$ survivors compared to *Mcm4*$^{Chaos3/Chaos3}$ *Mcm2*$^{Gt/+}$ animals produced from the same matings (Fig. 2.5B). *Mcm3* hemizygosity also significantly rescued the near 100% lethality of *Mcm4*$^{Chaos3/Gt}$ animals (nearly 6 fold increased viability), and doubled the viability of *Mcm4*$^{Chaos3/Chaos3}$ *Mcm6*$^{Gt/+}$ mice (Fig. 2.5A). Rescue of *Mcm4*$^{Chaos3/Chaos3}$ *Mcm7*$^{Gt/+}$ was not observed (not shown).

The rescue of the reduced growth phenotype by *Mcm3* hemizygosity led us to evaluate the proliferation of compound mutant cells. Whereas *Mcm4*$^{Chaos3/Chaos3}$ and *Mcm4*$^{Chaos3/Chaos3}$ *Mcm3*$^{Gt/+}$ primary MEFs proliferated at identical rates, *Mcm4*$^{Chaos3/Chaos3}$ *Mcm2*$^{Gt/+}$ MEFs showed a severe growth defect beginning ~5 days in culture (Fig. 2.5C). As with whole animals, MEF growth was partially but significantly rescued by *Mcm3* hemizygosity.

Since the *Mcm4*^{Chaos3} and *Mcm2*^{Gt} alleles causes elevated GIN (micronuclei in RBCs), we considered the possibility that the *Mcm3* rescue effect might be related to an attentuation of GIN. Accordingly, we measured MN levels in *Mcm4*$^{Chaos3/Chaos3}$ mice with different combinations of other Mcm mutations. As shown in Fig. 2.5D, hemizygosity for *Mcm2* and *Mcm7* caused a significant elevation in MN levels, unlike *Mcm3*. However, the increased MN in *Mcm4*$^{Chaos3/Chaos3}$ *Mcm2*$^{Gt/+}$ was not rescued by

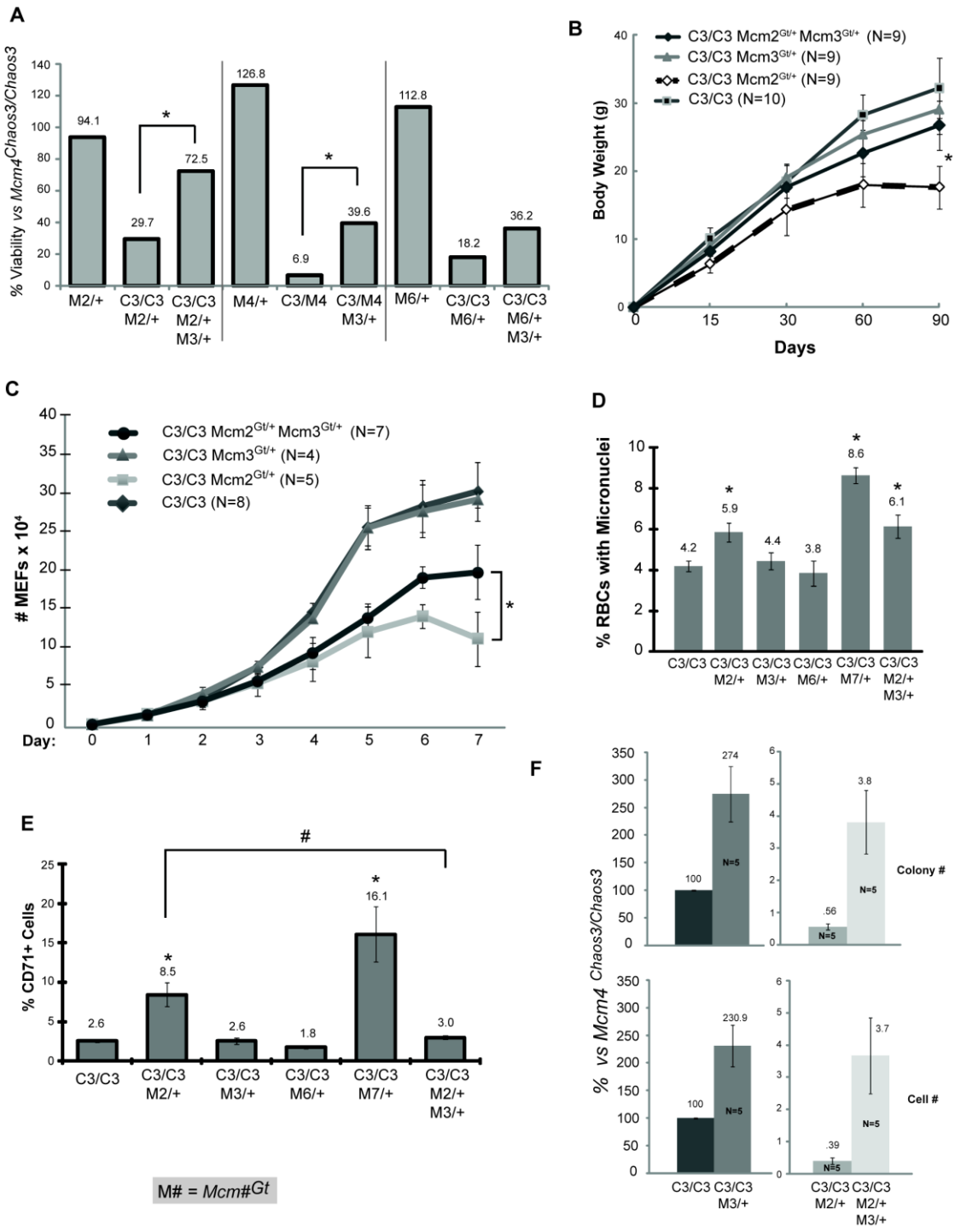

Figure 2.5. Rescue of phenotypes by *Mcm3* hemizygosity (A) Heterozygosity for *Mcm3*^{Gt} rescues the low viability of various mutant genotypes (asterisk indicates significance at $P< 0.05$ by FET). The raw data are presented in Figure S4. (B) Male

body weights of combination mutant mice. The weights of *Mcm4*$^{Chaos3/Chaos3}$ *Mcm2*$^{Gt/+}$ *Mcm3*$^{Gt/+}$ mice are significantly higher (asterisk; $P< 0.01$, Student's t-test) at 90 days than *Mcm4*$^{Chaos3/Chaos3}$ *Mcm2*$^{Gt/+}$ mice. Error bars represent SEM. (C) *Mcm4*$^{Chaos3/Chaos3}$ *Mcm2*$^{Gt/+}$ MEF proliferation defects are partially rescued by *Mcm3* hemizygosity. The effect is significant after 6 days in culture ($P< 0.05$, Student's t-test; Error bars represent SEM). (D) Micronucleus levels in *Mcm4*$^{Chaos3/Chaos3}$ mice bearing additional gene trap alleles. At least 5 males were analyzed for each genotype. Error bars represent SEM. Asterisk indicates $P< 0.05$ (student's t-test.) compared to *Mcm4*$^{Chaos3/Chaos3}$ alone. (E) CD71+ reticulocyte ratios in mutant male mice. At least 5 animals were analyzed from each class. The samples are identical to those in "D". All scored cells were anucleate peripheral blood cells Error bars represent SEM. Asterisks and "#" indicate $P< 0.05$ (Student's t-test) when compared to *Mcm4*$^{Chaos3/Chaos3}$ and *Mcm4*$^{Chaos3/Chaos3}$ *Mcm2*$^{Gt/+}$ cohorts, respectively. (F) *Mcm2* hemizygosity decreases efficiency of reprogramming *Mcm4*$^{Chaos3/Chaos3}$ MEFs into iPS cells, and *Mcm3* hemizygosity significantly increases reprogramming efficiency. Two methods of quanitifying reprogramming were used as described in Materials and Methods. "Cell number" refers flow cytometric quantification of LIN28/SSEA1 double positive cells from primary cultures of reprogrammed MEFs. Relative reprogramming efficiencies were normalized to *Mcm4*$^{Chaos3/Chaos3}$ MEFs (considered to be 100%). Error bars represent SEM. All samples within quantification class are significantly different from one another ($P< 0.05$, Student's t-test). C3 = *Mcm4*^{Chaos3}; M = *Mcm*.

Mcm3 hemizygosity. This suggests that the synthetic lethality and mouse/cell growth defects are not related to GIN *per se*. However, in the course of measuring MN in enucleated peripheral blood cells, we noticed that the ratio of CD71+ cells was significantly higher in both $Mcm4^{Chaos3/Chaos3}$ $Mcm2^{Gt/+}$ and $Mcm4^{Chaos3/Chaos3}$ $Mcm7^{Gt/+}$ mice (3.3 and 6.2 fold, respectively; Fig. 2.5E). This increase in the ratio of reticulocytes (erythrocyte precursors; immature RBCs) to total RBCs is characteristic of anemia. Hemizygosity for *Mcm3*, which alone had no effect on CD71 ratios of Chaos3 mice, corrected completely this abnormal phenotype in $Mcm4^{Chaos3/Chaos3}$ $Mcm2^{Gt/+}$animals (Fig. 2.5E).

Because MCM2-depleted mice were reported to have stem cell defects [20], and $Mcm4^{Chaos3/Chaos3}$ $Mcm\#^{Gt/+}$ mice had clear developmental abnormalities, we examined the efficiency of reprogramming mutant MEFs into induced pluripotent stem cells (iPS). The efficiency was quantified using either : 1) iPS-like colony formation, or 2) cells counts of SSEA1 and LIN28 positive cells by flow cytometry. Both gave similar results. $Mcm4^{Chaos3/Chaos3}$ $Mcm2^{Gt/+}$ cells were severely compromised in the ability to form iPS cells compared to $Mcm4^{Chaos3/Chaos3}$ (~ 200 fold less efficient; Fig. 2.5F). However, additionally reducing *Mcm3* by 50% increased iPS formation from both $Mcm4^{Chaos3/Chaos3}$and $Mcm4^{Chaos3/Chaos3}$ $Mcm2^{Gt/+}$ MEFs by ~2.5 and 10 fold, respectively.

Finally, we found that reduced MCM3 levels could rescue the cancer susceptibility of two different Chaos3 models. As shown earlier (Fig. 2.4), $Mcm4^{Chaos3/Chaos3}$ $Mcm2^{Gt/+}$ mice were highly cancer-prone with an average latency of <4 months. When a dose of Mcm3 was removed from mice of this genotype, lifespan was extended dramatically in both sexes as a consequence of delayed cancer onset, and the cancer spectrum shifted from lymphoma/thymoma towards mammary tumors (Fig. 2.6A). Additionally, hemizygosity of *Mcm3* delayed (or eliminated) the onset of mammary tumorigenesis in $Mcm4^{Chaos3/Chaos3}$ females by ~4 or more months (Fig. 2.6B). However, although *Mcm3* hemizygosity rescued viability of $Mcm4^{Chaos3/Gt}$

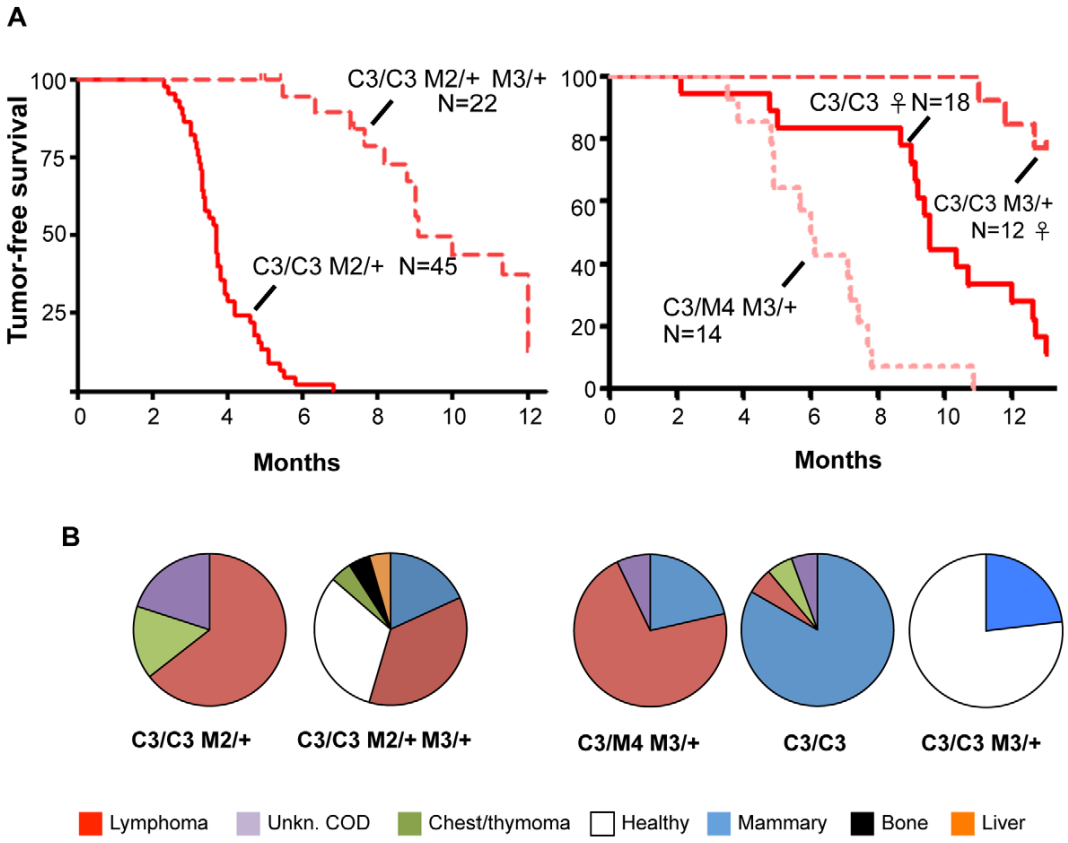

Figure 2.6. Inhibition of Chaos3 cancers by MCM3 reduction (A) Kaplan-Meier graphs of cohorts of the indicated genotypes. C3 = *Mcm4*^{Chaos3}; M# = *Mcm#*^{Gt}. In the left panel, the experiment was terminated at 12 months, with ~1/3 animals tumor-free and healthy at the time (see "B"). Unless otherwise indicated, the cohorts contained both sexes. (B) Pie charts of cancer types in mice from "A." COD= cause of death; Unkn = unknown. Classification of cancer types was assigned during necropsy, not from histological analysis.

mice (Fig. 2.5A), these animals were cancer prone with a shorter latency (by ~ 6 months) and different spectrum (primarily lymphomas) than *Mcm4*^{Chaos3} homozygotes.

Decreased MCM3 increases chromatin-bound levels of other MCMs.

We considered two possibilities to explain the surprising phenotypic rescues of reduced MCM genotypes (*Mcm4*$^{Chaos3/Chaos3}$; *Mcm4*$^{Chaos3/Chaos3}$ *Mcm2/6*$^{Gt/+}$; *Mcm4*$^{Chaos3/Gt}$) by additional MCM3 reduction (*Mcm3*$^{Gt/+}$). One is that the phenotypes are related to altered stoichiometry of MCM monomers, and that disproportionally high amounts of MCM3 relative to MCM4 and MCM2/6/7 have a dominant negative effect. However, as demonstrated above, levels of MCM3 are proportionally reduced in *Mcm4*$^{Chaos3/Chaos3}$ cells (Fig. 2.1). The second possibility is that decreased levels of MCM3 leads to a favorable change in the amounts or subcellular localization of MCMs. Various experiments have indicated that MCM2-7 hexamers or subcomplexes must be assembled in the cytoplasm before nuclear import in yeast [4], and in mice, nuclear import appears to require MCM2 and MCM3 [24]. MCMs shuttle between the nucleus and cytoplasm during the cell cycle in *S. cerevisiae*. Although in most other organisms MCMs are reported to be predominantly and constitutively nuclear localized throughout the cell cycle, dynamic redistribution between the nucleus and cytoplasm has been observed in hormonally-treated mouse uterine cells [25]. In budding yeast, nuclear export is dependent upon Mcm3, which has a nuclear export signal (NES) that is recognized by Cdc28 to promote export of MCM2-7 [22]. Analysis of mouse and human MCM3 using NES prediction software (www.cbs.dtu.dk/services/NetNES/)[26] revealed the presence of homologously-positioned, leucine-rich potential NESs (Fig. 2.7A). Therefore, we hypothesized that the rescue of phenotypes by *Mcm3* hemizygosity is due to decreased MCM protein export from the nucleus, or alternatively, increased nuclear import or stabilization that allows greater access of all MCMs for licensing chromatin.

To explore this hypothesis, we performed Western blot analysis of MCM levels in *Mcm4*$^{Chaos3/Chaos3}$ MEFs with or without the *Mcm3*^{Gt} and/or *Mcm2*^{Gt} alleles, and

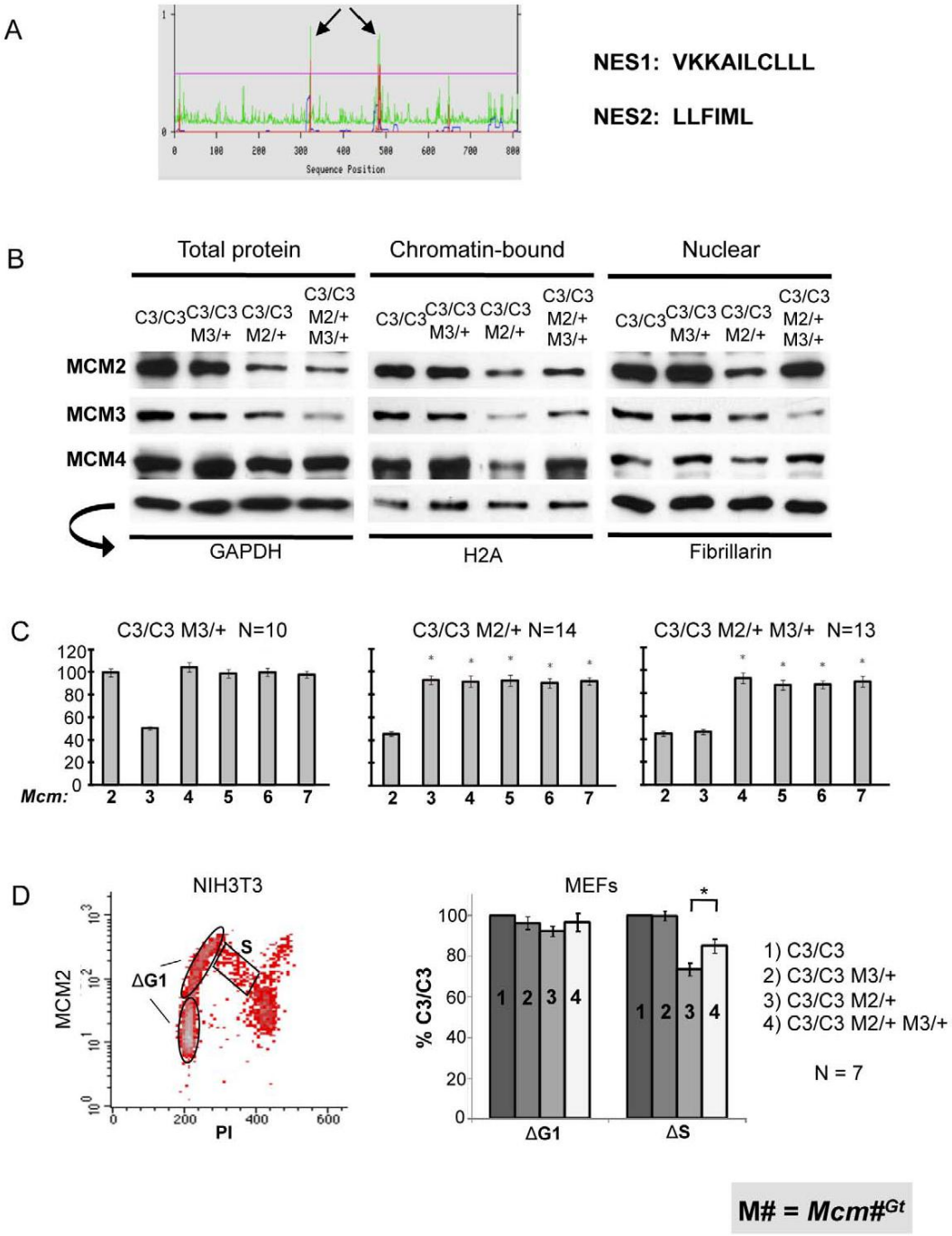

Figure 2.7. MCM3 regulates nuclear and chromatin-bound MCM levels (A) Predicted nuclear export sequences (NES) in mouse MCM3 (see text). (B) Western blot analysis of MCM2/3/4 in the indicated genotypes of MEFs. Three different

protein fractions were examined, with the indicated (arrow) loading controls at the bottom. (C) qRT-PCR analysis of Mcm2-7 mRNAs in MEFs of the indicated genotypes. (D) Nuclear MCM2 dynamics during the cell cycle. The flow plot is of isolated nuclei stained for DNA content (PI = propidium iodide) on the X-axis, and MCM2 on the Y-axis. NIH3T3 cells show dramatically the decrease in nuclear MCM2 through S phase. Flow cytometric data from the 4 MEF genotypes indicated in the right panel were used to calculate two values, ΔG1 and ΔS. The regions for the calculation of these values are indicated, and the values plotted in the right panel. The G1 (1N DNA content) phase nuclei were divided into two equal groups based on MCM2 signal intensity (Y-axis): the lower half, considered to be early-G1, and the upper half, considered to be late-G1. The ΔG1 value was calculated as the difference between the early and late MCM2 signal intensity averages. The ΔS value was calculated as : (average MCM2 intensity in the S population) – (early G1 average intensity). C3 = $Mcm4^{Chaos3}$; M# = $Mcm\#^{Gt}$. C3 is set at 100%. The asterisk indicates significance by Student's t-test ($P< 0.05$).

examined the effects of *Mcm3* dosage on the levels of nuclear and chromatin-bound MCM2 and MCM4. The results are presented in Fig. 2.7B. In all cases, the genetic reductions of *Mcm2* and *Mcm3* led to corresponding decreases in the cognate mRNA levels (Fig. 2.7C), with only minor additional decreases of other MCM mRNAs (beyond that already caused by homozygosity for $Mcm4^{Chaos3}$) occuring in the context of *Mcm2* hemizygosity (similar to $Mcm2^{Gt/+}$ MEFs in Fig. 2.2B). The overall levels of total, nuclear, and chromatin-bound MCM2 and MCM4 were unaffected by hemizygosity of *Mcm3* in $Mcm4^{Chaos3/Chaos3}$ cells (Fig. 2.7B). When *Mcm2* levels were genetically reduced by half, a condition causing the severe phenotypic effects described earlier, this caused a marked decrease in the level of chromatin-bound MCM3 and MCM4 (in addition to MCM2 itself), although total and nuclear MCM3/4 levels were affected to a lower degree or not at all. Strikingly, the decreased levels of chromatin-bound MCM2/3/4 in $Mcm4^{Chaos3/Chaos3}$ $Mcm2^{Gt/+}$ MEFs were reversed by *Mcm3* heterozygosity, but levels of total MCM2 and MCM4 were not restored. The increase of chromatin-bound MCMs occured despite the presence of less MCM3, suggesting that MCM3 is present at levels in excess of that needed to bind chromatin, presumably for pre-RC formation in the context of the MCM2-7 hexamer. In conclusion, a 50% reduction in total MCM3 increases MCM2/4 loading onto chromatin when MCM2 is otherwise limiting, and this rescue is associated with amelioration of several phenotypes.

We found that elevation of nuclear MCMs in the $Mcm3^{Gt/+}$ MEFs was often (as shown in Fig. 2.7B), but not consistently elevated across samples by Western analysis (not shown). Therefore, we quantified MCM2 during the cell cycle by flow cytometric analysis of nuclei from 7 replicate MEF cultures. Similar to WT MEFs (examples in Fig. 2.1B), NIH3T3 cells showed a decrease of nuclear MCM2 during S phase progression (Fig. 2.7D, left panel). However, all genotypes with in the $Mcm4^{Chaos3/Chaos3}$ background had a reduced decline. Thus, for comparative quantitation across genotypes, we compared the levels of MCM2 levels at the beginning of G1 *vs.* that in S phase (regions used for these calculations are indicated in

the left panel), using the calculation described in the Fig. 2.7 legend. The data are graphed in the right panel. The data revealed that regardless of genotype, the difference in average amounts of nuclear MCM2 at the beginning and end of G1 (ΔG1) did not vary. Compared to $Mcm4^{Chaos3/Chaos3}$, cells lacking 1 dose of *Mcm2* had relatively lower levels of S phase MCM2 (ΔS) compared to early G1. Additional removal of an *Mcm3* dose partially rescued the ΔS value, indicating that these cells had ~16% more nuclear MCM2 in S phase compared to $Mcm4^{Chaos3/Chaos3}$ cells hemizygous for *Mcm2* alone, despite overall reduced MCM2 levels in the cell (Fig. 2.7B, left panel).

Discussion

MCM2-7 proteins exist abundantly in proliferating cells and are bound to chromatin in amounts exceeding that required to license all replication origins that initiate DNA synthesis [9-12, 14]. The role of excess chromatin-bound MCM2-7 has been a mystery referred to as the "MCM paradox" [27], perpetuated by observations that drastic MCM reductions in certain systems can be compatible with normal DNA replication or cell proliferation [13, 28-30]. However, these circumstances are not universal, and reductions are not entirely without consequences. Early studies showed that a reduction in MCMs resulted in decreased usage of certain ARSs [12] and conferred genome instability [31] in yeasts. In cell culture systems, depletion of certain MCMs have been found to cause cell cycle defects, checkpoint abberations and GIN [13, 16, 17, 29, 32].

Recent work has shed light on aspects of the MCM paradox. Using *Xenopus* egg extracts attenuated for licensing by addition of geminin (an inhibitor of CDT1, which is required for MCM loading onto origins), one study proposed that excess chromatin-bound MCM2-7 complexes license "dormant" origins that can be activated to rescue stalled or damaged replication forks, a situation that can become important under conditions of replication stress [11]. Similar results were subsequently reported for

human cells depleted of MCMs by siRNA [15, 16], and for replication stressed MCM2-deficient MEFs [21]. Our finding that nuclear MCM2 levels decrease as S-phase progresses, and moreso in WT than in *Mcm4*$^{Chaos3/Chaos3}$ MEFs, is consistent with the dormant origin hypothesis. The decrease may reflect displacement of dormant hexamers by active replisomes, followed by subsequent degradation or nuclear export. If WT nuclei have more dormant licensed origins than Chaos3 mutants, then WT cells would be expected show a greater loss of MCMs.

The isolation of *Mcm4*^{Chaos3} provided the first demonstration that mutant alleles of essential replication licensing proteins can cause GIN and cancer [17]. Diploid budding yeast containing the same amino acid change in scMcm4 as the mouse *Mcm4*^{Chaos3} exhibited Rad9-dependent G2/M delay (Rad9 is a DNA damage checkpoint protein), elevated mitotic recombination, chromosome rearrangements, and intralocus mutations [19](Li, X. and Tye, B., personal communication). One explanation for these outcomes is that the *Chaos3* mutation impairs MCM4 biochemically in a manner leading to elevated replication fork defects, and that these defects lead to the GIN and cancer phenotypes. Alternatively, and/or in addition, the observed associated pan-reductions of MCMs in mouse cells [17] raised the possibility that decreased replication licensing might be the primary or ancillary cause for the mouse phenotypes.

The subsequent finding that mice (*Mcm2*$^{IRES\text{-}CreERT}$) containing ~1/3 the normal level of MCM2 had GIN and and cancer lent support for the idea that reductions in MCMs contribute to the Chaos3 phenotypes [20]. Although amounts of all MCMs were not investigated in *Mcm2*$^{IRES\text{-}CreERT/IRES\text{-}CreERT}$ mice, 65% reduction of MCM2 caused a reduction of dormant replication origins in MEFs that were replication stressed by hydroxyurea [21]. In *Mcm4*$^{Chaos3/Chaos3}$ mice, we hypothesize that in the context of *Mcm2*, *6* or *7* heterozygosity, which further reduces overall and chromatin-bound MCM levels below that already caused by *Mcm4*^{Chaos3} (measured to be <20% of WT mRNA levels for *Mcm2)*, MCMs are reduced to a degree that compromises cell proliferation. This then translates into the various developmental defects and

increased cancer susceptibility we observed. Whatever the exact mechanistic cause of these phenotypes, it is clear that the phenotypes are related to reduction of one or more MCMs below a threshold level that is <50%. The severe developmental consequences of MCM depletion in mice suggests that certain cell types in the developing embryo are highly sensitive to the effects of replicative stress, and/or that relatively minor cell growth perturbations of such cells are not well-tolerated in the context of complex, rapidly-occuring developmental events. The molecular basis for these phenotypes does not appear to be directly related to GIN, because whereas *Mcm3* hemizygosity rescued several phenotypes, and delayed cancer latency in $Mcm4^{Chaos3/Chaos3}$ mice, it did not concommitantly decrease MN. This suggests that phenotypes such as decreased proliferation and embryonic death are caused by genetically-induced replication stress, moreso (or in addition to) than GIN alone.

Our genetic studies indicate that there is a quantitative MCM threshold required for embryonic viability, as demonstrated by the synthetic lethalities we observed when combining homozygosity of $Mcm4^{Chaos3}$ with $Mcm2^{Gt}$, $Mcm6^{Gt}$ or $Mcm7^{Gt}$ heterozygosity, but not in the heterozygous single mutants. Additionally, the $Mcm4^{Chaos3/Gt}$ genotype, which reduced MCM levels below 50%, caused embryonic and neonatal lethality [17]. Underscoring the exquisite sensitivity of whole animals to subtle perturbations in the DNA replication machinery were the remarkable phenotypic rescues (viability, growth, iPS efficiency, etc.) by *Mcm3* hemizygosity. The decreased MCM dosage led to increases in S phase nuclear MCMs and chromatin-bound MCMs, presumably reflecting increased replication origin formation. The various single and compound mutants described here and elsewhere [20], which show that 50% reductions of any one MCM is well-tolerated but decreases of ~2/3 are not, supports the idea of a threshold effect, and suggests that the threshold lies somewhere between 1/3 and 1/2 of normal MCM levels (at least in the cases of MCM2, MCM6 and MCM7).

These results also emphasize the importance of relevant physiological models, both in general and with respect to the MCMs. RNAi knockdown of MCM3 in human cells to ~ 3% normal levels was still compatible with normal short-term proliferation, although the cells had GIN and high sensitivity to replication stress [16]. It is doubtful such a drastic situation would be recapitulated *in vivo* (it would likely result in embryonic lethality as in $Mcm3^{Gt/Gt}$ mice). Nevertheless, it is noteworthy in that study that MCM3 depletion was better tolerated than knockdowns of any other member of the replicative helicase.

The finding that reductions in MCM3 rescued MCM2/4/6 depletion phenotypes lends insight into dynamics and regulation of mammalian DNA replication. In budding yeast, MCMs shuttle between the nucleus and cytoplasm during the cell cycle. MCM2-7 multimers must be assembled in the cytoplasm before being imported into the nucleus during G1 phase [4]. The MCM2-7 importation is dependent upon synergistic nuclear localization signals (NLS) on Mcm2 and Mcm3 [22]. In order to prevent over-replication of the genome, MCMs are exported from the nucleus during S, G2 and M [4]. This export is dependent upon Mcm3, which has a nuclear export signal (NES) that is recognized by Cdc28 to promote MCM2-7 export in a Crm1-dependent manner [22].

In contrast to budding yeast, MCMs that have been studied (MCM2/3/7) are primarily nuclear-localized throughout the cell cycle in metazoans and in fission yeast [4]. Upon dissociation from chromatin during S phase, MCM2-7 complexes are reported to remain in the nucleus but are sequestered via attachement to the nuclear envelope or other nuclear structures [24, 33-35]. Interestingly, *mcm* mutations in fission yeast that disrupt intact MCM2-7 heterohexamers triggers active redistribution of MCMs to the cytoplasm [36]. Additionally, re-distribution of MCMs between the cytoplasmic and nuclear compartments has been observed in hormonally-treated mouse uterine cells [25].

Our observations support the idea that intracellular re-distribution of MCMs also occurs in mammals, and that it is an important regulatory process. Staining of MCM2 in intact nuclei of normal NIH 3T3 fibroblasts and MEFs show a steady decline (but not elimination) as S phase progresses. Furthermore, it appears that the process of nuclear MCM2 elimination during S phase is regulated, since in situations of decreased MCMs (as in the *Mcm4*$^{Chaos3/Chaos3}$ mutant), there is decreased loss of nuclear MCM2 during S phase.

Three lines of experimentation implicate MCM3 as playing a key role in regulating intracellular MCM localization: 1) Rescue of reduced-MCM phenotypes by genetic reduction of MCM3; 2) Increased S-phase nuclear MCM2 by *Mcm3* hemizygosity in MCM-depleted cells (Figure 7D); and increased chromatin-bound MCM2/4 by *Mcm3* hemizygosity in MCM-depleted cells. Our data suggests that MCM3 acts as a negative regulator that prevents re-assembly or reloading of MCM complexes as they dissociate from DNA during replication. As described earlier, mouse and human MCM3 have predicted NESs in similar positions of their primary amino acid sequences as do the yeast genes. Thus, one explanation for these phenomena is that decreased MCM3 suppresses MCM2-7 nuclear export, which occurs normally and which may be accentuated by the *Chaos3* mutation in a fashion analogous to *mcm* mutant fission yeast discussed above [36]. This would effectively increase the amounts of MCMs available for replication licensing. More work is required to determine if the rescue mechanism is indeed related to a decrease in MCMs export, as opposed to direct or indirect involvement in other events such as increased nuclear import or enhanced chromatin loading.

With respect to the early lymphoma susceptibility phenotype in *Mcm4*$^{Chaos3/Chaos3}$ *Mcm2*$^{Gt/+}$ mice, it is unclear whether the type of tumor is dictated primarily by the particular Mcm depletion (in this case MCM2, thus resembling *Mcm2*$^{IRES\text{-}CreERT2/\ IRES\text{-}CreERT2}$ animals), the genetic background, or the age of particular cancer onset (if animals die of thymic lymphoma at an early age, they will be unable to manifest later-

arising mammary tumors). The compound mutant mice used for the aging aspects of this study were bred to at least the N3 generation in strain C3H. *Mcm4*$^{Chaos3/Chaos3}$ mice congenic in this background are predisposed exclusively to mammary tumors, whereas lymphomas were observed in mutants of mixed background [17]. Presently, we favor the idea that genetic background and age of tumor type onset are primary determinants of the cancers that arise in the mice we have studied thus far. Genetic background has also been reported to influence tumor latency in MCM2-deficient mice [21].

The MCM2-7 pan-reduction in Chaos3 cells is consistent with other studies involving mutation or knockdown of a single MCM in mammalian cells [16, 20, 29, 37]. In these examples of parallel MCM decreases, the general assumption is that there is hexamer destabilization or impaired MCM chromatin loading followed by degradation of monomers. However, we found that the protein decreases are related to decreased mRNA levels. These large (~40%) decreases do not appear to be attributable to transcriptional alterations from cell cycle disruptions (these cells have a small elevation in the G2/M population), but rather occur at the post-transcriptional level (unpublished observations). Since we also found that MEFs carrying only 1 functional *Mcm2* allele caused ~20% decreases of *Mcm3-7* mRNAs, it is possible that mRNA downregulation drove MCM reductions in these other model systems. However, the mechanism for coordinated mRNA regulation, and what triggers it, is a mystery that we are currently investigating.

Our data contribute to a growing body of data that replication stress, which can occur via perturbations of the DNA replication machinery, plays a significant role in driving cancer [38-41]. While the *Mcm4*^{Chaos3} mutation is an unique case, the deleterious consequences of MCM reductions suggest that genetically-based variability in DNA replication factors can have physiological consequences. Such variability in functions or levels may be caused by Mendelian mutations or multigenic allele interactions. Mutations affecting transcriptional activity of one or more Mcms,

which might occur in non-coding *cis*-linked sequences or unlinked transcription factors, could have such effects. This has implications for cancer genome resequencing projects, whereby such mutations would not be obviously associated with MCM expression. The allelic collection we generated, when used alone or in combination with each other or *Mcm4*$^{Chaos3/\ Chaos3}$ mice, allow the generation of mouse models with a graded range of MCM levels. These should be valuable for investigations into the impact of replication stress on animal development, cancer formation, and cellular homeostasis.

Materials and Methods

MEF culture and proliferation assays

MEFs from 12.5- to 14.5-dpc embryos were cultured in DMEM + 10% FBS, 2 mM GlutaMAX, and penicillin-streptomycin (100 units/ml). Assays were conducted on cells at early passages (up to P3). For cell proliferation assays, $5x10^4$ cells were seeded per well of a 6 well plate. They were then cultured and harvested at the indicated time points to perform cell counts.

iPS Induction from MEFs using Lentiviral Vectors

Doxycycline inducible lentiviral vectors [42] were prepared by co-transecting viral packaging plasmids psPAX2 and and pMD2.G along with vectors encoding rtTA, *Oct4*, *Sox2*, *Klf4*, or *c-Myc* (plasmids were obtained from Addgene.org, serial numbers 12259, 12260, 20323, 20322, 20324, and 20326) into 293T cells using TransIT-Lt1 transfection reagent (Mirus). Viral supernatants were collected at 48 and 72 hours, and concentrated using a 30kd NMWL centrifugal concentrator. MEFs from 13.5d embryos, up to P3, were seeded to gelatin coated tissue plates at a density of $6.75x10^3$ cells/cm^2 and allowed to attach in standard MEF media for 24 hours before infection with lentiviral vectors. After 24 hours incubation the culture media was changed to KO-DMEM supplemented with 15% KO serum replacement (Gibco), recombinant LIF, 2 µg/mL doxycycline (Sigma), 100 µm MEM non-essential amino acids solution, 2mM GlutaMax, 100 units/mL penicillin and 100 µg/mL streptomycin (Gibco). The induction media was refreshed daily for 13 days until the cells were passaged to 100 mm plates prepared with irradiated feeders. Cells were cultured for an additional 10 days in the induction media in the absence of doxycyline before iPS colony counting, cell counts, and flow cytometry.

For flow cytometric quantification of iPS cells derived from reprogramming of MEFs, ~1 x 10^6 cells were trypsinized for 10 minutes, then washed twice with cold PBS. They were gently but completely resuspended in 1ml of 4% paraformaldehyde

in PBS at room temperature for 30 minutes. The fixed cells were pelleted by centrifugation at 500 x G for 2 minutes and washed twice with 10 ml TBS-TX (0.1% Triton X-100) buffer. For antibody staining, the cells were blocked with 1ml TBS-TX buffer with 1% BSA for 15 min at room temperature, then stained with primary "stemness" antibodies (monoclonal anti-SSEA1, Millipore; rabbit polyclonal anti-LIN28, Abcam) for 60 min, washed twice, then secondary antibody was applied for 60 minutes. Immunolabeled cells were analyzed by flow cytometry using a 488nm laser. Secondary antibodies were goat anti-mouse IgG-FITC (South Biotech) and goat anti-rabbit IgG-594 (Molecular Probes). Cells were considered to be iPS cells if they were LIN28/SSEA1 positive. Calibration of the flow cytometer and gates were set using untransfected MEFs as negative controls, and v6.4 ES cells as positive controls.

For quantification by colony formation, plates containing the passaged reprogrammed cells were examined microscopically at 20X, and 4 fields were scored and averaged. Colonies were considered as iPS clones based on morphological criteria: well defined border, three-dimensionality, and tight packing of cells.

Flow cytometric analyses of micronuclei and iPS cells

Micronucleus assays, which include CD71 staining, were performed essentially as described [43].

Nuclei isolation and immunofluorescence staining

MEFs were plated at 4 x 10^6 cells/150 mm culture dish for 60 hr, trypsinized, then resuspended in 1ml PBS. To the suspension was added TX-NE (320 mM sucrose, 7.5 mM $MgCl_2$, 10 mM HEPES, 1% Triton X-100, and a protease inhibitor cocktail). The cells were gently vortexed for 10 seconds and incubated on ice for 30 min. Dounce homogenization was unnecessary. Nuclei were then pelleted by centrifugation at 500xG for 2 min and washed twice with 10 ml TX-NE, then resuspended in 1ml TX-NE. Nuclei yield and integrity was monitored microscopically with trypan blue staining. The nuclei were fixed by adding 15ml cold methanol for 60 min on ice. The

fixed nuclei were pelleted by centrifugation at 500xG for 2 min, then washed twice with 10 ml TBS-TX (0.1% TX-100). 1 x 10^6 nuclei were placed into 1.5ml tubes in 1ml TBS-TX buffer + 1% BSA for 15 min at room temperature. The primary antibody (Rabbit anti-mouse MCM2) was added for 60 min, then secondary antibody (FITC goat anti-rabbit) was added for 60 min. Finally, the nuclei were stained with propidium iodide (PI), and RNAse treated (batches optimized empirically) for 30 mins. Immunolabeled nuclei were analyzed by flow cytometry (using a BD FACSCalibur cytometer with CellQuest software), exciting the PI and FITC with a 488nm laser.

Generation and validation of mouse lines bearing mutant Mcm alleles

ES cell lines containing gene trap insertions in Mcm genes were obtained from Bay Genomics [*Mcm3* (RRR002), *Mcm6* (YHD248), *Mcm7* (YTA285)] or the Sanger Institute [*Mcm2* (ABO178)]. The *Mcm4* line was previously reported [17]. Allele names are abbreviated as, for example, $Mcm3^{Gt}$ instead of the full name $Mcm3^{Gt(RRR002)Byg}$. All of the original ES cells were of strain 129 origin, and the alleles were backcrossed into C3HeB/FeJ for ≥4 generations.

To identify the exact insertion sites of the gene trap vectors, a "primer walking" procedure was used. This involved priming PCR reactions with :1) a fixed vector primer, and 2) one of a series of primers series corresponding to the intron in which the vector presumably integrated. PCR products were then sequenced. Genotyping of gene-trap-bearing mice was performed either by PCR amplification of the neomycin resistance gene within the vector, or by using insertion-specific assays (Table 2.1).

Western blot analysis.

Cytosolic and chromatin-bound protein was extracted as described [44]. Antibody binding was detected with a Pierce ECL kit. Band were quantified using NIH Image J software. Antibodies- aMCM2: ab31159 (Abcam); aMCM3: 4012 (Cell Signaling); aMCM4: ab4459 (Abcam); aMCM5: NB100-78261 (Novus); aMCM6: NB100-78262

(Novus); aMCM7: ab2360 (Abcam); aBeta-actin: A1978 (Sigma); aTBP: NB500-700 (Novus).

Quantitative RT-PCR (qPCR).

Total RNA from P1 MEFs was DNAse I treated, then cDNA was synthesized from 1 μg of total RNA using the Invitrogen SuperScript III ReverseTranscriptase kit with the supplied Olige-dT or random-hexamer primers. qPCR reactions were performed in triplicate on 1 ng or 10 ng of cDNA by using the SYBR power green RT-PCR Master kit (Applied Biosystems; 40 cycles at 95℃ for 10 s and at 60℃ for 1 min), and real-time detection was performed on an ABI PRISM 7300 and analyzed with Geneamp 5700 software. The specificity of the PCR amplification procedures was checked with a heat-dissociation step (from 60℃ to 95℃) at the end of the run and by gel electrophoresis. Results were standardized to β-actin. The PCR primers are listed in Table 2.1.

Acknowledgements

The authors thank B. Tye and S. Pruitt for helpful comments on the manuscript, and R. Munroe for generating chimeric mice.

Name	Sequence 5'->3'	Usage
mMcm2 mRNA-F (2Q1)	AGA AGT TCA GCG TCA TGC GGA GTA	mRNA qPCR
mMcm2 mRNA-R (2Q2)	CCC AAA GCG GTT GCG TTG ATA TGT	
mMcm3 mRNA-F (3Q1)	AGG AAG ACT CAT GCC AAG GAT GGA	mRNA qPCR
mMcm3 mRNA-R (3Q2)	TGG GCT CAC TGA GTT CCA CTT TCT	
mMcm4 mRNA-F (4Q1)	ACA GGA ATG AGT GCC ACT TCT CGT	mRNA qPCR
mMcm4 mRNA-R (4Q2)	AAA GCT CGC AGG GCT TCT TCA AAC	
mMcm5 mRNA-F (5Q1)	CTG GAT GCT GCT TTG TCT GGC AAT	mRNA qPCR
mMcm5 mRNA-R (5Q2)	TGT GTT CAG ACA CCT GAG AGC CAA	
mMcm6 mRNA-F (6Q1)	TCA CCA AGT CCT CGT GGA GAA TCA	mRNA qPCR
mMcm6 mRNA-R (6Q2)	TTT AGG CTG AAC CTC GTC ACA GCA	
mMcm7 mRNA-F (7Q1)	CCC TGC CCA ATT TGA ACC TTT GGA	mRNA qPCR
mMcm7 mRNA-R (7Q2)	TCT CCA CAT ATG CTG CGG TGA TGT	
mbeta-actin Frd RT	CAT CCT CTT CCT CCC TGG AGA AGA	mRNA qPCR
mbeta-actin Rev RT	ACA GGA TTC CAT ACC CAA GAA GGA AGG	
IMR13	CTT GGT GGA GAG GCT ATT C	beta-geo genotyping PCR
IMR14	AGG TGA GAT GAC AGG AGA TC	
IMR15	CAA ATG TTG CTT GTC TGG TG	postive control for genotyping PCR
IMR16	GTC AGT CGA GTG CAC AGT TT	
ABO178-R (2G2)	GCA GTA GAG TTC CCA GGA GGA GCC	ABO178 genotyping PCR
ABO178-F (2G1)	CCC TCC TCC TGC AGG TGG AAA GCA C	
ABO178-WR (2G3)	GGT GGT GTA AGG AAC AGA TGG AC	
RR0002-R (3G2)	GGA TGA GGG AGC AGG GCT CGG CAC	RRR002 genotyping PCR
RR0002-F (3G1)	CAC TGT TTA TAT GTG CAC GTG TAC C	
RR0002-WR (3G3)	CTT CTG TCG CTT TCA GAC CAG AAG C	
RRE056WR (4G3)	GAC ACA TAA ATC TTG CCA ATG AGG	RRE056 genotyping PCR
Mcm4 e12L (4G1)	AAA TGT CAG ATG AAG ATG GTT T	
Vector R (4G2)	CCA TAC AGT CCT CTT CAC ATC CAT GC	
Mcm6e9L2 (6G1)	GAC GTT GAA TCC GTT TTA GA	YHD248genotyping PCR
Mcm6e9R (6G3)	GCA CCA ACT AAT GAT GAG TCT T	
YHD248R (6G2)	AGT AGA TCC CGG CGC TCT TAC CAA	
YTA185R (7G2)	GGG AAA GAG GGC TCT GTC CTC CAG	YTA285 genotyping PCR
mMcm7intron1F (7G1)	AAG GGA CTA GGT TAC TGG GCC AGC	
mMcm7intron1R (7G3)	CCT TTC GCC ACC GGG CGC TTA GCC	
Chaos3type831L	CAT TGA TCA GCT CAT CAC CA	Chaos3 mutant genotyping PCR
Chaos3typeR	CAC ATA CCA TTT GCT TGT CAG	

Table 2.1. Primer used in this chapter

References

1. Gilbert, D.M., *Making sense of eukaryotic DNA replication origins.* Science, 2001. **294**(5540): p. 96-100.
2. Blow, J.J. and A. Dutta, *Preventing re-replication of chromosomal DNA.* Nat Rev Mol Cell Biol, 2005. **6**(6): p. 476-86.
3. Lei, M., *The MCM complex: its role in DNA replication and implications for cancer therapy.* Curr Cancer Drug Targets, 2005. **5**(5): p. 365-80.
4. Forsburg, S.L., *Eukaryotic MCM proteins: beyond replication initiation.* Microbiol Mol Biol Rev, 2004. **68**(1): p. 109-31.
5. Tye, B.K., *MCM proteins in DNA replication.* Annu Rev Biochem, 1999. **68**: p. 649-86.
6. Moyer, S.E., P.W. Lewis, and M.R. Botchan, *Isolation of the Cdc45/Mcm2-7/GINS (CMG) complex, a candidate for the eukaryotic DNA replication fork helicase.* Proc Natl Acad Sci U S A, 2006. **103**(27): p. 10236-41.
7. Labib, K., J.A. Tercero, and J.F. Diffley, *Uninterrupted MCM2-7 function required for DNA replication fork progression.* Science, 2000. **288**(5471): p. 1643-7.
8. Bochman, M.L. and A. Schwacha, *The Mcm2-7 complex has in vitro helicase activity.* Mol Cell, 2008. **31**(2): p. 287-93.
9. Stoeber, K., et al., *DNA replication licensing and human cell proliferation.* J Cell Sci, 2001. **114**(Pt 11): p. 2027-41.
10. Edwards, M.C., et al., *MCM2-7 complexes bind chromatin in a distributed pattern surrounding the origin recognition complex in Xenopus egg extracts.* J Biol Chem, 2002. **277**(36): p. 33049-57.
11. Woodward, A.M., et al., *Excess Mcm2-7 license dormant origins of replication that can be used under conditions of replicative stress.* J Cell Biol, 2006. **173**(5): p. 673-83.
12. Lei, M., Y. Kawasaki, and B.K. Tye, *Physical interactions among Mcm proteins and effects of Mcm dosage on DNA replication in Saccharomyces cerevisiae.* Mol Cell Biol, 1996. **16**(9): p. 5081-90.
13. Crevel, G., et al., *Differential requirements for MCM proteins in DNA replication in Drosophila S2 cells.* PLoS ONE, 2007. **2**(9): p. e833.
14. Young, M.R. and B.K. Tye, *Mcm2 and Mcm3 are constitutive nuclear proteins that exhibit distinct isoforms and bind chromatin during specific cell cycle stages of Saccharomyces cerevisiae.* Mol Biol Cell, 1997. **8**(8): p. 1587-601.
15. Ge, X., D.A. Jackson, and J.J. Blow, *Dormant origins licensed by excess Mcm2-7 are required for human cells to survive replicative stress.* Genes Dev, 2007. **21**(24): p. 3331-3341.
16. Ibarra, A., E. Schwob, and J. Mendez, *Excess MCM proteins protect human cells from replicative stress by licensing backup origins of replication.* Proc Natl Acad Sci U S A, 2008. **105**(26): p. 8956-61.
17. Shima, N., et al., *A viable allele of Mcm4 causes chromosome instability and mammary adenocarcinomas in mice.* Nat Genet, 2007. **39**(1): p. 93-98.

18. Fletcher, R.J., et al., *The structure and function of MCM from archaeal M. Thermoautotrophicum.* Nat Struct Biol, 2003. **10**(3): p. 160-7.
19. Li, X., J. Schimenti, and B. Tye, *Aneuploidy and improved growth are coincident but not causal in a yeast cancer model.* PLoS Biology, 2009. **7**: p. e1000161.
20. Pruitt, S.C., K.J. Bailey, and A. Freeland, *Reduced Mcm2 expression results in severe stem/progenitor cell deficiency and cancer.* Stem Cells, 2007. **25**(12): p. 3121-32.
21. Kunnev, D., et al., *DNA damage response and tumorigenesis in Mcm2-deficient mice.* Oncogene.
22. Liku, M.E., et al., *CDK phosphorylation of a novel NLS-NES module distributed between two subunits of the Mcm2-7 complex prevents chromosomal rereplication.* Mol Biol Cell, 2005. **16**(10): p. 5026-39.
23. Shima, N., T.R. Buske, and J.C. Schimenti, *Genetic screen for chromosome instability in mice: Mcm4 and breast cancer.* Cell Cycle, 2007. **6**(10): p. 1135-40.
24. Kimura, H., et al., *Mouse MCM proteins: complex formation and transportation to the nucleus.* Genes Cells, 1996. **1**(11): p. 977-93.
25. Pan, H., Y. Deng, and J.W. Pollard, *Progesterone blocks estrogen-induced DNA synthesis through the inhibition of replication licensing.* Proc Natl Acad Sci U S A, 2006. **103**(38): p. 14021-6.
26. la Cour, T., et al., *Analysis and prediction of leucine-rich nuclear export signals.* Protein Eng Des Sel, 2004. **17**(6): p. 527-36.
27. Hyrien, O., K. Marheineke, and A. Goldar, *Paradoxes of eukaryotic DNA replication: MCM proteins and the random completion problem.* Bioessays, 2003. **25**(2): p. 116-25.
28. Tsao, C.C., C. Geisen, and R.T. Abraham, *Interaction between human MCM7 and Rad17 proteins is required for replication checkpoint signaling.* Embo J, 2004. **23**(23): p. 4660-9.
29. Cortez, D., G. Glick, and S.J. Elledge, *Minichromosome maintenance proteins are direct targets of the ATM and ATR checkpoint kinases.* Proc Natl Acad Sci U S A, 2004. **101**(27): p. 10078-83.
30. Oehlmann, M., A.J. Score, and J.J. Blow, *The role of Cdc6 in ensuring complete genome licensing and S phase checkpoint activation.* J Cell Biol, 2004. **165**(2): p. 181-90.
31. Liang, D.T., J.A. Hodson, and S.L. Forsburg, *Reduced dosage of a single fission yeast MCM protein causes genetic instability and S phase delay.* J Cell Sci, 1999. **112 (Pt 4)**: p. 559-67.
32. Ekholm-Reed, S., et al., *Deregulation of cyclin E in human cells interferes with prereplication complex assembly.* J Cell Biol, 2004. **165**(6): p. 789-800.
33. Madine, M.A., et al., *The nuclear envelope prevents reinitiation of replication by regulating the binding of MCM3 to chromatin in Xenopus egg extracts.* Curr Biol, 1995. **5**(11): p. 1270-9.
34. Kimura, H., N. Nozaki, and K. Sugimoto, *DNA polymerase alpha associated protein P1, a murine homolog of yeast MCM3, changes its intranuclear*

distribution during the DNA synthetic period. Embo J, 1994. **13**(18): p. 4311-20.
35. Fujita, M., et al., *hCDC47, a human member of the MCM family. Dissociation of the nucleus-bound form during S phase.* J Biol Chem, 1996. **271**(8): p. 4349-54.
36. Pasion, S.G. and S.L. Forsburg, *Nuclear localization of Schizosaccharomyces pombe Mcm2/Cdc19p requires MCM complex assembly.* Mol Biol Cell, 1999. **10**(12): p. 4043-57.
37. Lin, D.I., P. Aggarwal, and J.A. Diehl, *Phosphorylation of MCM3 on Ser-112 regulates its incorporation into the MCM2-7 complex.* Proc Natl Acad Sci U S A, 2008. **105**(23): p. 8079-84.
38. Bartkova, J., et al., *DNA damage response as a candidate anti-cancer barrier in early human tumorigenesis.* Nature, 2005. **434**(7035): p. 864-70.
39. Gorgoulis, V.G., et al., *Activation of the DNA damage checkpoint and genomic instability in human precancerous lesions.* Nature, 2005. **434**(7035): p. 907-13.
40. Di Micco, R., et al., *Oncogene-induced senescence is a DNA damage response triggered by DNA hyper-replication.* Nature, 2006. **444**(7119): p. 638-42.
41. Bartkova, J., et al., *Oncogene-induced senescence is part of the tumorigenesis barrier imposed by DNA damage checkpoints.* Nature, 2006. **444**(7119): p. 633-7.
42. Brambrink, T., et al., *Sequential expression of pluripotency markers during direct reprogramming of mouse somatic cells.* Cell Stem Cell, 2008. **2**(2): p. 151-9.
43. Reinholdt, L., et al., *Forward genetic screens for meiotic and mitotic recombination-defective mutants in mice.* Methods Mol Biol, 2004. **262**: p. 87-107.
44. Fujita, M., et al., *In vivo interaction of human MCM heterohexameric complexes with chromatin. Possible involvement of ATP.* J Biol Chem, 1997. **272**(16): p. 10928-35.

CHAPTER III
POST-TRANSCRIPTIONAL HOMEOSTASIS OF MCM LEVELS IN MAMMALIAN CELLS

Abstract

The MCM2-7 complex provides essential replicative helicase function. Insufficient MCMs impair the cell cycle and cause genomic instability (GIN), leading to cancer and developmental defects in mice. Depletion or mutation of one MCM can destabilize the hexamer and decrease all MCMs levels. Here, we use mice and cells bearing a GIN-causing hypomophic allele of MCM4 (*Chaos3*), in conjunction with disruption alleles of other Mcms, to reveal new mechanisms of coordinate MCM pan down-regulation at two levels. First, MCM4^{Chaos3} specifically destroys MCM4:MCM6 interaction, triggering a ~40% reduction in all MCM proteins that is attributable to *Dicer1* or *Drosha* –dependent post-transcriptional reduction of *Mcm2-7* mRNA in *Mcm4*$^{Chaos3/Chaos3}$ embryonic fibroblasts. Second, we build upon genetic and biochemical evidence to show, *in vivo*, that MCM3 is a negative regulator of the MCM2-7 helicase. Whereas the overexpression of WT MCM3 exacerbates cell cycle defects in MCM2-7 depleted *Mcm4*^{Chaos3} embryonic fibroblasts, the opposite occurs with hemizygosity of MCM3 or overexpression of a mutant MCM3 (MCM3^{L4A}) that destroys helicase-inhibiting MCM3:MCM5 complexes. Unlike WT MCM3, MCM3^{L4A} does not block the recruitment of helicase onto chromatin *in vivo*. These data show that proper stoichiometry of MCM components is controlled post-transcriptionally at both the mRNA and protein levels, and is the first *in vivo* evidence that a MCM3/5 complex negatively regulates assembly of the MCM2-7 helicase onto chromatin.

Introduction

In eukaryotes, the amount and timing of DNA replication is tightly controlled to conduct a single duplication of the genome during S phase [1]. Perturbations of the underlying replication machinery can alter ploidy, genome stability, and the cell cycle. In late mitosis to early G1 phase, replication machinery assembles at numerous replication origins in the genome, beginning with the ORC complex, followed by CDC6 and CDT1 which load the MCM2-7 replicative helicase [2], then other factors needed for helicase activity [3] and full competence ("licensing") of this pre-replicative complex (pre-RC) to initiate DNA replication. Although MCM2-7 proteins are bound to chromatin in amounts exceeding that which is required for complete DNA replication the excess chromatin-bound MCM2-7 complexes occupy dormant or "backup" origins which are needed under the conditions of replication stress, compensating for stalled or disrupted primary replication forks [4-6]. Humans with mutations in any of several pre-RC components are afflicted with a severe developmental syndrome known as Meier-Gorlin [7-9]. Mice with decreased (40% or more) levels of MCMs are highly susceptible to genomic instability, cancers and developmental defects [10-13].

While these studies demonstrate that proper homeostasis of the DNA licensing process is critical for health, little is known about the regulation of these factors in mammals. However, multiple studies in cultured cells and mice reported a phenomenon whereby genetic- or siRNA-induced depletion of a single MCM causes depletion of the other MCMs [5, 6, 10, 11, 13-16]. It was generally assumed that the pan-decreases were due to MCM2-7 hexamer destabilization. However, single MCM knockdown in Drosophila, induced MCM2-7 instability in human cultured cells, and a hypomorphic allele of mouse *Mcm4* (*Mcm4*^{Chaos3}) all showed an mRNA pandownregulation coordinate with decreased protein levels [12, 17, 18]. The underlying mechanism is unknown.

DNA replication can also be regulated at the level of loading the existing pool of pre-RC components. The six MCM proteins form a ring-shaped toroidal heterohexamer in yeast [19-21]. Nevertheless, in mammalian cells, the MCM3/5 dimer and MCM4/6/7 trimer are the main complexes instead of the MCM2-7 heterohexamex [22-25]. MCM4/6/7 are typically co-isolated as a dimerized $(MCM4/6/7)_2$ sub-complex during biochemical purifications, the "MCM core," which has helicase activity *in vitro* [26, 27]. MCM3 and MCM5 dimer bind weakly to the MCM core, probably *via* Mcm7 [28]. However, this binding disrupts $(MCM4/6/7)_2$ formation and inhibits robustly its helicase activity [26, 28, 29]. These biochemical observations suggest that the degree and level of individual MCM components will influence the dynamics and degree of helicase loading and activity. In previous work, we found that genetic reduction of MCM3 ameliorates numerous mutant phenotypes exhibited by MCM-depleted mice and cells, including cancer susceptibility, embryonic lethality, and cell cycle/proliferation [12]. Paradoxically, this occurred by increasing the amounts of the other MCMs bound to chromatin *in vivo*.

In this study, we exploit the *Mcm4*^{Chaos3} model to reveal two novel mechanisms for post-transcriptional regulation of replication licensing in vivo. One occurs at the mRNA level and is modulated by the small RNA regulatory pathway to trigger pan-downregulation of all MCMs. This suggests the existence of a novel regulatory relationship for governing the stoichiometry of the MCM DNA replication licensing complex. The other mechanism involves negative regulation of MCM2-7 access to chromatin by a MCM3:MCM5-containing complex, possibly involving the nuclear export factor XPO1.

Results

The *Mcm4*^{Chaos3} mutation disrupts MCM4:MCM6 interaction

The *Mcm4*^{Chaos3} allele (hereafter abbreviated as "C3") encodes a PHE>ILE change at a highly conserved residue (Phe345Ile) [10]. This ultimately causes a reduction in both mRNA and protein levels for MCM2-7, a decrease of dormant origins, high GIN,

and extreme cancer susceptibility in homozygous mice [10, 12, 13]. We considered two possibilities to explain these consequences. The first is that the *Chaos3* mutation disrupts an intra-hexamer interaction(s) between MCM4 and another MCM(s). This idea is based on the structural prediction that Phe345 resides at the protein-protein interface region of MCM2-7 monomers [30]. Biochemical studies have indicated most MCMs also exists in several major subcomplexes, such as MCM4/6/7 and MCM3/5 [26, 31-34], so the mutation might disrupt interactions within or between subcomplexes. The second possibility, based on the finding that MCM2-7 complexes are loaded as double hexamers into pre-RCs [21], is that inter-hexamer interactions are disrupted, which might somehow affect the coordination of firing in S, or stability of the pre-RC.

To distinguish between these possibilities, we determined the ability of $MCM4^{C3}$ to associate with other MCMs in HEK cells. Whereas MCM7 could be co-immunoprecipitated with epitope-tagged mouse $MCM4^{+}$ or $MCM4^{C3}$, MCM6 was only pulled down with $MCM4^{+}$ (Fig. 3.1A). Little or no MCM2, 3, or 5 was co-precipitated with $MCM4^{+}$ or $MCM4^{C3}$. These results are consistent with MCM4, 6, 7 forming a sub-complex in human cells, and the Phe345Ile mutation disrupting MCM4/6 intrasubunit interaction. Furthermore, since $MCM4^{+}$ and $MCM4^{C3}$ co-immunoprecipitated each other but not MCM2,3 or 5, we conclude that there are little or no stable inter-MCM2-7 hexamer interactions in unsynchronized HEK cells, but rather that MCM4,6,7 may form a double-trimer as reported in yeast [31].

To assess how the $Mcm4^{C3}$ mutation affects MCM4,6,7 interactions in a more physiological context, we immunoprecipitated protein complexes from WT or $Mcm4^{Chaos3/Chaos3}$ immortalized MEFs with anti-MCM6 or 7. Consistent with the co-transfection studies, no detectable MCM4 could be immunoprecipitated by anti-MCM6 in $Mcm4^{C3/C3}$ MEFs. Additionally, although anti-MCM6 immunoprecipitated MCM7 in WT cells, it did not immunoprecipitate detectible MCM7 in mutant cells (Fig. 3.1B). However, $MCM4^{Chaos3}$-MCM7 interaction remained, albeit at a slightly

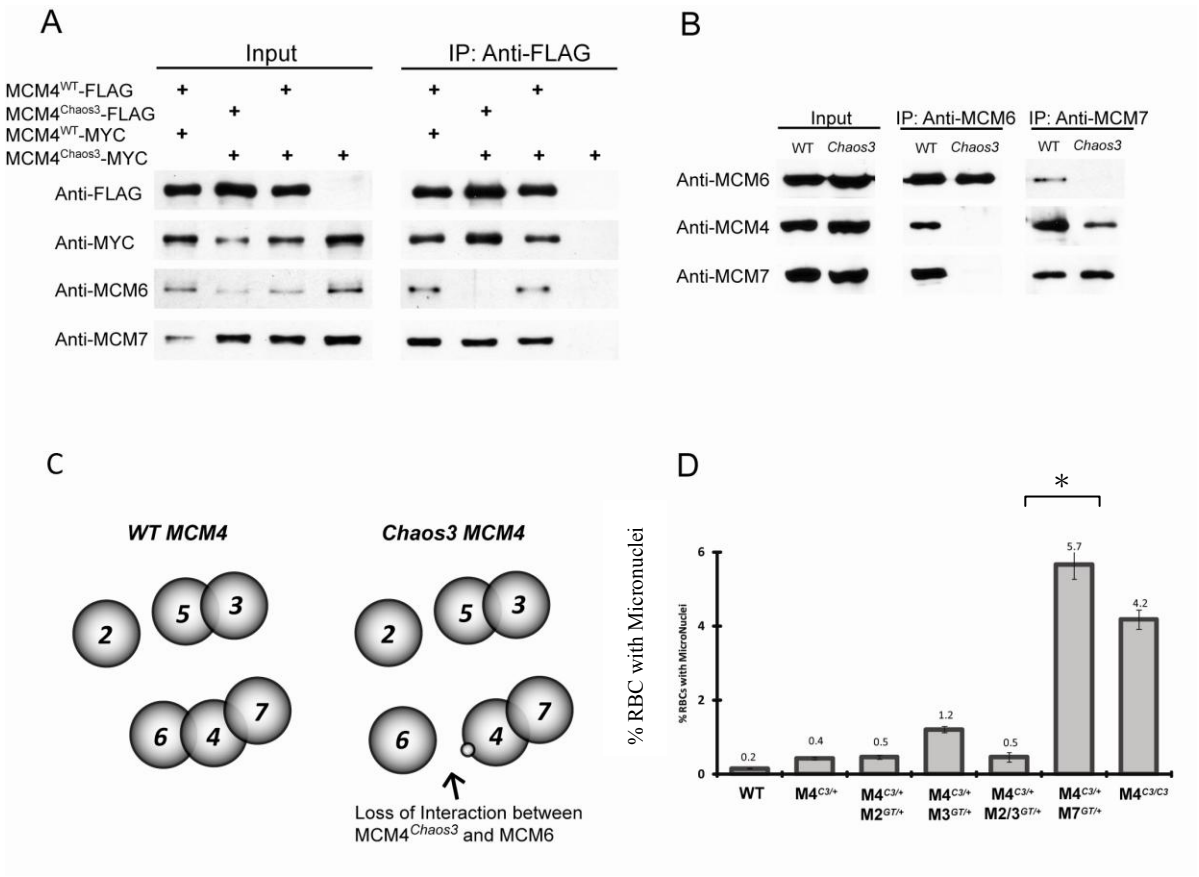

Figure 3.1. MCM4^{C3} disrupts interaction with MCM6 specifically. (A) Western blot analysis of proteins immunoprecipitated with ectopically-expressed epitope-tagged MCM4 in HEK cells. (B) Western blot analysis of proteins immunoprecipitated with MCM6 or 7 in the indicated genotypes of immortalized MEFs. (C) Consequence of *Chaos3* mutation on MCM2-7 interactions. "X" = *Chaos3* mutation. (D) Micronucleus levels in indicated genotypes of male MEFs. "C3" = *Chaos3*. "M4" = *Mcm4*. Asterisk indicates $P< 0.05$ (student's t-test.) compared to *Mcm4*$^{Chaos3/Chaos3}$ alone. At least 5 embryos were analyzed for each genotype. ±SEM bars are shown.

lower level than between the MCM4-MCM7 (Fig. 3.1B). The disrupted MCM4/6 interaction likely causes the MCM2-7 to break into sub- complexes (Fig. 3.1C), as was also suggested by gel filtration studies [13]. Taken together, these results show that the Phe345Ile change in MCM4^{Chaos3} greatly weakens the MCM4/6 interaction, possibly destabilizing the entire MCM2-7 complex, and ultimately leading to downstream consequences such as GIN and tumorigenesis.

Given the known relationship amongst MCM2-7 monomers in the intact hexamer (Fig. 3.1C) and the disrupted MCM4/6 interaction in *Mcm4*$^{C3/C3}$ cells, we surmised that the already reduced MCM4^{C3}-MCM7 interaction becomes critical for hexamer function, since this link is the only one left tethering MCM4 to the rest of the MCM2-7 complex. If true, we would expect severe phenotypic consequences if this interaction were compromised. To test this, we assessed GIN (measured as micronucleus levels in peripheral blood) in *Mcm4*$^{C3/+}$ and *Mcm4*$^{C3/C3}$ mice combined with heterozygosities for Mcm gene trap ("Gt") mutations. *Mcm7* heterozygosity cause a dramatic increase of micronuclei in *Mcm4*^{C3}/+ mice that was even higher than in *Mcm4*$^{C3/C3}$ cells. Notably, the genotype *Mcm4*$^{C3/C3}$ *Mcm7*$^{Gt/+}$ also causes higher embryonic or neonatal lethality in 97% of mice, compared to 70% lethality for *Mcm4*$^{C3/C3}$ *Mcm2*$^{Gt/+}$, 80% lethality for *Mcm4*$^{C3/C3}$ *Mcm6*$^{Gt/+}$, and no lethality for *Mcm4*$^{C3/C3}$ *Mcm3*$^{Gt/+}$ [12]. This underscores that the MCM4^{C3}:MCM7 interaction becomes critical when the MCM4/6 interaction is abolished.

Mcm RNA levels are regulated posttranscriptionally.

We reported previously [12] that the ~40% decreases of MCM2-7 protein levels in *Chaos3* cells were mirrored by similar reductions in *Mcm2-7* mRNA (Fig. 3.2A). One possible explanation is that *Mcm2-7* transcription is differentially regulated during the cell cycle, and that alterations of cell cycle distribution in mutant cell populations underlie the changes. However, the cycle profile in *Mcm4*$^{C3/C3}$ cells has only minor differences relative to WT: 10% more G1, 10% fewer S, and 20% more G2/M cells [12]. qRT-PCR analysis of a cadre of cell-cycle regulated genes revealed only

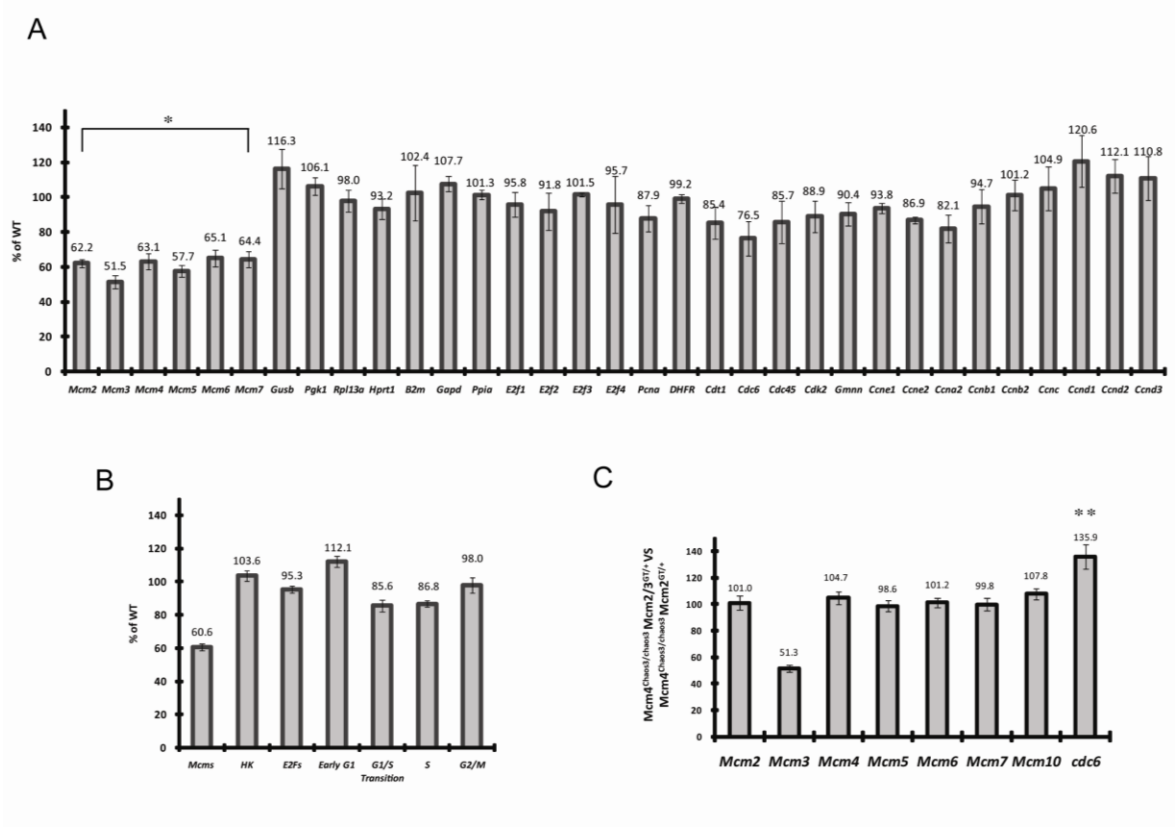

Figure 3.2. Mcm2-7 mRNAs are reduced in *Mcm4*$^{Chaos3/Chaos3}$ cells (A), (B), (C) qRT-PCR analysis of *Mcm* mRNAs, control genes, and cell cycle related genes in the WT or *Chaos3* MEFs. Relative transcript levels were normalized to -actin. Charted are the percent levels of the indicated RNAs in mutant compared to WT (considered to be 100%). At least 3 replicate cultures were analyzed for each genotype. Error bars are ±SEM. *p<0.01 vs WT, **p<0.05 vs *Mcm4*$^{C3/C3}$ *Mcm2*$^{GT/+}$.

minimal (<14%) alterations of the G1/S and S gene mRNA levels (Fig. 3.2B). The most "dysregulated" non-MCM gene was *Cdc6*, but the 24% decrease was not nearly as drastic as the 40~50% decrease in *Mcm2-7* (Fig. 3.2A). Additionally, there was no evidence for involvement of the E2F transcription factor family in downregulating Mcm2-7 transcription in *Chaos3* cells, which was a potential consideration given that the promoter regions of *Mcm3, 5 ,6, and 7* contain potential E2F binding sequences [35]. Neither the E2F family, nor key downstream targets of E2F (*Pcna*, *Dhfr* and *Ccne1/2*) [36], were downregulated at all or nearly as much as *Mcm2-7*. Furthermore, upon rescue of the abnormal cell cycle and *cdc6* mRNA level (Fig. 3.2 C) by reduction of *Mcm3* as previously described [12], *Mcm2-7* mRNA levels were not restored (Fig. 3.2 C). These results suggest the drastic pan-reduction of Mcm mRNAs is not due to abnormal cell cycle distribution *per se*, but rather to another consequence of the *Chaos3* mutation.

Mcm2-7 mRNA pan-reduction could be due to decreased transcription or increased postranscriptional degradation. We tested the former using four approaches. First, we quantified *Mcm2-7* heterogeneous nuclear RNA (hnRNA; pre-spliced transcripts) which, due to its short half-life, reflects transcriptional activity [37, 38]. In contrast to the mRNA (Fig. 3.2A), *Mcm* hnRNAs were at WT levels in *Chaos3* MEFs (Fig. 3.3A). Second, we compared the activity of luciferase reporters under the control of *Mcm2*, *Mcm5* and *Mcm7* promoters in WT and *Chaos3* MEFs. There were no significant differences for any of the promoters (Fig. 3.4A). Third, we measured LacZ reporter mRNAs in MEFs bearing gene trap alleles. These transcripts are driven by their respective Mcm promoters. There was no decrease in $Mcm2^{Gt}$ or $Mcm3^{Gt}$ mRNA in *Chaos3* vs WT MEFs; in fact, the levels of these mRNAs were actually slightly higher in the mutant cells (Fig. 3.4B). Fourth, we measured RNA polymerase II occupancy within Mcm transcriptional units by ChIP-qPCR. The levels in mutant cells were similar to or higher than in WT (Fig. 3.3B). These four lines of experimentation show that the reduction of Mcm2-7 mRNAs in *Chaos3* cells is not due to decreased

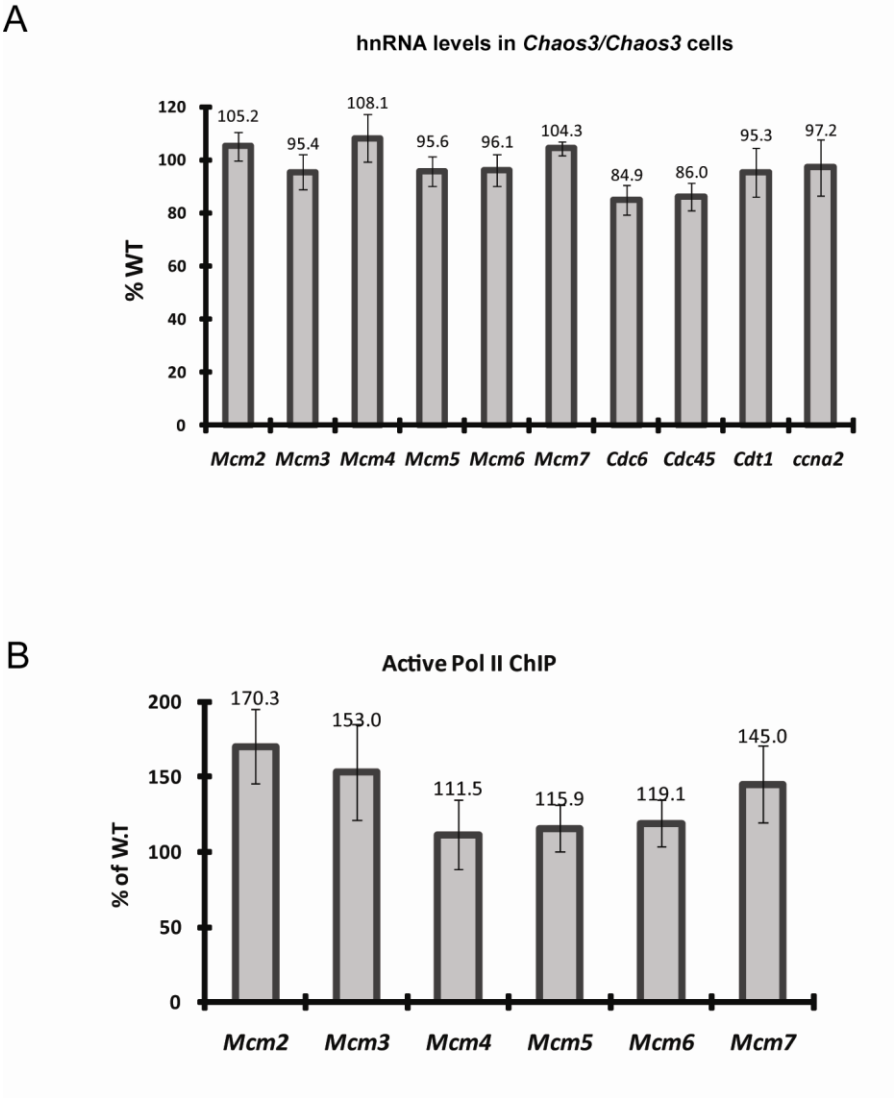

Figure 3.3. Depletion of Mcm2-7 mRNAs in *Mcm4*$^{Chaos3/Chaos3}$ cells occurs postranscriptionally (A) Mcm2-7 hnRNA levels in *Mcm4*$^{Chaos3/Chaos3}$ MEFs are unchanged compared to WT. Plotted are qRT-PCR data (% compared to WT), of intron/exon amplimers produced with primers listed in Supplemental Table 2. N = 3 replicates; ±SEM bars are shown. (B) ChIP-qPCR analysis of RNA Pol II occupancy within the Mcm2-7 transcription units of *Mcm4*^{Chaos3} mutant MEFs. N = 4 replicates; ±SEM bars are shown.

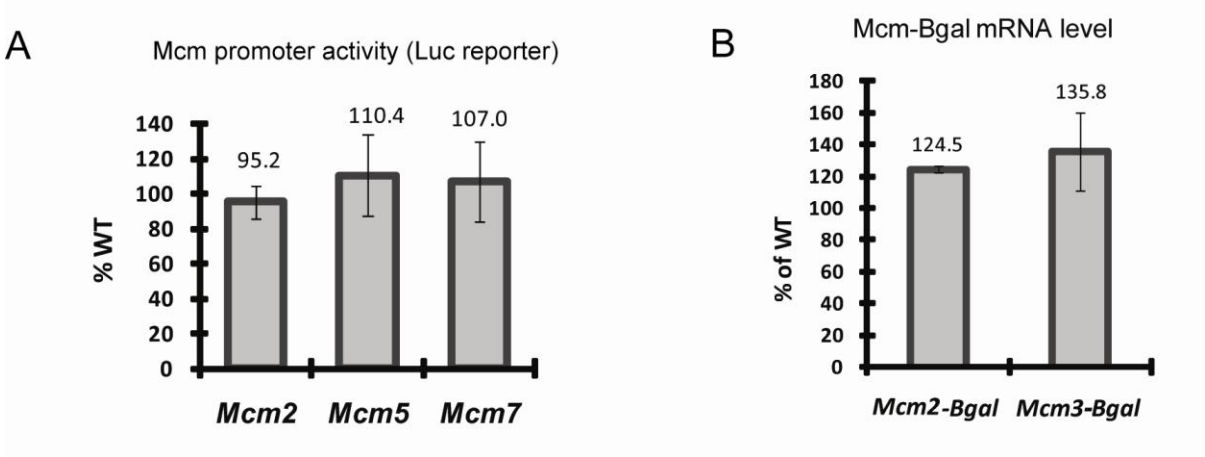

Figure 3.4. MCMs promoter activity does not decrease in *Mcm4*$^{Chaos3/Chaos3}$ cells

Luciferase reporter assays. Plotted are the luciferase activities of in *Mcm4*$^{Chaos3/Chaos3}$ MEFs transfected with the indicated promoter-luciferase (Luc) expression constructs (see Methods), with the values relative to transfections into WT MEFs. N = 5 replicates; ±SEM bars are shown. (B) LacZ mRNA levels in *Mcm4*$^{Chaos3/Chaos3}$ MEFs are unchanged compared to WT. N = 3 replicates; ±SEM bars are shown.

transcription or alterations in cell cycle distribution, but rather to post-transcriptional mechanisms.

Mcm mRNA levels are affected by RNAi machinery.

Because the decrease in *Mcm* mRNAs occurs post-transcriptionally, we hypothesized that an RNAi-mediated mechanism might be involved. To test this, *Chaos3* MEFs were transfected with siRNAs against *Drosha* or *Dicer1*, followed by measurement of Mcm transcripts by qRT-PCR. Depletion of *Dicer1* mRNA by ~68% was accompanied by increases in *Mcm2, 3, 4, 5,* and *7* (Fig. 3.5A) by up to 1.6 fold compared to scrambled siRNA controls. Knockdown of *Drosha* by ~72% caused 1.3-1.7 fold increases of *Mcm* RNAs (Fig. 3.5B). These data are consistent with the possibility that endogenous RNAi is responsible for depletion of *Mcm* mRNAs in $Mcm4^{Chaos3}$ cells. Interestingly, *Dicer* mRNA itself also increased (Fig. 3.5B), indicating a regulatory relationship between these components as observed by others [39]

MCM3 interaction with MCM5 via a Leucine rich motif correlates with chromatin-bound MCM levels

In previous work, we reported that genetic reductions of MCM2, 6 and 7 in *Chaos3* mice had severe phenotypic consequences including embryonic lethality, growth defects, anemia and early onset cancer [12]. Surprisingly, further reducing MCM3 was found to rescue most of these detrimental phenotypes. This rescue was associated with increased chromatin-bound MCMs, presumably improving pre-RC density that is already decreased in *Chaos3* cells [13]. Based on the following observations: 1) mammalian MCM3 encodes two predicted leucine-rich potential nuclear export signals (NES) in the same approximate location as a functional NES in yeast Mcm3 (scMcm3) [12, 40]; 2) the scMcm3 NES interacts with Crm1 to export Mcms through nuclear pores at after DNA synthesis [40]; and 3) MCM interaction with nuclear pore complex components regulates binding of MCMs to chromatin and replication licensing in *Xenopus* egg extracts [41, 42]; we speculated that this redistribution of the chromatin depleted MCM pool was attributable to a reduction in

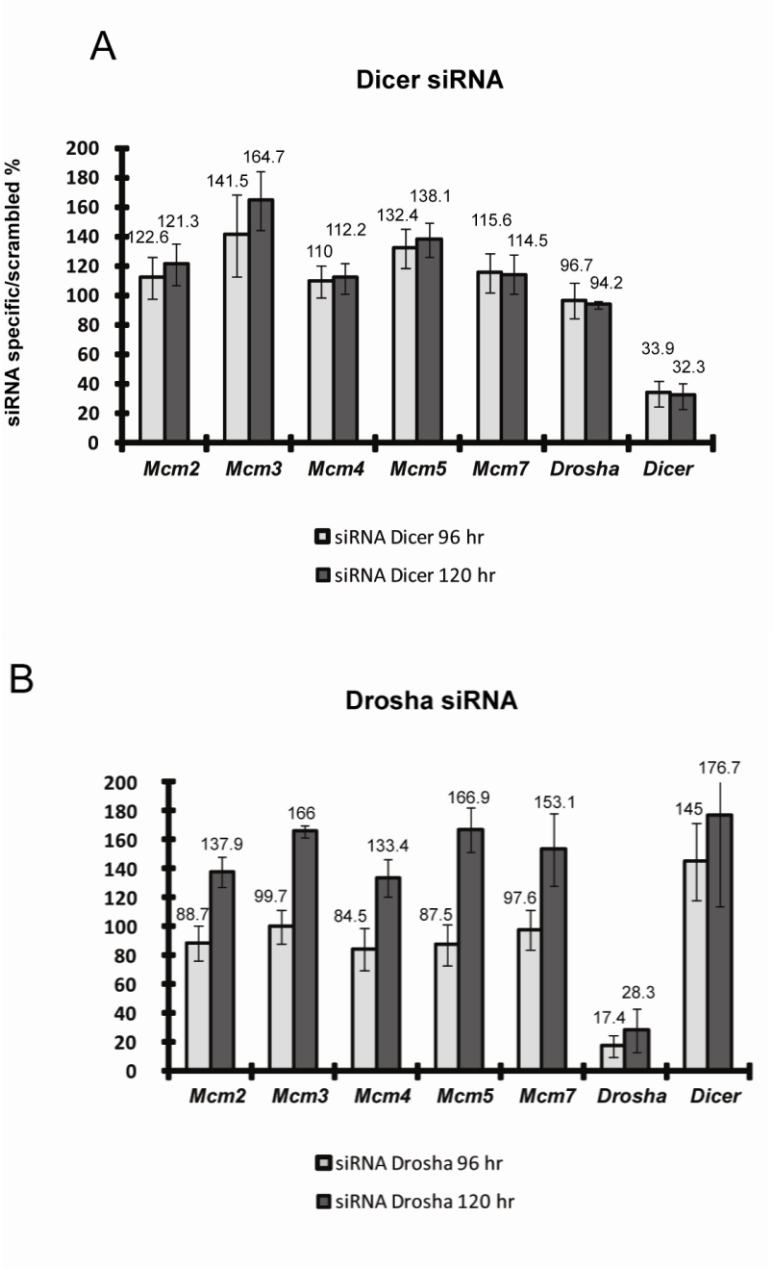

Figure 3.5. Depletion of Mcm2-7 mRNAs in *Mcm4*$^{Chaos3/Chaos3}$ cells is *Dicer1* and *Drosha* dependent. The graphs showed qRT-PCR analysis of the indicated genes in *Mcm4*$^{Chaos3/Chaos3}$ MEFs that were treated with siRNA against (A) *Dicer1* and (B) *Drosha*. The values shown are % of levels in the same cells treated with scrambled siRNA controls. N = 3 replicates; SEM bars are shown. Data were standardized against -actin as control.

MCM3-mediated MCM2-7: XPO1 (exportin 1; the mammalian ortholog of Crm1) interaction.

Consistent with this hypothesis, lentivirally-expressed MYC-tagged mouse MCM3 indeed co-immunoprecipitated XPO1 in HEK cells (Fig. 3.6B, first lane), whereas a mutant version in which 3 leucines and 1 isoleucine within the predicted NES were changed to alanines ("L4A") abolished MCM3:XPO1 interaction. To test the consequences of the leucine mutations on MCM2-7 chromatin loading, we infected HeLa cells with control (LacZ), MCM3, $MCM3^{S5A}$, and $MCM3^{L4A}$ lentiviral expression constructs. Cell extracts were divided into a detergent-soluble fraction ("Soluble" control for which was GAPDH, Fig. 3.7A) and a fraction containing nuclear scaffold protein, DNA, and chromatin binding forms of MCMs ("Chromatin" controls = Fibrillarin and Lamin A/C; Fig. 3.7A). Overexpression of MCM3 but not $MCM3^{L4A}$ caused a decrease of chromatin-bound MCM2,4,5,6, and 7, as detected both by Western blot (Fig. 3.7A). This thereby increased the soluble/chromatin MCM ratio (Fig. 3.7B). These changes in MCM2-7 localization had functional correlates with cell growth; overexpression of MCM3 markedly decreased colony formation compared to $MCM3^{L4A}$. Since CDK phosphorylation of scMcm3 regulates its nuclear transport ability [40], we also tested whether a presumed phosphorylation-dead version of MCM3 ($MCM3^{S5A}$), in which 5 predicted MCM3 CDK phosphorylation sites were mutagenized (Fig. 3.6), would also abolish the ability to increase MCM2-7 loading and improve cell growth. However, this was not the case (Fig. 3.7A&B); $MCM3^{S5A}$ transfection had similar effects as the WT construct. Furthermore, dephosphorylation of protein extracts did not disrupt MCM3:XPO1 interaction (Fig. 3.6B), suggesting that the anti-licensing effects of MCM3 may occur via a mechanism not involving, or in addition to, XPO1 interaction. We posited that these anti-licensing effects involve interaction with another protein at the mutated leucine rich domain.

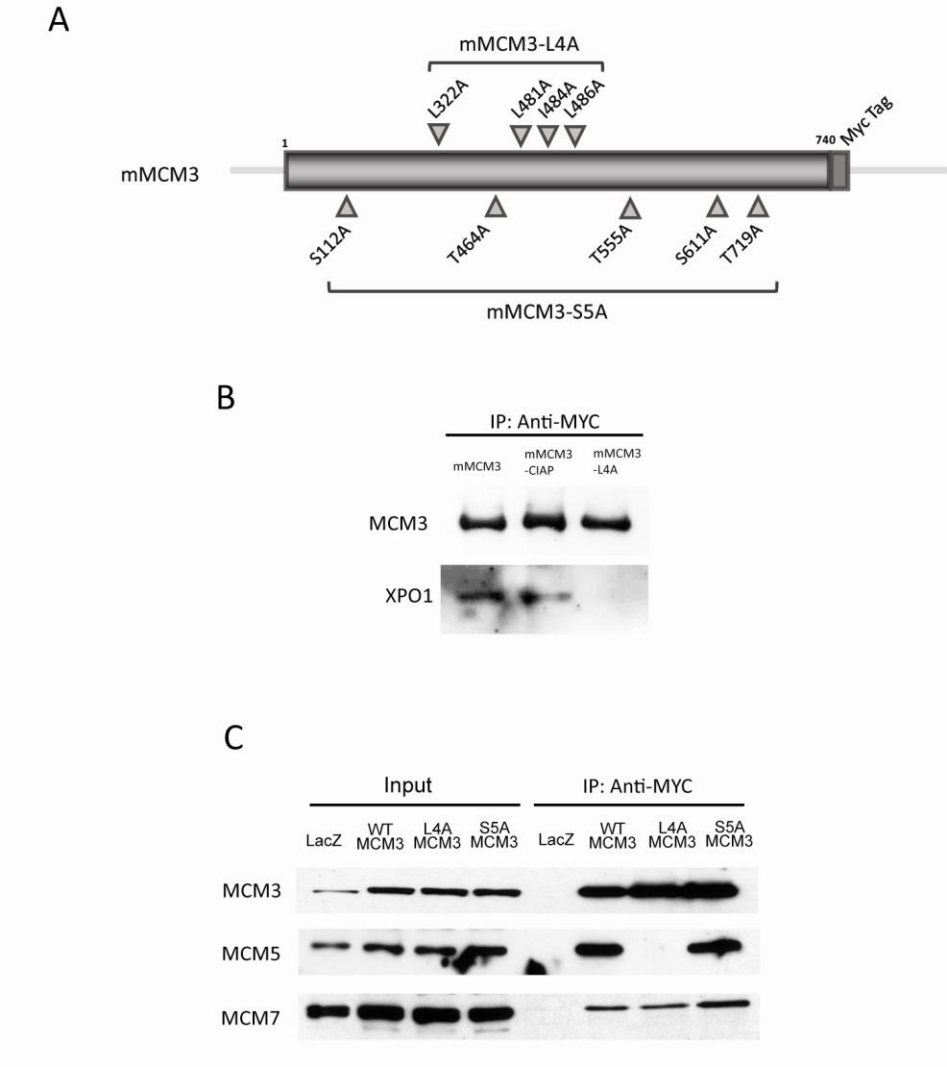

Figure 3.6. The mutation of MCM3 NES motif disrupts interaction with XPO1 and MCM5. (A) Schematic of putative NES motif and CDK phosphorylation sites within MCM3. mMcm3^{L4A} represent mMcm3-L322A/L481A/I484A/L485/A; mMcm3^{S5A} represents mMcm3-S112A/T464A/T555A/S611A/T719A. (B) MCM3 loses interaction with XPO1 after mutation of the NES motif. Western blot analysis of ectopic mMCM3-WT (with or without Calf intestinal alkaline *phosphatase* (*CIAP*)) and mMCM3-L4A precipitation and probed for MCM3 and XPO1. (C) MCM3 loses interaction with MCM5 after the NES motif is mutated. Interaction of MCM3-MCM5 or MCM3-MCM7 is evaluated by Western blot analysis. Hela cells were transduced with vectors expressing LacZ, MCM3^{WT} , MCM3^{L4A} , and MCM3^{S5A} , and cell lysates were immunoprecipitated with Anti-Myc and probed for MCM3 ,MCM5, and MCM7.

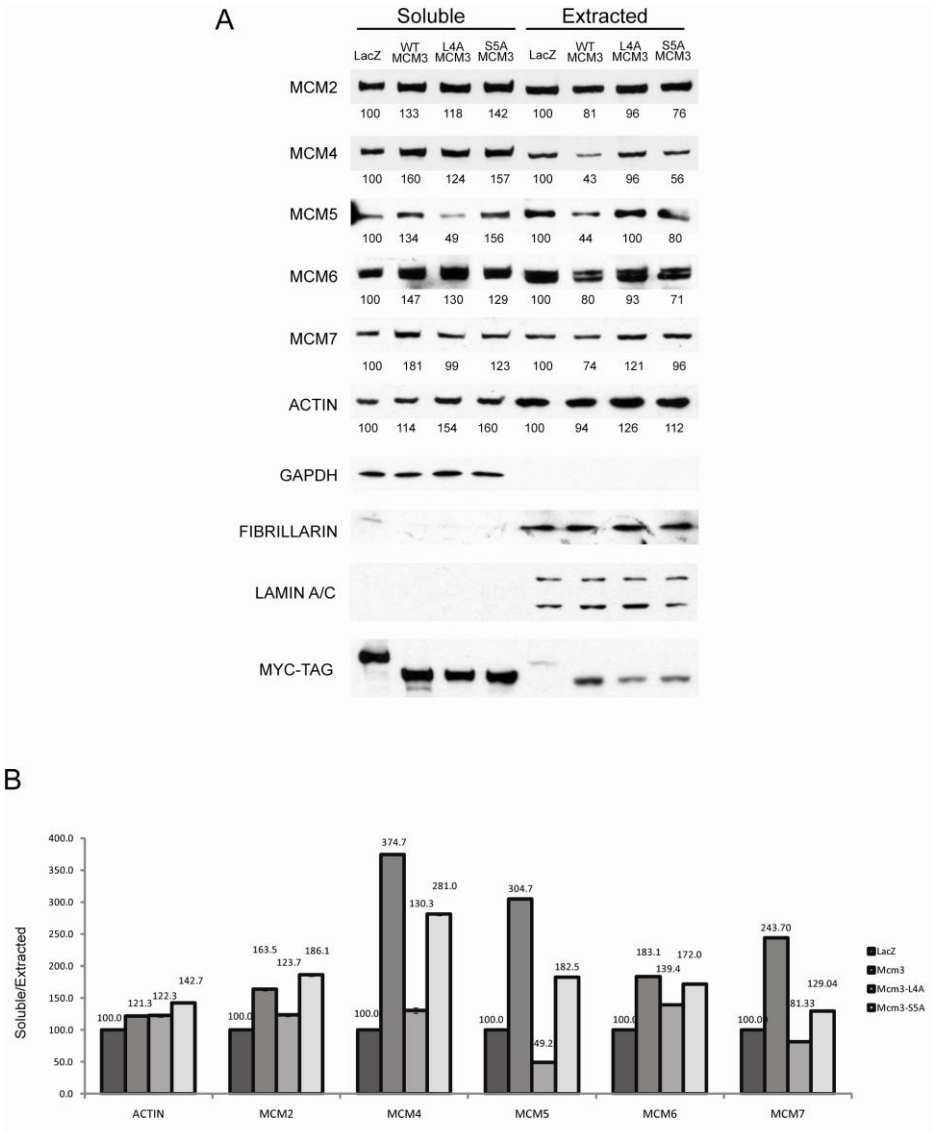

Figure 3.7. Mutation of the MCM3 NES motif disrupts the ability of MCM3 to reduce chromatin MCMs levels. (A) Cells that express ectopic LacZ, MCM3WT, MCM3L4A, and MCM3S5A were fractionated into Soluble and Extracted fractions. Western blot analysis of different fractions were probed for MCM2 , MCM4, MCM5, MCM6, MCM7, ACTIN, GAPDH, FIBRILLARIN, LAMIN A/C, and Myc-TAG. Numbers represent normalized values of band intensity against GAPDH in soluble fractions, or fibrillarin in extracted fractions (B) Quantification of Western blot data by densitometry is shown in the center panel. The amounts relative to WT cells (after normalization to the controls) are plotted. Experiments are repeated twice with reproducible results.

In mammalian cells, MCM3 dimerizes robustly with MCM5. It also binds MCM7, but with lower affinity [28]. To determine if the Leucine rich motifs in MCM3 mediate these interactions, the abilities of MYC-tagged MCM3 and MCM3^{L4A} to bind these partners were compared in co-IP experiments. As expected, WT MCM3 bound both MCM5 and MCM7, but the L4A mutation completely abolished intreraction with MCM5 specifically (Fig. 3.6C). Although CDK phosphorylation of Mcm3 S/T sites is believed to modulate Mcm3 to bind other MCMs [22], MCM3^{S5A} maintained robust interactions with MCM5 and MCM7.

MCM3 modulates cell cycle via controlling MCM2-7 loading onto chromatin

To investigate MCM3's apparent role as a negative cell cycle regulator in a physiologically accurate system, we utilized primary, non-transformed cells (MEFs) with well-characterized phenotypic consequences of MCM modulation. *Chaos3* MEFs, with ~60% WT of MCM2-7, exhibit a mild accumulation of G2/M stage cells [10, 12]. Further genetic reduction of MCM2 to ~17% WT levels (in *Mcm4*$^{Chaos3/Chaos3}$ *Mcm2*$^{Gt/+}$ cells) severely impacted cell growth and viability of mice [12]. Cells of this genotype had a dramatically increased G2/M population, indicative of cell cycle arrest (Fig. 3.8A). Further genetic reduction of MCM3 (*Mcm4*$^{Chaos3/Chaos3}$ *Mcm2*$^{Gt/+}$ *Mcm3*$^{Gt/+}$), which was shown to partially rescue the poor growth and early senescence of *Mcm4*$^{Chaos3/Chaos3}$ *Mcm2*$^{Gt/+}$ MEFs by increasing MCM binding to chromatin [12], also decreased the degree of G2/M arrest (Fig. 3.8A). This genotype of MEFs has ~17% of WT MCM2-7 levels, but mice do not suffer the extreme embryonic lethality as do those of the *Mcm4*$^{Chaos3/Chaos3}$ *Mcm2*$^{GT/+}$ genotype. The half dose of *Mcm3* also permits sufficiently adequate growth of MEFs, which, as mentioned above, otherwise undergo growth arrest beginning at early passages [12]. Another advantage of this model is that the decreased MCM3 levels allow us to replace the "lost" MCM3 with mutant versions (see below) without necessitating an overall level above WT.

In the first set of experiments, these cells were infected with lentiviruses encoding MYC-tagged expression vectors for *Mcm2*, *3*, or *4*. The epitope tag was used to

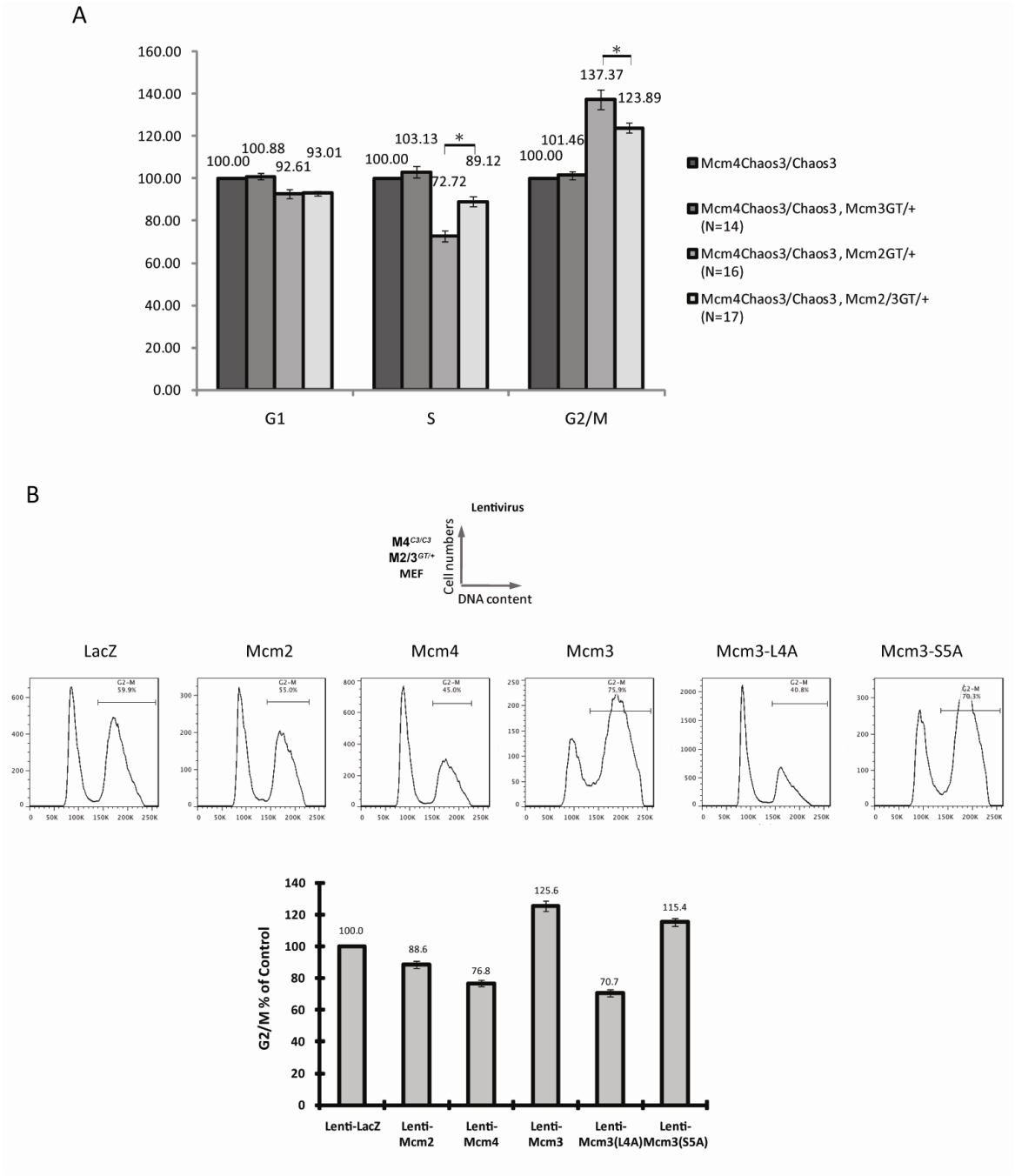

Figure 3.8. MCM3 NES motifs are required for causing G2/M arrest in MCM-depleted cells. (A) Flow cytometric analysis of unsynchronized MEF culture cell cycle profiles, based on DNA content. The MEF culture cells established from littermates include *Mcm4* $^{Chaos3/Choas4}$, *Mcm4* $^{Chaos3/Choas4}$ *Mcm2*$^{+/-}$, *Mcm4* $^{Chaos3/Choas4}$ *Mcm3* $^{+/-}$, and *Mcm4* $^{Chaos3/Choas4}$ *Mcm2/3* $^{+/-}$. Results show *Mcm4* $^{Chaos3/Choas4}$ *Mcm2*$^{+/-}$

have significant G2/M arrest when compared to *Mcm4* $^{Chaos3/Choas4}$, whereas *Mcm4* $^{Chaos3/Choas4}$ *Mcm2/3* $^{+/-}$ showed a reduction of G2/M arrest phenotype. Error bars represent SEM, derived from at least 14 independent experiments.

(B) Cell cycle histograms of *Mcm4* $^{Chaos3/Choas4}$*Mcm2/3* $^{+/-}$ MEF cells expressing LacZ, Mcm2, Mcm4, Mcm3, Mcm3-L4A, Mcm3-S5A by lentviral transduction. Only Express MCM3 and MCM3^{S5A} cause more G2/M arrest. (C) Quantification of G2/M population data. The percentages of G2/M population were normalized against LacZ controls (set to 100%). Error bars represent SEM from 3 independent experiments.

specifically analyze the growth of cells expressing the transfected Mcm. As expected, ectopic *Mcm2* or *Mcm4* expression rescued the G2/M delay (Fig. 3.8A&B). In contrast, the expression of WT *Mcm3* aggravated the G2/M arrest (Fig. 3.8A&B), consistent with our model. Whereas ectopic WT *Mcm3* increased the G2/M population, expression of Mcm3-L4A rescued the G2/M arrest even more efficiently than *Mcm2* or *Mcm4* (Fig. 3.7A&B).

Discussion

Post-transcriptional regulation of MCM mRNA levels

The pan downregulation of Mcm mRNAs in *Mcm4*$^{Chaos3/Chaos3}$ cells constitutes a previously unrecognized mode of regulation of replication licensing. Because transcriptional activity of the Mcm genes appears normal, we propose 3 potential explanations for this reduction: 1) decreased splicing of the primary transcripts; 2) decreased mRNA stability; or 3) active degradation of the mRNAs. Since knockdown of *Dicer1* or *Drosha* increased *Mcm2-7* mRNA levels, this lends support for the latter, and suggests that miRNAs might be responsible for mRNA degradation. If true, the regulation could be indirect. In support of this are observations that *Mcm4*^{Chaos3} causes detectable alterations in cell cycle (G2/M delay; [10, 30]), and that miRNAs are involved in cell cycle control [43]. Therefore, the MCM downregulation may be just one component of a more general impact of miRNAs on cell cycle perturbation. Alternatively, the coordinate decrease of all the *Mcm2-7* RNAs might be controlled by a single miRNA that binds multiple Mcm mRNAs. To explore this possibility, we used (primarily) the TargetScan algorithm (www.targetscan.org) to identify candidates. Most notable were predicted binding sites for the following miRNAs in 3 or more Mcm 3'UTRs: miR-103/107 (*Mcm4,5,6,7*); miR-465a,b,c-5p (*Mcm2,3,4*); miR-495/1192 (*Mcm2,3,4,5*); and miR-214/761 (*Mcm2,6,7*). We do not know if any of these miRNAs actually bind the predicted targets *in vivo*. However, all Mcms were found to carry multiple cleavage sites targeted by unknown small RNAs [44].

In cell culture [6] and mouse studies [11] showing that MCM2 depletion caused decreases in other MCM proteins, the corresponding mRNA levels were not investigated. Since we found that MEFs carrying only 1 functional *Mcm2* allele caused ~20% decreases of *Mcm3-7* mRNAs [12], it is possible that mRNA downregulation drove MCM reductions in those other systems. However, MEFs hemizygous for *Mcm4* or *Mcm6*, while having 50% or lower levels of the corresponding mRNAs, did not exhibit a decrease in the other Mcm mRNAs. This suggests that decreased levels of some (including *Mcm2* and *Mcm3* but not *Mcm4* or *Mcm6*) but not all MCM proteins/mRNAs are sensed by a novel mechanism in mammals, leading to mRNA degradation or decrease. In the case of $Mcm4^{Chaos3}$, it is possible that the destabilized MCM2-7 hexamer, or the consequence thereof, generates the signal.

Observations in other systems indicate that the coordinated downregulation phenomenon is complicated, and may vary according to organism, system, and particular MCM. Numerous studies have reported MCM protein decreases in response to mutation or knockdown of a single MCM, including *Drosophila* [17] and human cells [15, 22]. In these examples of parallel MCM decreases, the general assumption is that there is hexamer destabilization or impaired loading followed by degradation of monomers. This may indeed be true in some cases, but mRNA levels were rarely assessed. The nature of the MCM sensing mechanism that reduces Mcm mRNA levels in response to decreased MCMs (the data presented here) is a matter of speculation and the subject of ongoing research.

Inter-MCM regulation

Electron microscopy studies indicate that MCM2-7 forms a ring-shaped toroidal heterohexamer on DNA [19, 20] [21]. Furthermore, gel filtration analyses in a variety of systems identify a ~600 kDa MCM complex that is consistent with each subunit being present in a 1:1:1:1:1:1 stoichiometry [33, 34, 45]. However, *in vitro* studies have shown that a dimeric trimer of MCM4/6/7 has helicase activity, and that MCM2, 3, and 5 function as negative regulators [26, 27, 31, 46, 47]. The exact relationship

between *in vitro* helicase activity of reconstituted MCM components and the constitution of *in vivo* complexes remains unclear. The situation in mammalian cells appears to be more complex, in that a variety of MCM sub-complexes have been identified *in vivo*, especially the MCM4/6/7 sub-complex [22-25]. In this study, only MCM6 and MCM7 were robustly coimmunoprecipitated by anti-MCM4 from total cell extracts, consistent with our data and other reports [24, 29]. Interestingly, we also found that $MCM4^{Chaos3}$, like WT MCM4, immunoprecipitates other MCM4 molecules in addition to MCM7, indicating that an MCM4/7 double dimer is stable even in the absence of MCM6.

Our results showing that MCM3:MCM5 blocks the assembly of MCMs onto chromatin *in vivo*, and that alteration of MCM3 levels has phenotypic consequences in parallel with the effects upon MCM loading, support the idea that the primary function of certain MCMs are regulatory in nature. Regarding the exact mechanism behind the inhibitory role of MCM3, we suggest two models that are not necessarily mutually exclusive, and are based upon prior knowledge that are consistent with our observations. Model 1: since the stoichiometry of MCM2-7 in mammalian cells has been reported to be 1:2:1:1:1:1 [25, 48], the excess MCM3 obstructs the assembly of toroidal heterohexamers by binding other MCMs (especially MCM5 and MCM7). However, since $MCM3^{L4A}$ lacks negative effects on MCM2-7 loading but retains the ability to interact with MCM7, the obstructive effect would be due to interaction with MCM5. It would therefore be of interest to test the effects of MCM5 knockdown in cells and mice. Our finding that MCM3 interacts with XPO1 (similar to interaction between the yeast orthologs) raises the possibility that the MCM3/5 interaction occurs in the context of nuclear pore association.

Model 2 is based on two prior sets of data. The first is that $(MCM4/6/7)_2$ appears to be the "core complex" of the replicative helicase. Not only is it a major complex isolated from mammalian cells, but it has several *in vitro* activities expected for a replicative helicase. These include DNA binding, ATP hydrolysis, and DNA unwinding [49-51]. $(MCM4/6/7)_2$ can bind and unwind the circular DNA, suggesting

an ability to load and clamp DNA at positions without open ends, such as genomic DNA [19]. $(MCM4/6/7)_2$ can also bind CDC45, which links to DNA polymerase [52]. The second set of data is that MCM3/5 not only blocks the formation of $(MCM4/6/7)_2$ but also inhibits $(MCM4/6/7)_2$ helicase activity *in vitro* [32, 53]. Therefore, we suggest that mammalian cells may utilize $(MCM4/6/7)_2$ as the replicative helicase at least to some extent, and that the MCM3/5 dimers negatively regulate the formation of these double heterotrimers. This model does not negate the existence and the function of MCM2-7 heterohexamers, but it is possible that two forms of helicase might be employed under different circumstances. The existence of two distinct subcomplexes could explain the beneficial effects of reducing MCM3 levels in Chaos3 cells and mice.

Materials and Methods

MEF culture

Mouse embryonic fibroblasts (MEFs) from 12.5- to 14.5-dpc embryos were cultured in Dulbecco's Modified Eagle's Medium (DMEM) supplemented with 10% FBS, 2 mM GlutaMAX, penicillin-streptomycin (100 units/ml) and b-mercaptoethanol. All assays were conducted on cells at early passages (up to P3).

RNA interference

ON-TARGETplus SMARTpool small interfering RNA (siRNA) was purchased from Dharmacon (Lafayette, CO). MEFs were seeded on six-well plates at 1×10^5 cells/well and grown for 12 hr. The cells were then transfected with siRNA against mouse *DicerI* (Dicer I: 5-GGUAGACUGUGGACCGUUU; Dicer II: GGAAAUACCUGUACAACCA; Dicer III:GCAAUUUGGUGGUUGGUUU; Dicer IV: ACAGGAAUCAGGAUAAUUA), *Rnasen* (Rnasen I:UGGAAGGAGUUACG-CUUUA; Rnasen II: GCCAAAUACGGAUCGGCAA ; Rnasen III: UGUGUAA-AGUGAUUCGAUU ; Rnasen IV: GGAUGGAAUUUCUGGGCGA), or a nonrelated scrambled siRNA (CCUACUAAGCGACACCAUUdTdT) at a final concentration of

100 nM using DharmaFECT1 (Dharmacon). After 24 h, the transfection medium was replaced with DMEM. The cells were harvested 96 or 120 hr posttransfection.

Micronucleus assays

These were performed essentially as described [54].

Chromatin immunoprecipitation assays

MEFs were plated at 4 x 10^6 cells/150 mm culture plate for 60 hr, then treated for 10 min at room temperature in 1% formaldehyde to crosslink chromatin proteins to DNA. The reaction was stopped with 0.125M glycine for 5 min. Cells were pelleted and resuspended in 1 ml sonication buffer (Upstate) for 10 min on ice. 450 µl were sonicated to generated 500-bp fragments on average (300–700 bp). 100ug of DNA-chromatin complexes were processed according to the *EZ ChIP*™ (Upstate) kit protocol. Monoclonal anti-RNA polymerase II (phospho S2; Covance) and rabbit anti-mouse IgM antibody (Millipore) were incubated together for immunoprecipitation. DNA was purified by phenol-chloroform extraction and ethanol precipitation.

For quantitative PCR analysis of RNA polymerase II -bound targets, the immunoprecipitated DNA was resuspended in 100 µl of water. Input DNA was used as reference.

Co-immunoprecipitation

1 x10^6 cells were transfected with expression plasmid using Lipofectamine™ 2000. After 72 hours, the total proteins were extracted using RIPA buffer (50mM Tris-HCl pH 8.0, 150mM NaCl, 0.1% SDS, 1% NP-40, 1mM EDTA, 0.5% Sodium Deoxycholate, 50mM NaF) with proteinase inhibitor (Protease Inhibitor Cocktail Tablets, Roche Cat. No. 11836153001). After centrifugation (10,000 xg for 10 mins), the supernatant was incubated with primary antibody at 4 C overnight and then with Protein A Agarose (Millipore, Cat. No. 16-125) at room temperature for1h, followed by 3 Washs using RIPA buffer. Bound proteins were denatured by boiling in Sample buffer and used for western blotting.

For Mcm4 over-expression in HEK cells, anti-FLAG (Sigma F3165) was used for Co-IP. For reciprocal co-IPs, anti-MCM6 (Santa Cruz sc-9843) and anti-MCM7(cell signaling #4176) were used separately.

Protein and cellular fractionation

These were performed essentially as described [55]. A Triton-100 based fractionation of chromatin-bound vs non-chromatin-bound proteins was used. In this protocol, nuclei pelleted from lysed cells contained nuclear scaffold proteins, DNA, and chromatin binding forms of MCMs. The supernatant ("detergent soluble fraction") contained proteins of the cell membrane, cytosol, and free forms of MCMs (4, 24). For protein extraction, the nuclear pellet was washed 2X with 1ml TX-NE (320 mM sucrose, 7.5 mM MgCl2, 10 mM HEPES, 1% Triton X-100, and a protease inhibitor cocktail) and resuspended in 0.5ml RIPA. Successful partitioning was assessed not only with Western blotting controls, but with flow cytometric analysis of detergent-extracted whole nucleus preps, which were consistent with prior studies (25).

Western blot analysis.

The concentration of protein samples were quantified with a BCA kit (Pierce). 15 μg of total protein were separated by SDS-PAGE, electrotransferred onto a pure nitrocellulose membrane (Bio-Rad), and probed with the relevant antibodies. Binding was detected with a Pierce ECL kit. The antibodies used were as follows. aMCM2: ab31159 (Abcam); aMCM3: 4012 (Cell Signaling); aMCM4: ab4459 (Abcam); aMCM5: NB100-78261 (Novus); aMCM6: NB100-78262 (Novus); aMCM7: ab2360 (Abcam); aMYC: Mouse Monoclonal Anti-c- Myc M4439 (Sigma); aFLAG: Rabbit Polyclonal Anti-FLAG #2368 (Cell Signaling)

Luciferase constructs and assays

The promoter regions of *Mcm2*, *Mcm5*, *Mcm7* and *Pgk2* (300 bp upstream of the annotated transcriptional start sites) were PCR amplified from mouse genomic DNA

(PCR primers are listed in Table 3.1) and cloned into the pGL4.14 luciferase-containing plasmid (Promega). MEFs were plated at 7.5 x 10^4 cells/well in 24-well plates. Cells were transfected using FuGENE HD reagent and a total of 850ng DNA/well consisting of mouse Mcms (2, 5, or 7) and *Pgk2* reporter contructs. Cells were transfected then lysed in reporter lysis buffer (Promega) after 24 hr, and assayed for luciferase (Promega) activity. Results were standardized to the *Pgk2*-Luc activity levels.

Quantitative RT-PCR (qPCR).

Passage 1 MEFs were plated at 1 x 10^6 cells/100 mm culture plate for 24 hr. Total RNA isolated from passage 1 MEFs was isolated using Qiagen RNeasy kits. After DNAse I (Invitrogen) treatment, cDNA was synthesized from 1 μg of total RNA using the Invitrogen SuperScript III ReverseTranscriptase kit in a total volume of 20 μl with the supplied Olige-dT or random-hexamer primers. qPCR reactions were performed in triplicate on 1 ng or 10 ng of cDNA by using the SYBR power green RT-PCR Master kit (PerkinElmer Applied Biosystems; 40 cycles at 95℃ for 10 s and at 60℃ for 1 min), and real-time detection was performed on an ABI PRISM 7300 (Applied Biosystems) and analyzed with the Geneamp 5700 sds program (PerkinElmer/Applied Biosystems). The specificity of the PCR amplification procedures was checked with a heat-dissociation step (from 60℃ to 95℃) at the end of the run and by agarose gel electrophoresis. Results were standardized to -actin expression levels. The PCR primers are listed in Table 3.1.

Construction of Mcm2,3,4 and Mcm3 mutants.

Mouse *Mcm2*, 3, 4 DNA fragment were amplified from the cDNA library which generated from a C3HfeB strain mouse. *Chaos3* Mcm4 DNA fragment were amplified from *Chaos3* mouse. Those DNA were clone into pCDNA4-TO-His-Myc express plasmid for transient transfection, and pFUW vectors for Lentiviral infection. Mcm3 mutants were generated by site-directed mutagenesis with the QuikChange kit (Stratagene) according to the manufacturer's instructions. Total sequences were

confirmed after finishing the mutagenesis. The primers used in plasmid construction are listed in Table 3.1.

Expression of Mcms in primary MEFs using Lentiviral Vectors

Doxycycline inducible lentiviral vectors [56] were prepared by co-transecting viral packaging plasmids psPAX2 and and pMD2.G along with vectors encoding rtTA, LacZ, *Mcm2, Mcm3, Mcm4, or Mcm3 mutant* into 293T cells using TransIT-Lt1 transfection reagent (Mirus). Viral supernatants were collected at 48 and 72 hours, and concentrated using a 30kd NMWL centrifugal concentrator. MEFs from 14.5d embryos, up to P3, were seeded to gelatin coated tissue plates at a density of $6.75x10^3$ cells/cm^2 and allowed to attach in standard MEF media for 24 hours before infection with lentiviral vectors. After 24 hours incubation the culture media was changed to normal medium with 2 µg/mL doxycycline (Sigma). Cells were cultured for an additional 5 days in the induction media and then analyzed by flow cytometry.

For flow cytometric quantification of virus infected MEFs; ~1 x 10^6 cells were trypsinized for 10 minutes, then washed twice with cold PBS. They were gently but completely resuspended in 1ml of 4% paraformaldehyde in PBS at room temperature for 30 minutes. The fixed cells were pelleted by centrifugation at 500 x G for 2 minutes and washed twice with 10 ml TBS-TX (0.1% Triton X-100) buffer. For antibody staining, the cells were blocked with 1ml TBS-TX buffer with 1% BSA for 15 min at room temperature, then stained with anti-Myc antibodies for 60 min, washed twice, then secondary antibody goat anti-mouse IgG-FITC (South Biotech) with Hoechst 33258 DNA dye was applied for 60 minutes. Immunolabeled cells were analyzed by flow cytometry using a 488nm laser. Cells were considered to be virus infected cells if they were FITC positive. Only FITC positive cells were future estimated cell cycle prolifiles which were determined by Hoechst 33258 staining. Calibration of the flow cytometer and gates were set using uninfected MEFs as negative controls.

	Table 3.1 Primers used in this chapter	
Name	Sequencing 5'->3'	Usage
mMcm2 mRNA-F (2Q1)	AGA AGT TCA GCG TCA TGC GGA GTA	mRNA qPCR
mMcm2 mRNA-R (2Q3)	CCC AAA GCG GTT GCG TTG ATA TGT	
mMcm3 mRNA-F (3Q1)	AGG AAG ACT CAT GCC AAG GAT GGA	
mMcm3 mRNA-R (3Q3)	TGG GCT CAC TGA GTT CCA CTT TCT	
mMcm4 mRNA-F (4Q1)	ACA GGA ATG AGT GCC ACT TCT CGT	
mMcm4 mRNA-R (4Q3)	AAA GCT CGC AGG GCT TCT TCA AAC	
mMcm5 mRNA-F	CTG GAT GCT GCT TTG TCT GGC AAT	
mMcm5 mRNA-R	TGT GTT CAG ACA CCT GAG AGC CAA	
mMcm6 mRNA-F (6Q1)	TCA CCA AGT CCT CGT GGA GAA TCA	
mMcm6 mRNA-R (6Q3)	TTT AGG CTG AAC CTC GTC ACA GCA	
mMcm7 mRNA-F	CCC TGC CCA ATT TGA ACC TTT GGA	
mMcm7 mRNA-R	TCT CCA CAT ATG CTG CGG TGA TGT	
mMcm10 mRNA-F	ACG GGA TGG AAT GCT GAA GGA GAA	
mMcm10 mRNA-R	AGG ACA GCA CAG AGC CAA TCT CTT	
mbeta-actin Frd RT	CAT CCT CTT CCT CCC TGG AGA AGA	
mbeta-actin Rev RT	ACA GGA TTC CAT ACC CAA GAA GGA AGG	
Gusb mRNA-F	AAT GAG CCT TCC TCT GCT CT	
Gusb mRNA-R	AAC TGG CTA TTC AGC TGT GG	
B2m mRNA-F	GGC CTG TAT GCT ATC CAG AA	
B2m mRNA-R	GAA AGA CCA GTC CTT GCT GA	
Gapd mRNA-F	CTG GAG AAA CCT GCC AAG TA	
Gapd mRNA-R	TGT TGC TGT AGC CGT ATT CA	
Hprt1 mRNA-F	GCT GAC CTG CTG GAT TAC AT	
Hprt1 mRNA-R	TTG GGG CTG TAC TGC TTA AC	
Pgk mRNA-F	GCA GAT TGT TTG GAA TGG TC	
Pgk mRNA-R	TGC TCA CAT GGC TGA CTT TA	
Pp1a mRNA-F	AGC TCTGAG CAC TGG AGA GA	
Pp1a mRNA-R	GCC AGG ACC TGT ATG CTT TA	
Rpl13a mRNA-F	ATG ACA AGA AAA AGC GGA TG	
Rpl13a mRNA-R	CTT TTC TGC CTG TTT CCG TA	
E2f1 mRNA-F	ACT GTG ACT TTG GGG ACC TG	
E2f1 mRNA-R	CCC ATT TTG GTC TGC TCA AT	
E2f2 mRNA-F	TCA GAG TTG CTC CCT GAG CTT CAA	
E2f2 mRNA-R	TTG AAG TTG CCT ACG GCA CGG ATA	
E2f3 mRNA-F	GGT CCT AGC TGA AGC ACT GG	
E2f3 mRNA-R	ATG CAG CTG GCA AAG AGA AT	
E2f4 mRNA-F	CTG GCA CTT GTG ACT GTG CT	
E2f4 mRNA-R	AGC ACC ACC CTC TCT CTG AA	
Pcna mRNA-F	GGG TTG GTA GTT GTC GCT GT	
Pcna mRNA-R	TCC AGC ACC TTC TTC AGG AT	
DHFR mRNA-F	AGC ACC ACC ACG AGG AGC TCA TTT	
DHFR mRNA-R	TCT GAG GTG GCC TGG TTG ATT CAT	
Cdt1 mRNA-F	TCC AAG AGA ATG CTG TGG AGC CTA	
Cdt1 mRNA-R	TGC GGA ACA TCT CAA CTA GCA CCT	
Cdc6 mRNA-F	GCT GCC CTG GAC TTT TTA AG	
Cdc6 mRNA-R	GCT GCT TGA CTC GGA TAT GA	
Cdc45 mRNA-F	ATG TGT CCC GTC ATA ACC ACC GAA	
Cdc45 mRNA-R	TGT GTA GCT GGT GTT GTA CAG GCT	
Gmnn mRNA-F	ACG CTG AAG ATG ATC CAG CCT TCT	

Gmnn mRNA-R	TAG CTG GTC ATC CCA AAG CTT CCT	
Ccna2 mRNA-F	CTT GGC TGC ACC AAC AGT AA	
Ccna2 mRNA-R	ATG ACT CAG GCC AGC TCT GT	
Ccnb1 mRNA-F	AAG TCA GCG AAG AGC TAC AGG CAA	
Ccnb1 mRNA-R	AGT TCC ACC TCT GGT TCA CAC ACA	
Ccnb2 mRNA-F	TGA AGT CCT GGA AGT CAT GC	
Ccnb2 mRNA-R	GAG GCC AGG TCT TTG ATG AT	
Ccnc mRNA-F	GTA GGG TGG CCA TCT CTT GT	
Ccnc mRNA-R	GAA ACC CAA CAT GTT TGC AC	
Ccnd1 mRNA-F	ATT GGT CTT TCA TTG GGC AAC GGG	
Ccnd1 mRNA-R	GGC CAA TTG GGT TGG GAA AGT CAA	
Ccnd3 mRNA-F	TGC CGT GGT CAT TTT AAT TT	
Ccnd3 mRNA-R	CCT AAC CCT GCT CTG ATG AA	
Ccnd2 mRNA-F	GCT GCT TTG GTT TGA ACT GT	
Ccnd2 mRNA-R	ACC CTG CTA GCA ACA AGA TG	
Cdt1 mRNA-F	TCC AAG AGA ATG CTG TGG AGC CTA	
Cdt1 mRNA-R	TGC GGA ACA TCT CAA CTA GCA CCT	
Ccne1 mRNA-F	CCT CCA AAG TTG CAC CAG TTT GCT	
Ccne1 mRNA-R	TCG TTG ACA TAG GCC ACT TGG ACA	
Cdk2 mRNA-F	ATG AGG TGG TTT GGC CAG GAG TTA	
Cdk2 mRNA-R	CTG CTT TGG CTG AAA TCC GCT TGT	
Ccne2 mRNA-F	GAC GCA GTA GCC GTT TAC AA	
Ccne2 mRNA-R	ATA ATG CAA GGG CTG ATT CC	
mMcm2-intron14F (2Q2)	GGT GTG TAT GGC TGA GGC CAG GTT	hRNA qPCR (with mMcm2 mRNA-R
mMcm3-intron13F (3Q2)	CTG GAA ATG GCT TCA CCT TGC TGT	hRNA qPCR (with mMcm3 mRNA-R
mMcm4-intron15F (4Q2)	CAT TAA AGC ATG TGT GCC TGA CAG	hRNA qPCR (with mMcm4 mRNA-R
mMcm5-intron14F	TCT AGC ACC CAG TTT CCC TAT TGC	hRNA qPCR (with mMcm5 mRNA-R
mMcm6-intron13R (6Q2)	ACT CAT GCA TTC CTG TTC CCG TGT	hRNA qPCR (with mMcm6 mRNA-F
mMcm7-intron12F	TTT CCC GCT TTC CCA TGA ACC TTG	hRNA qPCR (with mMcm7 mRNA-R
Cdc6 hnRNA-F	GCC TGT TTA AGC CGG ATT CTG CAA	hnRNA qPCR (with Cdc6 mRNA-R)
Cdc45 hnRNA-R	ACC ACA ATC ACA CTG GTC ACA GGA	nRNA qPCR (with Cdc45 mRNA-F
Cdt1 hnRNA-F	TTC TGG GTC ACA GTG TCC TCT CCT A	hnRNA qPCR (with Cdt1 mRNA-R)
mbeta-actin-intron4R	AAC TTG TAC TAT GGC CTC AGG AGT	RNA qPCR (with mbeta-actin Frd R
IMR13	CTT GGT GGA GAG GCT ATT C	beta-geo genotyping PCR
IMR14	AGG TGA GAT GAC AGG AGA TC	
IMR15	CAA ATG TTG CTT GTC TGG TG	postive comtrol for genotyping PCR
IMR16	GTC AGT CGA GTG CAC AGT TT	
ABO178-R (2G2)	GCA GTA GAG TTC CCA GGA GGA GCC	ABO178 genotyping PCR
ABO178-F (2G1)	CCC TCC TCC TGC AGG TGG AAA GCA C	
ABO178-WR (2G3)	GGT GGT GTA AGG AAC AGA TGG AC	
RR0002-R (3G2)	GGA TGA GGG AGC AGG GCT CGG CAC	RRR002 genotyping PCR
RR0002-F (3G1)	CAC TGT TTA TAT GTG CAC GTG TAC C	
RR0002-WR (3G3)	CTT CTG TCG CTT TCA GAC CAG AAG C	
RRE056WR (4G3)	GAC ACA TAA ATC TTG CCA ATG AGG	RRE056 genotyping PCR
Mcm4 e12L (4G1)	AAA TGT CAG ATG AAG ATG GTT T	
Vector R (4G2)	CCA TAC AGT CCT CTT CAC ATC CAT GC	
Mcm6e9L2 (6G1)	GAC GTT GAA TCC GTT TTA GA	YHD248 genotyping PCR
Mcm6e9R (6G3)	GCA CCA ACT AAT GAT GAG TCT T	
YHD248R (6G2)	AGT AGA TCC CGG CGC TCT TAC CAA	
YTA185R	GGG AAA GAG GGC TCT GTC CTC CAG	

mMcm7intron1F	AAG GGA CTA GGT TAC TGG GCC AGC	YTA285 genotyping PCR
mMcm7intron1R	CCT TTC GCC ACC GGG CGC TTA GCC	
Chaos3type831L	CAT TGA TCA GCT CAT CAC CA	Chaos3 mutant genotyping PCR
Chaos3typeR	CAC ATA CCA TTT GCT TGT CAG	
mMcm2 -300-F(XhoI)	AAA CTC GAG ACG CTG AAG GGT TAA GCC TAG GTG	Ampify mMcm2 promoter
mMcm2 -1-R(BglII)	AAA AGA TCT GTC TGC GCT AGC TCC ACC GCA CCA	
mMcm5 -300-F(XhoI)	AAA CTC GAG ACG CCA CAG CCA ATC ATC TTG GGA	Ampify mMcm5 promoter
mMcm5 -1-R(BglII)	AAA AGA TCT GAC TGT ACC TGG GTC AAG GGA GAC	
mMcm7 -300-F(NheI)	AAA GCT AGC CAT TAA TTT CGA ACC GCG GGA AAC	Ampify mMcm7 promoter
mMcm7 -1-R(XhoI)	AAA CTC GAG CGC TGC CGG GGA CGG TGT GGC AGG	
PKGrev (NheI)	GTC AAG CTT ACA GGC TGC AGG TCG AAA GG	Ampify pgk promoter
PGKNeoF (HindIII)	AAA GCT AGC TTG GCT GCA GGT CGT CGA AA	
mMCM2-F (BamHI)	AAA GGA TCC GCT ATG GCG GAG TCT TCT GAG TCT CTCT C	Ampify mMcm2 gene and cloned into pCDNA4/TO/His-Myc vector
mMCM2-R (XhoI)	AAA CTC GAG ACA GAA CTG CTG TAG GAT CAG TTT GCG	
mMCM3-F (HindIII)	AAA AAG CTT GCT ATG GCG GGC ACA GTA GTG CTG GAT G	Ampify mMcm3 gene and cloned into pCDNA4/TO/His-Myc vector
mMCM3-R (XhoI)	AAA CTC GAG ACA GAT AAG GAA GAC GAT GCC CTC AG	
mMCM4-F (BamHI)	AAA GGA TCC GCT ATG TCG TCC CCG GCA TCC ACC CCG AG	Ampify mMcm4 gene and cloned into pCDNA4/TO/His-Myc vector
mMCM4-R (XhoI)	AAA CTC GAG ACA GAG CAG GCG GAC AGT CTT CCC AG	
pCDNA4toFUW-F	CAG CCT CCG CGG CCC CGA ATT CAG CCT CCG GAC TCT AGC GTT	Ampify gene from pCDNA4/TO/His-Myc vector and clone into pFUW vector
pCDNA4toFUW-R	CGA TAA GCT TGA TAT CGA ATT CTG ATC AGC GGG TTT AAA CTC	
S112A-F	GCT CAA AGC ACG TCG CTC CCC GGA CTC TC	neration of Site-Directed Mutagene
S112A-R	GAG AGT CCG GGG AGC GAC GTG CTT TGA GC	
T464A-F	GGC AGG TAT GAT CAG TAT AAG GCG CCC ATG GAG AAC	
T464A-R	GTT CTC CAT GGG CGC CTT ATA CTG ATC ATA CCT GCC	
T555A-F	ACA GCC TTC TAC ATG GGG CCA AGA AGA AAA AGG AG	
T555A-R	CTC CTT TTT CTT CTT GGC CCC ATG TAG AAG GCT GT	
S611A-F	GAC ACT GCC CGG ACA GCT CCA GTT ACA GCA C	
S611A-R	GTG CTG TAA CTG GAG CTG TCC GGG CAG TGT C	
T719A-F	ATG CCT CAA GTG CAC GCC CCA AAG ACT GAC G	
T719A-R	CGT CAG TCT TTG GGG CGT GCA CTT GAG GCA T	
L322A-F	CCT CTG CTT GCT CGC GGG AGG GGT GGA G	
L322A-R	CTC CAC CCC TCC CGC GAG CAA GCA GAG G	
L481A-F	ACT GCT GTC TAG ATT TGA CGC GCT CTT CAT CAT GCT GGA T	
L481A-R	ATC CAG CAT GAT GAA GAG CGC GTC AAA TCT AGA CAG CAG T	
L481A/ I484A-F	TAG ATT TGA CGC GCT CTT CGC CAT GCT GGA TCA GAT GGA T	
L481A/ I484A-R	ATC CAT CTG ATC CAG CAT GGC GAA GAG CGC GTC AAA TCT A	
L481A/ I484A/ L486A-F	ACG CGC TCT TCG CCA TGG CGG ATC AGA TGG ATC CTG	
L481A/ I484A L486A-R	CAG GAT CCA TCT GAT CCG CCA TGG CGA AGA GCG CGT	
Flag-F （XhoI）	AAA CTC GAG GAC TAG ACC ATG ACG GT	Ampify Flag-tag from pBICEP-CMV-2 and cloned into pCDNA4/TO/His-Myc vector
Flag-R （AgeI）	AAA ACC GGT CAC TCG TCA TCC TTG TA	

Table 3.1. Primers used in this chapter.

References

1. Blow, J.J. and A. Dutta, *Preventing re-replication of chromosomal DNA.* Nat Rev Mol Cell Biol, 2005. **6**(6): p. 476-86.
2. Bochman, M.L. and A. Schwacha, *The Mcm2-7 complex has in vitro helicase activity.* Mol Cell, 2008. **31**(2): p. 287-93.
3. Remus, D. and J.F. Diffley, *Eukaryotic DNA replication control: lock and load, then fire.* Current opinion in cell biology, 2009. **21**(6): p. 771-7.
4. Woodward, A.M., et al., *Excess Mcm2-7 license dormant origins of replication that can be used under conditions of replicative stress.* J Cell Biol, 2006. **173**(5): p. 673-83.
5. Ge, X., D.A. Jackson, and J.J. Blow, *Dormant origins licensed by excess Mcm2-7 are required for human cells to survive replicative stress.* Genes Dev, 2007. **21**(24): p. 3331-3341.
6. Ibarra, A., E. Schwob, and J. Mendez, *Excess MCM proteins protect human cells from replicative stress by licensing backup origins of replication.* Proc Natl Acad Sci U S A, 2008. **105**(26): p. 8956-61.
7. Bicknell, L.S., et al., *Mutations in ORC1, encoding the largest subunit of the origin recognition complex, cause microcephalic primordial dwarfism resembling Meier-Gorlin syndrome.* Nature genetics, 2011. **43**(4): p. 350-5.
8. Bicknell, L.S., et al., *Mutations in the pre-replication complex cause Meier-Gorlin syndrome.* Nature genetics, 2011. **43**(4): p. 356-9.
9. Guernsey, D.L., et al., *Mutations in origin recognition complex gene ORC4 cause Meier-Gorlin syndrome.* Nature genetics, 2011. **43**(4): p. 360-4.
10. Shima, N., et al., *A viable allele of Mcm4 causes chromosome instability and mammary adenocarcinomas in mice.* Nat Genet, 2007. **39**(1): p. 93-98.
11. Pruitt, S.C., K.J. Bailey, and A. Freeland, *Reduced Mcm2 expression results in severe stem/progenitor cell deficiency and cancer.* Stem Cells, 2007. **25**(12): p. 3121-32.
12. Chuang, C.H., et al., *Incremental genetic perturbations to MCM2-7 expression and subcellular distribution reveal exquisite sensitivity of mice to DNA replication stress.* PLoS Genet, 2010. **6**(9).
13. Kawabata, T., et al., *Stalled Fork Rescue via Dormant Replication Origins in Unchallenged S Phase Promotes Proper Chromosome Segregation and Tumor Suppression.* Molecular Cell, 2011. **41**(5): p. 543-53.
14. Tsao, C.C., C. Geisen, and R.T. Abraham, *Interaction between human MCM7 and Rad17 proteins is required for replication checkpoint signaling.* Embo J, 2004. **23**(23): p. 4660-9.
15. Cortez, D., G. Glick, and S.J. Elledge, *Minichromosome maintenance proteins are direct targets of the ATM and ATR checkpoint kinases.* Proc Natl Acad Sci U S A, 2004. **101**(27): p. 10078-83.
16. Orr, S.J., et al., *Reducing MCM levels in human primary T cells during the G(0)-->G(1) transition causes genomic instability during the first cell cycle.* Oncogene, 2010. **29**(26): p. 3803-14.

17. Crevel, G., et al., *Differential requirements for MCM proteins in DNA replication in Drosophila S2 cells.* PLoS ONE, 2007. **2**(9): p. e833.
18. Buchsbaum, S., et al., *Human INT6 interacts with MCM7 and regulates its stability during S phase of the cell cycle.* Oncogene, 2007. **26**(35): p. 5132-44.
19. Bochman, M.L. and A. Schwacha, *Differences in the single-stranded DNA binding activities of MCM2-7 and MCM467: MCM2 and MCM5 define a slow ATP-dependent step.* J Biol Chem, 2007. **282**(46): p. 33795-804.
20. Adachi, Y., J. Usukura, and M. Yanagida, *A globular complex formation by Nda1 and the other five members of the MCM protein family in fission yeast.* Genes Cells, 1997. **2**(7): p. 467-79.
21. Remus, D., et al., *Concerted loading of Mcm2-7 double hexamers around DNA during DNA replication origin licensing.* Cell, 2009. **139**(4): p. 719-30.
22. Lin, D.I., P. Aggarwal, and J.A. Diehl, *Phosphorylation of MCM3 on Ser-112 regulates its incorporation into the MCM2-7 complex.* Proc Natl Acad Sci U S A, 2008. **105**(23): p. 8079-84.
23. Musahl, C., et al., *A human homologue of the yeast replication protein Cdc21. Interactions with other Mcm proteins.* Eur J Biochem, 1995. **230**(3): p. 1096-101.
24. Ritzi, M., et al., *Human minichromosome maintenance proteins and human origin recognition complex 2 protein on chromatin.* J Biol Chem, 1998. **273**(38): p. 24543-9.
25. Burkhart, R., et al., *Interactions of human nuclear proteins P1Mcm3 and P1Cdc46.* Eur J Biochem, 1995. **228**(2): p. 431-8.
26. Ishimi, Y., *A DNA helicase activity is associated with an MCM4, -6, and -7 protein complex.* J Biol Chem, 1997. **272**(39): p. 24508-13.
27. Lee, J.K. and J. Hurwitz, *Processive DNA helicase activity of the minichromosome maintenance proteins 4, 6, and 7 complex requires forked DNA structures.* Proc Natl Acad Sci U S A, 2001. **98**(1): p. 54-9.
28. Prokhorova, T.A. and J.J. Blow, *Sequential MCM/P1 subcomplex assembly is required to form a heterohexamer with replication licensing activity.* J Biol Chem, 2000. **275**(4): p. 2491-8.
29. Mendez, J. and B. Stillman, *Chromatin association of human origin recognition complex, cdc6, and minichromosome maintenance proteins during the cell cycle: assembly of prereplication complexes in late mitosis.* Mol Cell Biol, 2000. **20**(22): p. 8602-12.
30. Li, X., J. Schimenti, and B. Tye, *Aneuploidy and improved growth are coincident but not causal in a yeast cancer model.* PLoS Biology, 2009. **7**: p. e1000161.
31. Ma, X., et al., *The effects of oligomerization on Saccharomyces cerevisiae Mcm4/6/7 function.* BMC biochemistry, 2010. **11**: p. 37.
32. Sato, M., et al., *Electron microscopic observation and single-stranded DNA binding activity of the Mcm4,6,7 complex.* J Mol Biol, 2000. **300**(3): p. 421-31.
33. Schwacha, A. and S.P. Bell, *Interactions between two catalytically distinct MCM subgroups are essential for coordinated ATP hydrolysis and DNA replication.* Mol Cell, 2001. **8**(5): p. 1093-104.

34. Lee, J.K. and J. Hurwitz, *Isolation and characterization of various complexes of the minichromosome maintenance proteins of Schizosaccharomyces pombe.* J Biol Chem, 2000. **275**(25): p. 18871-8.
35. Ohtani, K., et al., *Cell growth-regulated expression of mammalian MCM5 and MCM6 genes mediated by the transcription factor E2F.* Oncogene, 1999. **18**(14): p. 2299-309.
36. Berckmans, B. and V.L. De, *Transcriptional control of the cell cycle.* Current opinion in plant biology, 2009. **12**(5): p. 599-605.
37. Elferink, C.J. and J.J. Reiners, Jr., *Quantitative RT-PCR on CYP1A1 heterogeneous nuclear RNA: a surrogate for the in vitro transcription run-on assay.* Biotechniques, 1996. **20**(3): p. 470-7.
38. Sugimoto, K., et al., *Quantitative analysis of thyroid-stimulating hormone messenger RNA and heterogeneous nuclear RNA in hypothyroid rats.* Brain Res Bull, 2007. **74**(1-3): p. 142-6.
39. Kuehbacher, A., et al., *Role of Dicer and Drosha for endothelial microRNA expression and angiogenesis.* Circ Res, 2007. **101**(1): p. 59-68.
40. Liku, M.E., et al., *CDK phosphorylation of a novel NLS-NES module distributed between two subunits of the Mcm2-7 complex prevents chromosomal rereplication.* Mol Biol Cell, 2005. **16**(10): p. 5026-39.
41. Madine, M.A., et al., *The nuclear envelope prevents reinitiation of replication by regulating the binding of MCM3 to chromatin in Xenopus egg extracts.* Curr Biol, 1995. **5**(11): p. 1270-9.
42. Gillespie, P.J., et al., *ELYS/MEL-28 chromatin association coordinates nuclear pore complex assembly and replication licensing.* Current biology : CB, 2007. **17**(19): p. 1657-62.
43. Carleton, M., M.A. Cleary, and P.S. Linsley, *MicroRNAs and cell cycle regulation.* Cell Cycle, 2007. **6**(17): p. 2127-32.
44. Karginov, F.V., et al., *Diverse endonucleolytic cleavage sites in the mammalian transcriptome depend upon microRNAs, Drosha, and additional nucleases.* Molecular cell, 2010. **38**(6): p. 781-8.
45. Davey, M.J., C. Indiani, and M. O'Donnell, *Reconstitution of the Mcm2-7p heterohexamer, subunit arrangement, and ATP site architecture.* J Biol Chem, 2003. **278**(7): p. 4491-9.
46. You, Z., Y. Komamura, and Y. Ishimi, *Biochemical analysis of the intrinsic Mcm4-Mcm6-mcm7 DNA helicase activity.* Mol Cell Biol, 1999. **19**(12): p. 8003-15.
47. Bochman, M.L. and A. Schwacha, *The Mcm complex: unwinding the mechanism of a replicative helicase.* Microbiol Mol Biol Rev, 2009. **73**(4): p. 652-83.
48. Wong, P.G., et al., *Cdc45 limits replicon usage from a low density of preRCs in mammalian cells.* PLoS One, 2011. **6**(3): p. e17533.
49. You, Z., et al., *Roles of Mcm7 and Mcm4 subunits in the DNA helicase activity of the mouse Mcm4/6/7 complex.* J Biol Chem, 2002. **277**(45): p. 42471-9.
50. Coue, M., et al., *Evidence for different MCM subcomplexes with differential binding to chromatin in Xenopus.* Exp Cell Res, 1998. **245**(2): p. 282-9.

51. Kanter, D.M., I. Bruck, and D.L. Kaplan, *Mcm subunits can assemble into two different active unwinding complexes.* J Biol Chem, 2008. **283**(45): p. 31172-82.
52. Bauerschmidt, C., et al., *Interactions of human Cdc45 with the Mcm2-7 complex, the GINS complex, and DNA polymerases delta and epsilon during S phase.* Genes Cells, 2007. **12**(6): p. 745-58.
53. Stead, B.E., et al., *ATP binding and hydrolysis by Mcm2 regulate DNA binding by Mcm complexes.* J Mol Biol, 2009. **391**(2): p. 301-13.
54. Reinholdt, L., et al., *Forward genetic screens for meiotic and mitotic recombination-defective mutants in mice.* Methods Mol Biol, 2004. **262**: p. 87-107.
55. Friedrich, T.D., et al., *Distinct patterns of MCM protein binding in nuclei of S phase and rereplicating SV40-infected monkey kidney cells.* Cytometry A, 2005. **68**(1): p. 10-8.
56. Brambrink, T., et al., *Sequential expression of pluripotency markers during direct reprogramming of mouse somatic cells.* Cell Stem Cell, 2008. **2**(2): p. 151-9.

CHAPTER IV

ANDROGEN PROTECTS MALE ANIMALS FROM MCMS INSUFFICIENCY

Abstract

The MCM2-7 proteins form the DNA replicative helicase and are essential for viability. In previous work, we generated Mcm hypomorphic mouse models using gene disruption alleles. Animals with a 50% reduction of *Mcms* mRNA levels are grossly normal and do not show any early stage abnormality. However, further reduction of *Mcms* mRNA levels to 30% by introducing the $Mcm4^{Chaos3}$ allele into these mice causes embryo lethality, growth retardation, and increased cancer incidence. These detrimental phenotypes are due to insufficient pre-replication complex formation and result in a slowed cell cycle.

From the genetic analyses, we observed a unique phenotype in $Mcm4^{Chaos3/Chaos3}$ *& Mcms* gene trap mice that only have 30% of WT *Mcms* mRNA levels. Females had higher embryonic and postnatal lethality than males, indicating the males are less susceptible to MCMs insufficiency. Furthermore, XX males bearing the "male determinant" *Sry* gene had increased viability, suggesting that androgen protects animals from MCMs insufficiency. Testosterone injection into pregnant females significantly rescued the viability of their daughters. Finally, we have shown that testosterone can up-regulate *Mcm2, 3, 5, 6, and 7* mRNA expression. Our results reveal a novel relationship between *Mcms* and androgens, which can influence the animals' phenotype when MCMs are insufficient.

Introduction

During the late M and early G1 phase of the cell cycle, the DNA origins of replication are bound by origin recognition complex (ORC1-6) [1, 2]. The binding of ORC1-6 in DNA is competent to recruit CDC6 and CDT1, which are required for the loading of MCMs complex [3]. As the cell enters S phase, the cyclin-dependent kinases (CDKs) and the Dbf4-dependent kinase (DDK) CDC7 activate the MCMs complex, therefore, the DNA can unwind and begin to replicate [2, 4]. Based on their function in DNA replication, *Mcms* are predicted to be highly transcribed in actively dividing cells. However, only E2F family is experimentally proved to regulate *Mcm5, 6, 7* which have E2F binding sites located on the promoter regions [5]. Although *Mcm7* was predicted to be up-regulated by E2F, which activate G1/S phase genes, evidence for increased transcription of *Mcm7* was shown in G2/M phase, suggesting that E2F is not the only regulating factor [6].

Sex steroid hormones, including estradiol, progesterone, and testosterone, play a very important role in many physiological processes by regulating cell proliferation [7-9]. The regulation of *Mcms* by steroid hormones remains unclear. The *Mcms* expression pattern from microarray analysis after hormone treatments showed that estradiol and testosterone up-regulate all *Mcms*, and progesterone has opposite effect [10-12]. The detailed mechanism that how steroid hormones regulate Mcms and the physiological relevance need to be future addressed.

In Chapter II, the results showed that 70% reductions of the *Mcms* mRNA cause elevated embryonic and neonatal lethality. Further analyses of the survival rate reported in this chapter indicate that the females are more susceptible to MCMs reduction. This gender bias correlates with embryonic lethality after 9.5 dpc. Mouse embryonic sexual development also occurs after 9.5 dpc, suggesting that the gender bias lethality relates to sexual differentiation. In early embryogenesis, the mammalian Y chromosome acts as a dominant male determinant due to the action of a single gene, *Sry* [13, 14]. The activation of *Sry* drives the production of testosterone to initiate testis rather than ovarian development from the early bipotential gonads [15], then it triggers the differentiation of Sertoli cells from supporting cell precursors, which

would otherwise become granulosa cells [16]. Sex determination and the activation of *Sry* occurs between 9.5 and 12.5 dpc, paralleling the gender bias lethality phenotype in Mcms deficient mice.

Based on the difference of embryonic lethality between genders, I hypothesized that *Sry* expression, and elevated testosterone that comes with maleness, is responsible for the protection of MCM-depleted animals. In this chapter, I describe genetic evidence that embryonic and neonatal lethality in Mcms deficient animals exhibit a female preference and that hormones are specifically responsible.

Results

Female newborn mice are more susceptible to Mcms insufficiency than males.

The genetic interaction results from chapter II showed that 70% reduction of the *Mcms* mRNA level caused a high incidence of embryonic or neonatal lethality. Interestingly, males and females were affected differentially. (Fig. 4.1A); the numbers of viable female newborns with the MCM-depleted genotype were significantly lower than males of the same mutant genotype. There was no gender bias in animals of non-lethal genotypes. For example, the ratio of females vs males ("F/M ratio") in $Mcm4^{Chaos3/Chaos3}$ and $Mcm4^{Chaos3/Chaos3}$ $Mcm3^{GT/+}$ are 100.7% and 90.3% (Fig. 4.1A). In the Mcms deficient animals such as $Mcm4^{Chaos3/Chaos3}$ $Mcm2^{GT/+}$, $Mcm4^{Chaos3/GT}$, $Mcm4^{Chaos3/Chaos3}$ $Mcm6^{GT/+}$, and $Mcm4^{Chaos3/Chaos3}$ $Mcm7^{GT/+}$, the F/M ratio are 32.1%, 0%, 16%, and 47.89%, respectively (Fig. 4.1A). Heterozygosity of Mcm3 rescued this bias in the $Mcm4^{Chaos3/GT}$ and $Mcm4^{Chaos3/Chaos3}$ $Mcm6^{GT/+}$ animals.

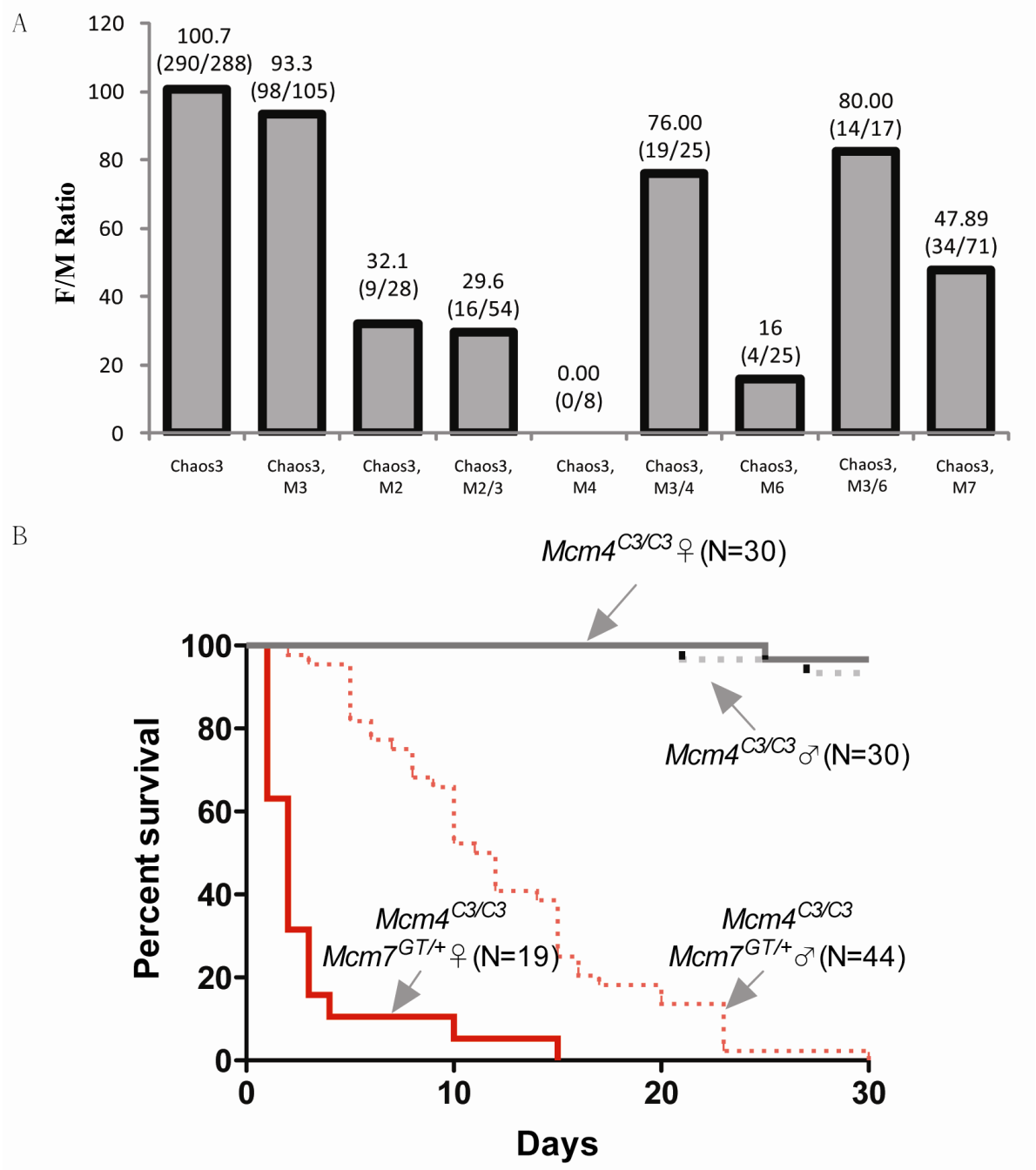

Figure 4.1. Female newborn mice are more susceptible to MCMs insufficiency than males. (A) Graphed are F/M ratios of different genotypes. Viable newborn mice from different crosses were genotyped by *Mcms* and *Sry* PCR. "*Chaos3*" in the X axis represents $Mcm4^{Chaos3/Chaos3}$. *M"s"* represents $Mcm"s"^{GT/+}$. (B) Neonatal lethality occurs in $Mcm4^{Chaos3/Chaos3}$ $Mcm7^{Gt/+}$ animals, and it occurs earlier in females than in males.

The F/M ratios in the *Mcm4*$^{Chaos3/Chaos3}$ *Mcm3*$^{GT/+}$ and *Mcm4*$^{Chaos3/Chaos3}$ *Mcm3/6*$^{GT/+}$ are 76% and 80%. However, the reduction of MCM3 does not rescue this bias in the *Mcm4*$^{Chaos3/Chaos3}$ *Mcm2*$^{GT/+}$ animals, because the F/M ratio in *Mcm4*$^{Chaos3/Chaos3}$ *Mcm2/3*$^{GT/+}$ is 29.6% which similar to 32.1% in the *Mcm4*$^{Chaos3/Chaos3}$ *Mcm2*$^{GT/+}$ animals (Fig. 4.1A). The gender bias also appears in neonatal lethal phenotype in the *Mcm4*$^{Chaos3/Chaos3}$ *Mcm7*$^{GT/+}$ animals. The life span for male pups is significantly longer than female pups (Fig. 4.1B)

Gender bias occurs coincident with the appearance of the embryonic lethal phenotype

To further characterize this phenomenon, several timed mating experiments conducted to identify when females loss occurs in *Mcm4*$^{Chaos3/Chaos3}$ *Mcm2*$^{GT/+}$ embryos. Viable 9.5dpc, 12.5dpc, 14.5dpc embryos and newborn pups were genotyped by *Mcms* and *Sry* PCR. The F/M ratios were 100%, 73.1%, 50%, and 32.1%, respectively (Fig. 4.2A). Therefore, the gender bias starts between 9.5 dpc to 12.5 dpc. We also observed that the embryonic lethal phenotype starts as early as between 9.5 dpc to 12.5 dpc (Fig. 4.2B). The simultaneous occurrences of two phenotypes suggest that the gender bias is due to the female embryos undergoing death.

***Sry* expression or Testosterone administration rescues Mcms-insufficient embryos from lethality**

The time mating experiment shows that the gender bias starts from 9.5dpc to 12.5dpc when sex determination occurs. Therefore, gender bias may be due to the activation of sex determination events. In early embryogenesis, the mammalian Y chromosome acts as a dominant male determinant due to the action of a single gene, *Sry*. Because only males have a Y chromosome, *Sry* is only expressed in males. Based on the fact that male embryos tolerate Mcms-insufficiency better than females, the activation of *Sry* was speculated to protect embryos. Therefore, an *Sry* transgene was introduced into *Mcm4*$^{Chaos3/Chaos3}$, *Mcm2*$^{Gt/+}$ and *Mcm4*$^{Chaos3/Chaos3}$ *Mcm2/3*$^{GT/+}$mice

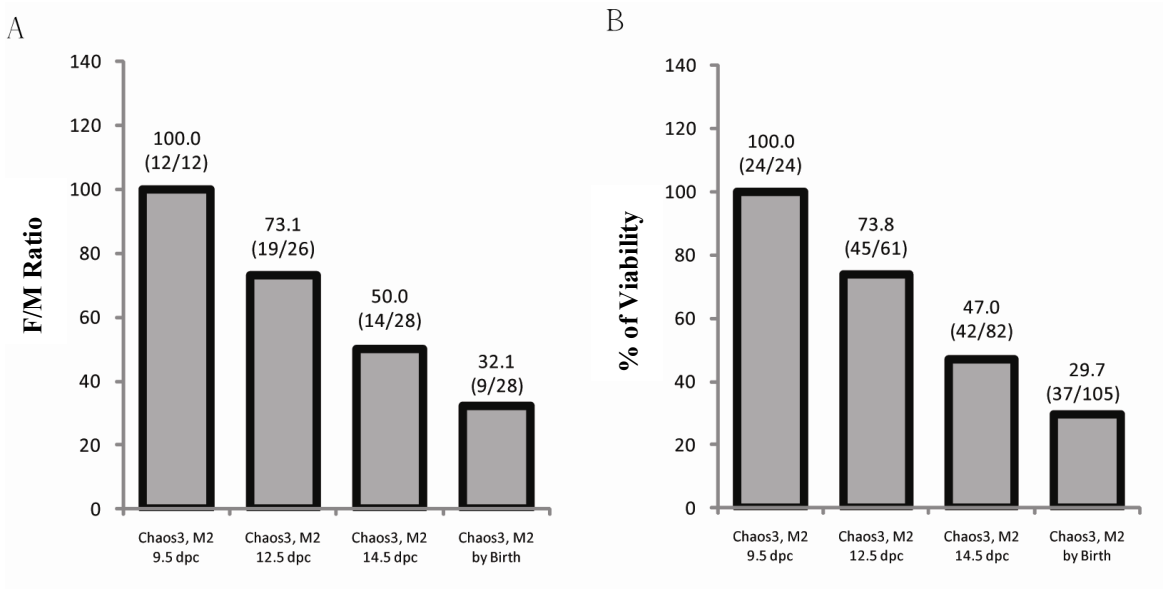

Figure 4.2. Gender bias correlates with embryonic lethality. (A) Viable embryos were genotyped by PCR and the gender was determined by *Sry* gene. Gender bias occurs between 9.5 dpc to 12.5 dpc. "*Chaos3*" in the X axis represents $Mcm4^{Chaos3/Chaos3}$. *M"s"* represents *Mcm"s"* $^{GT/+.}$ (B) Viable embryos were genotyped by PCR. Embryonic lethality occurs between 9.5 dpc to 12.5 dpc.

and sex ratios of offspring were measured. The results show that, in the groups of *Sry* transgene animals, the viable F/M ratios increased in both $Mcm4^{Chaos3/Chaos3}$ $Mcm2^{GT/+}$ and $Mcm4^{Chaos3/Chaos3}$ $Mcm2/3^{GT}$ animals while compared to non-*Sry* transgene animals (Fig 4.3), demonstrating a protective effect of *Sry*.

The expression of *Sry* is critical for appropriate male genital development during the 9.5 dpc to 12.5 dpc time period. By coordinating with *Sox9*, *Sry* initiates testis development from early bipotential gonads [15], then it triggers the differentiation of Sertoli cells from supporting cell precursors. *Sry* also activates the downstream genes responsible for testosterone production. Therefore, the protective effect against Mcms-insufficiency may be due to testosterone. To test this, 7.5-14.5 dpc embryos were supplied with extra testosterone by injecting testosterone propionate into the pregnant mothers ($MCM4^{Chaos3/Chaos3}$ $MCM2/3^{GT/+}$♂ vs $MCM4^{Chaos3/Chaos3}$♀). Newborn offsprings were genotyped for *Mcms* and *Sry*. The survival rates of female embryos (both $MCM4^{Chaos3/Chaos3}$ $MCM2/3^{GT/+}$and $MCM4^{Chaos3/Chaos3}MCM2^{GT/+}$) treated with testosterone were significantly increased compared to the untreated embryos (Fig 4.3). These results demonstrate the protective effect of testosterone in aminals from Mcms-insufficiency.

Testosterone protects Mcms insufficient embryos by up-regulating Mcms mRNA levels

Given the fact that testosterone can protect male embryos from Mcms-insufficiency, one explanation is that androgen produced in the embryonic gonad after 9.5 dpc diffuses to other tissues. These trace amounts of androgen may directly stimulate *Mcm* expression to maintain in levels higher than female embryos. To test this hypothesis, the mRNA level of all six *Mcms* were measured in male and female MEFs that were generated from the following genotypes: $Mcm4^{Chaos3/Chaos3}$, $Mcm4^{Chaos3/Chaos3}$ $Mcm3^{GT/+}$, $Mcm4^{Chaos3/Chaos3}$ $Mcm2^{GT/+}$, and $Mcm4^{Chaos3/Chaos3}$ $Mcm2/3^{GT/+}$. In the groups of $Mcm4^{Chaos3/Chaos3}$ and $Mcm4^{Chaos3/Chaos3}$ $Mcm3^{GT/+}$ MEFs

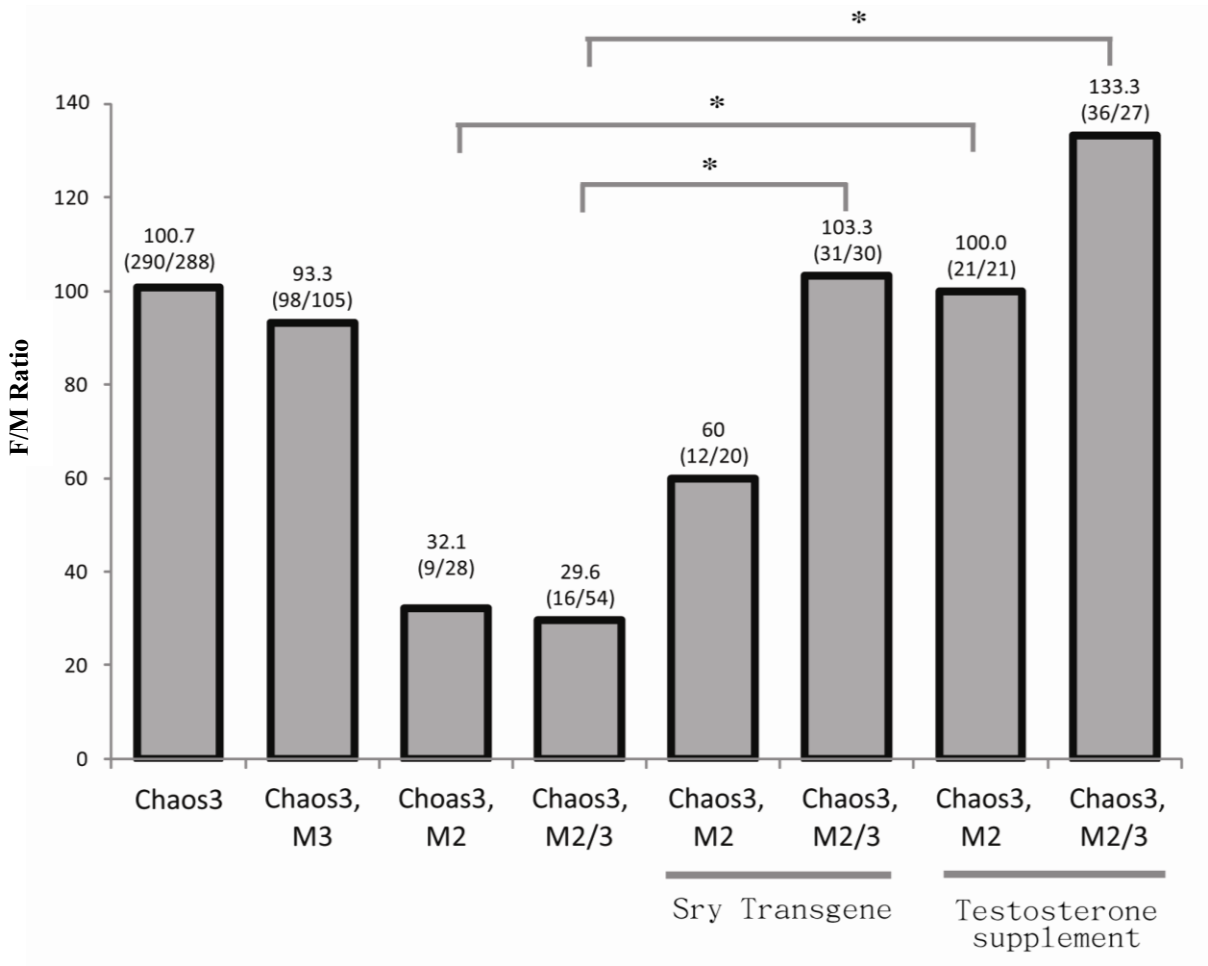

Figure 4.3. ***Sry*** **transgene and testosterone rescues lethality in female mice.** Viable newborns were genotyped by PCR and the gender was determined by *Sry* genotyping. Unless otherwise indicated, the values represent expected proportions of indicated genotypes that were present by birth. Both Sry transgene and testosterone treatment restore the viability. "*Chaos3*" in the X axis represents $Mcm4^{Chaos3/Chaos3}$. *M"s"* represents *Mcm"s"* $^{GT/+}$. Asterisk indicates $P< 0.05$ (Fisher exact test).

which do not have gender bias phenotype, the *Mcm2-7* mRNA levels were equal between sexes (Fig. 4.4A). However, in the groups of $Mcm4^{Chaos3/Chaos3}$ $Mcm3^{GT/+}$ and $Mcm4^{Chaos3/Chaos3}$ $Mcm2/3^{GT/+}$ MEFs which show gender bias, the mRNA levels in females were 60% ~ 70% of that in males (Fig. 4.4A). To test if testosterone alone is responsible for this difference in *Mcm* mRNAs, I treated both $Mcm4^{+/+}$ and $Mcm4^{Chaos3/Chaos3}$ immortalized MEFs with testosterone and measured mRNA level of *Mcms*. *Mcm3, 6* and *7* mRNA were increased after 8 hours treatment (Fig. 4.4B), and *Mcm2, 3, 5, 6,* and *7* are up regulated after 24 hours treatment (Fig. 4.4B). The results show that testosterone stimulates *Mcms* mRNA levels, and this is the basis for protection of males against Mcms insufficiency.

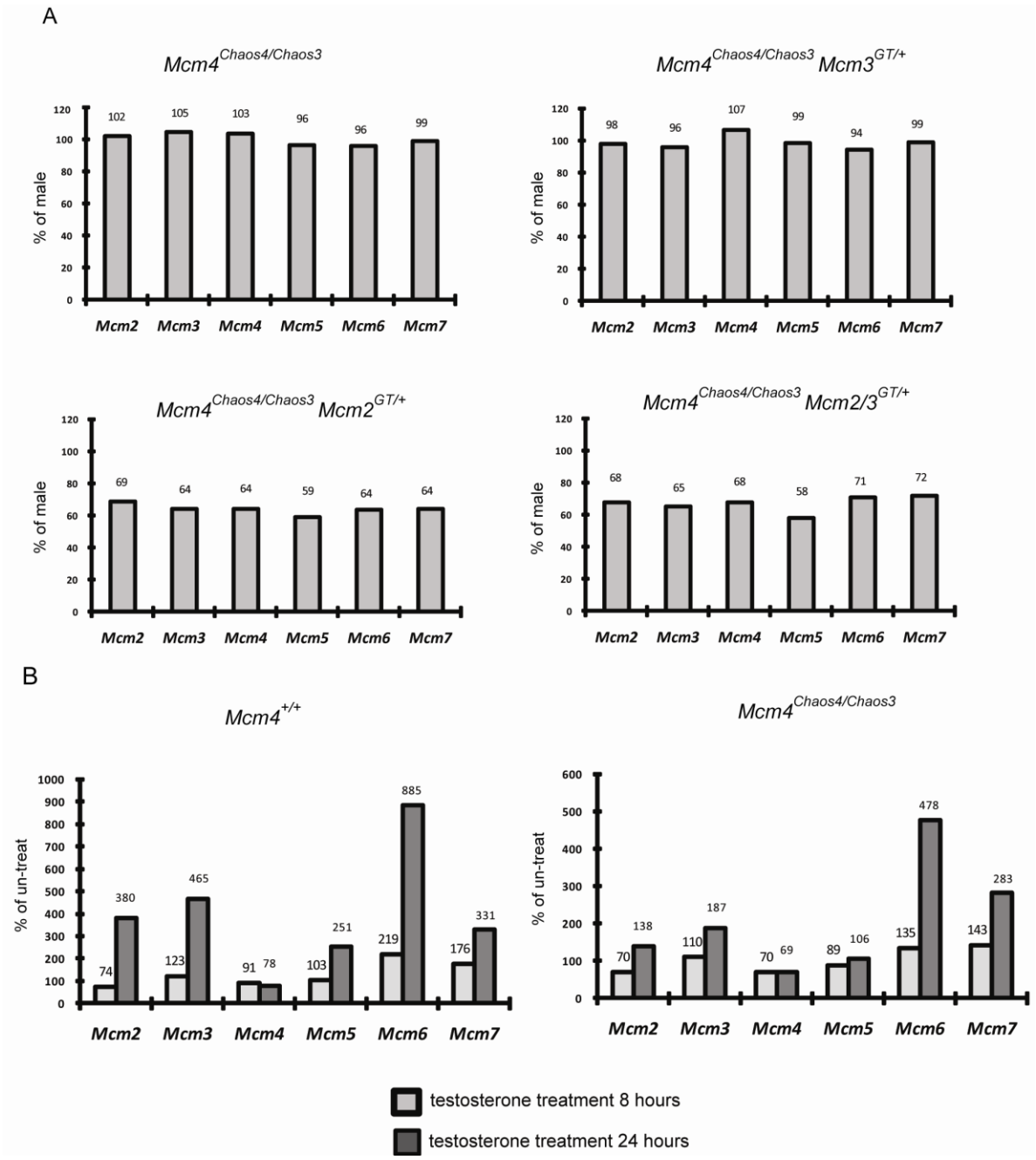

Figure 4.4. Testosterone up-regulate *Mcm2, 3, 5, 6, 7* mRNA expressions. (A) Mcm2-7 mRNAs are reduced in *Mcm4*$^{Chaos3/Chaos3}$ *Mcm2*$^{+/-}$ and *Mcm4*$^{Chaos3/Chaos3}$ *Mcm2/3*$^{+/-}$ female MEF cells. qRT-PCR analysis of Mcm mRNAs, control genes, and in the MEFs. Relative transcript levels were normalized to -actin. Charted are the percent levels of the indicated RNAs in mutant compared to male MEFs (considered

to be 100%). At least 5 replicate cultures were analyzed for each genotype. Error bars are SEM. (B) mRNA expression levels of *Mcm2, 3, 5, 6, 7* after 10nM testosterone treatment were quantified by Real-time PCR. Results showed up-regulation of *Mcm*3, 6, 7 after 8hr treatment, and *Mcm*2, 3, 5, 6, 7 after 24 hr treatment.

Discussion

Estradiol and progesterone modulate many physiological mechanisms predominantly in female animals [17, 18], whereas testosterone primarily plays a key role in the development of male reproductive tissues [19-21]. In general, steroid hormones promote cell proliferation and growth of those tissues with receptors. Therefore, steroid hormones have been proposed to be involved in regulating *Mcms* gene transcription or protein function [11, 22]. Mcms-insufficient mice exhibit many detrimental phenotypes, including early stage lethality, development retardation, genomic instability, and cancer formation [23]. The lethality phenotype occurs as early as 9.5 dpc, whereas cancer formation takes place after one-year of age. Interestingly, lethality phenotypes occur in a gender-dependent manner that is an unexpected finding. Given the fact that the gender bias was observed as early as 9.5 dpc when testosterone is the only steroid hormones begins produced, we speculate that testosterone protects embryo from Mcms insufficiency through an unknown mechanism.

There are at least two possibilities that can be addressed and the first was shown in this chapter. (1) The results from microarray analyses of testosterone-treatment cells show that testosterone can up-regulate almost all *Mcms* [24, 25]. Consistent with these results, mRNA levels of *Mcm2, 3, 5, 6,* and *7* in MEFs increased after testosterone treatment. This activation probably depends on the increased expression of E2F genes or a decreased in RB protein. (2) In Mcms-insufficient mice, stem cell deficiency has been report [23, 26-28]. One major consequence of stem cell deficiency is to hinder development of the embryo. However, the capacity of androgens to stimulate increased differentiation of mouse ES cells to cardiomyocytes has been demonstrated and it can take place as early as 5.5 dpc [29]. It is reasonable to speculate that testosterone might protect embryos from Mcms insufficiency via boosting stem cell activity.

Materials and Methods

MEF culture

MEFs from 12.5- to 14.5-dpc embryos were cultured in DMEM + 10% FBS, 2 mM GlutaMAX, and penicillin-streptomycin (100 units/ml). Assays were conducted on cells at early passages (up to P3).

Testosterone propionate (TP) injection in mouse and treatment in MEFs

To treat embryos, testosterone propionate (TP) (20ug/g/day in Corn oil) were *subcutaneously injected* (hind leg) into pregnant females, from days 7.5-14.5 post coitus. To treat MEFs, testosterone propionate was added into culture media in final concentration of 10 nM.

Validation of genotype in mouse lines

Genotyping of gene-trap-bearing mice or gender was performed either by PCR amplification of the neomycin resistance gene within the vector, or by using insertion-specific assays (Table 3.1). Primer SryT-F: 5' CTCAGTGTGGAATTCATCTGC 3' and SryT-R: 5' GAGGGCATGGTCAGTTGAAC 3' were used for *Sry* transgene genotyping.

Quantitative RT-PCR (qPCR).

Total RNA from P1 MEFs was DNAse I treated, then cDNA was synthesized from 1 μg of total RNA using the Invitrogen SuperScript III ReverseTranscriptase kit with the supplied Olige-dT or random-hexamer primers. qPCR reactions were performed in triplicate on 1 ng or 10 ng of cDNA by using the SYBR power green RT-PCR Master kit (Applied Biosystems; 40 cycles at 95℃ for 10 s and at 60℃ for 1 min), and real-time detection was performed on an ABI PRISM 7300 and analyzed with Geneamp 5700 software. The specificity of the PCR amplification procedures was checked with a heat-dissociation step (from 60℃ to 95℃) at the end of the run and by

gel electrophoresis. Results were standardized to β-actin. The PCR primers are listed in Table 3.1.

References

1. Aparicio, O.M., D.M. Weinstein, and S.P. Bell, *Components and dynamics of DNA replication complexes in S. cerevisiae: redistribution of MCM proteins and Cdc45p during S phase.* Cell, 1997. **91**(1): p. 59-69.
2. Bell, S.P. and A. Dutta, *DNA replication in eukaryotic cells.* Annu Rev Biochem, 2002. **71**: p. 333-74.
3. Randell, J.C., et al., *Sequential ATP hydrolysis by Cdc6 and ORC directs loading of the Mcm2-7 helicase.* Mol Cell, 2006. **21**(1): p. 29-39.
4. Nougarede, R., et al., *Hierarchy of S-phase-promoting factors: yeast Dbf4-Cdc7 kinase requires prior S-phase cyclin-dependent kinase activation.* Mol Cell Biol, 2000. **20**(11): p. 3795-806.
5. Ohtani, K., et al., *Cell growth-regulated expression of mammalian MCM5 and MCM6 genes mediated by the transcription factor E2F.* Oncogene, 1999. **18**(14): p. 2299-309.
6. Fitch, M.J., J.J. Donato, and B.K. Tye, *Mcm7, a subunit of the presumptive MCM helicase, modulates its own expression in conjunction with Mcm1.* J Biol Chem, 2003. **278**(28): p. 25408-16.
7. Guerriero, G., *Vertebrate sex steroid receptors: evolution, ligands, and neurodistribution.* Annals of the New York Academy of Sciences, 2009. **1163**: p. 154-68.
8. Copland, J.A., et al., *Sex steroid receptors in skeletal differentiation and epithelial neoplasia: is tissue-specific intervention possible?* BioEssays : news and reviews in molecular, cellular and developmental biology, 2009. **31**(6): p. 629-41.
9. Thakur, M.K. and V. Paramanik, *Role of steroid hormone coregulators in health and disease.* Hormone research, 2009. **71**(4): p. 194-200.
10. Sobrino, A., et al., *Estradiol stimulates vasodilatory and metabolic pathways in cultured human endothelial cells.* PLoS One, 2009. **4**(12): p. e8242.
11. Pan, H., Y. Deng, and J.W. Pollard, *Progesterone blocks estrogen-induced DNA synthesis through the inhibition of replication licensing.* Proc Natl Acad Sci U S A, 2006. **103**(38): p. 14021-6.
12. Wang, X.D., et al., *Expression profiling of the mouse prostate after castration and hormone replacement: implication of H-cadherin in prostate tumorigenesis.* Differentiation; research in biological diversity, 2007. **75**(3): p. 219-34.
13. Sekido, R. and R. Lovell-Badge, *Sex determination involves synergistic action of SRY and SF1 on a specific Sox9 enhancer.* Nature, 2008. **453**(7197): p. 930-4.
14. Lovell-Badge, R., *Sex determining gene expression during embryogenesis.* Philos Trans R Soc Lond B Biol Sci, 1993. **339**(1288): p. 159-64.
15. Hacker, A., et al., *Expression of Sry, the mouse sex determining gene.* Development, 1995. **121**(6): p. 1603-14.

16. Tilmann, C. and B. Capel, *Cellular and molecular pathways regulating mammalian sex determination.* Recent Prog Horm Res, 2002. **57**: p. 1-18.
17. Chaim, W. and M. Mazor, *The relationship between hormones and human parturition.* Archives of gynecology and obstetrics, 1998. **262**(1-2): p. 43-51.
18. Spitz, I.M., *Progesterone antagonists and progesterone receptor modulators: an overview.* Steroids, 2003. **68**(10-13): p. 981-93.
19. Swaab, D.F. and A. Garcia-Falgueras, *Sexual differentiation of the human brain in relation to gender identity and sexual orientation.* Functional neurology, 2009. **24**(1): p. 17-28.
20. Roy, A.K., et al., *Regulation of androgen action.* Vitamins and hormones, 1999. **55**: p. 309-52.
21. Roy, A.K. and B. Chatterjee, *Androgen action.* Critical reviews in eukaryotic gene expression, 1995. **5**(2): p. 157-76.
22. Shi, Y.K., et al., *MCM7 Interacts with Androgen Receptor.* American Journal Of Pathology, 2008. **173**(6): p. 1758-1767.
23. Chuang, C.H., et al., *Incremental genetic perturbations to MCM2-7 expression and subcellular distribution reveal exquisite sensitivity of mice to DNA replication stress.* PLoS Genet, 2010. **6**(9).
24. Wang, X.D., et al., *Expression profiling of the mouse prostate after castration and hormone replacement: implication of H-cadherin in prostate tumorigenesis.* Differentiation, 2007. **75**(3): p. 219-34.
25. Treister, N.S., et al., *Influence of testosterone on gene expression in the ovariectomized mouse submandibular gland.* Eur J Oral Sci, 2006. **114**(4): p. 328-36.
26. Maslov, A.Y., et al., *Stem/progenitor cell-specific enhanced green fluorescent protein expression driven by the endogenous Mcm2 promoter.* Stem Cells, 2007. **25**(1): p. 132-8.
27. Pruitt, S.C., K.J. Bailey, and A. Freeland, *Reduced Mcm2 expression results in severe stem/progenitor cell deficiency and cancer.* Stem Cells, 2007. **25**(12): p. 3121-32.
28. Kunnev, D., et al., *DNA damage response and tumorigenesis in Mcm2-deficient mice.* Oncogene, 2010. **29**(25): p. 3630-8.
29. Goldman-Johnson, D.R., D.M. de Kretser, and J.R. Morrison, *Evidence that androgens regulate early developmental events, prior to sexual differentiation.* Endocrinology, 2008. **149**(1): p. 5-14.

CHAPTER V

DISCUSSION AND FUTURE DIRECTIONS

1. Summary of findings

My thesis projects dealt with the organismal effects of MCM protein family deficiency, and the underlying mechanisms regulating MCM levels. I conducted these studies using several lines of mice containing gene trap disruption alleles of *Mcm* genes, a hypomorphic ENU-induced allele called *Chaos3*, and combinations of these mutations produced by breeding. My general conclusion was that whereas a 50% decrease in *Mcm* mRNA levels was well tolerated, >50% reduction resulted in multiple phenotypes including embryonic lethality, grow retardation, anemia, genomic instability, and increasing cancer formation (Fig. 5.1). Interestingly, the outcomes of individual MCMs reduction were quite different. Insufficient MCM2 caused significant embryonic lethality (70%) and early onset cancer formation in almost 100% of surviving animals. Insufficient MCM4 and MCM6 caused more than 80% embryonic lethality, though it was below 50% for insufficient MCM7. However, the surviving MCM7 deficient animals show the most severe growth retardation, anemia, and genomic instability phenotypes among all of the MCM deficient mice. My experiments also revealed a very unique function of MCM3. The reduction of MCM3 rescued almost all the detrimental phenotypes caused by insufficiency of MCM2, 4, 6, but not 7. The rescue function of MCM3 involves the re-distribution of soluble and chromatin bound forms of MCMs.

In Chapter III, the biochemical effect of *Chaos3* breast cancer susceptibility mutation in MCM4 was identified (Fig. 5.1). This mutation dramatically disrupts the interaction between MCM4 & 6 and causes instability of the MCM2-7 complex. Moreover, all of *Mcm* mRNAs are down-regulated posttranscriptionally in response to MCM2-7 complex instability, and this regulation is likely mediated via the miRNA pathway. One consequence of *Mcm* mRNA down-regulation is to decrease MCM3-MCM5 protein levels, and resulting reduction of MCM3:5 interaction complex which can block the MCM2-7 complex from binding to chromatin. My in vivo studies characterizing the MCM3-MCM5 interaction, which has negative regulatory effects on the MCM2-7 helicase, are the first ever conducted on animal models and

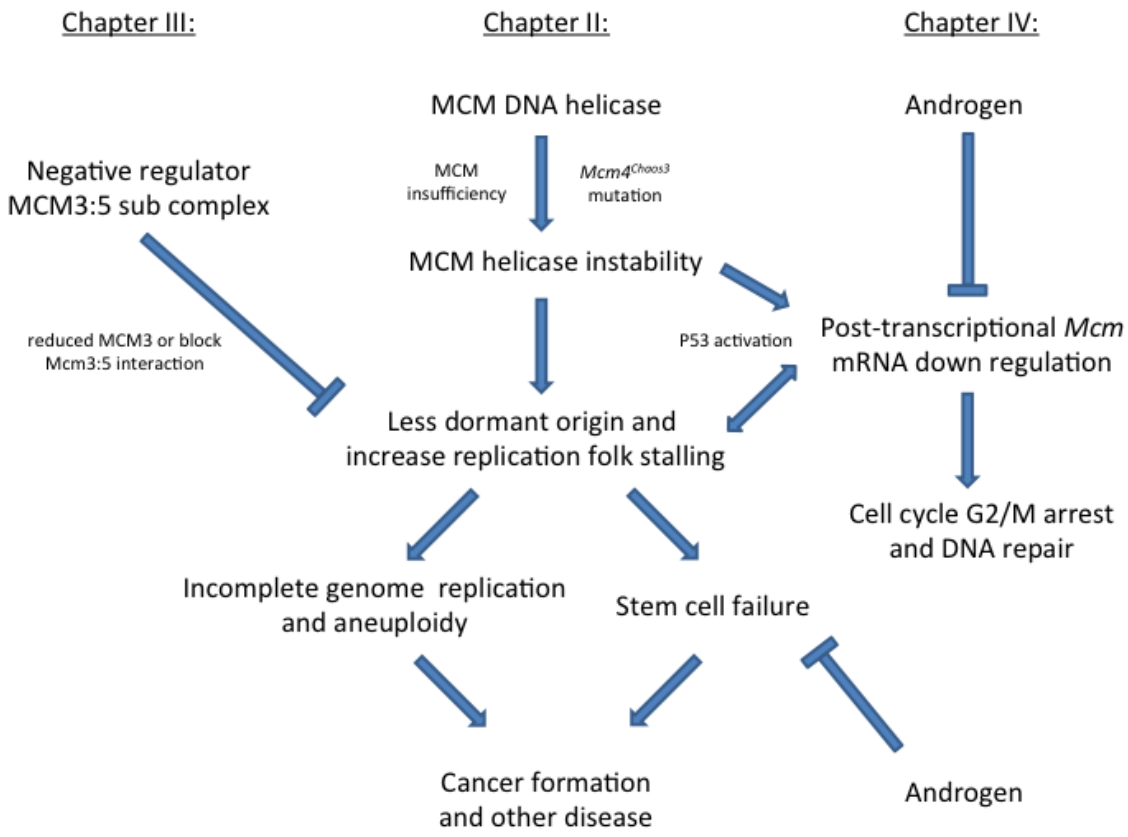

Figure 5.1 Thesis projects Summary. In chapter II, I report that genetically-induced reductions of MCM levels in mice caused several health-related defects including increased embryonic lethality, GIN, cancer susceptibility, growth retardation, defective cell proliferation, stem cell failure, and hematopoiesis defects. Remarkably, genetic reduction of MCM3 rescued many of these defects, presumably attributable to observed increases in chromatin-bound MCM levels. This chapter suggests that relatively minor misregulation or destabilization of MCM homeostasis can have serious consequences for health, viability and cancer susceptibility of animals. In chapter III, I identify the MCM3/5 interaction as negative regulator, which blocks the assembly of MCMs onto chromatin in vivo. Therefore, MCM3 reduction benefits the MCM deficient cells and animals from detrimental phenotypes or disease. In chapter III, I descripted how androgen protects male embryos from MCM insufficiency by up regulating Mcm mRNA levels.

underscore the physiological intracacies of regulating DNA replication (Fig. 5.1).

In Chapter IV, a unique gender bias phenotype was described for MCM deficient mice. I found that male embryos and animals are more resistant to MCMs insufficiency. Furthermore, "Male determinant" *Sry* gene and testosterone rescue the high lethality in female MCM deficient embryos. We also proved that testosterone up-regulates *Mcms* mRNA level. Based on the observation that female MCM deficient embryos have lower *Mcm*s mRNA levels, I conclude that testosterone protects male MCM deficient embryos by maintaining the higher transcription of *Mcm*s than in females (Fig. 5.1).

2. The function of excess MCMs

In *Xenopus* egg extracts, each preRC (pre-replication complex) contains approximately 20–50 MCM hexamers that attract only 1–2 Cdc45 molecules during initiation of replication. Also in mammalian somatic cells, for each origin of replication there are 4–5 total MCM hexamers on average, and only two Cdc45 recurred in ~15 origins. It is clear that Cdc45 is the rate-liming factor and MCMs are in excess [1]. The function of excess MCMs was unclear and known as "MCM paradox". In both *Xenopus* egg and cultured cells, these excess MCMs were found to be "dormant helicases" that are activated under stress conditions [2, 3]. Insufficient levels of dormant helicases fail to respond to spontaneous replication fork stalling and resulting DNA breaks. In this thesis, I initially used a mouse model to study the response to MCMs insufficiency. Consistent with previous studies, I observed the induction of genomic instability and the pathogenic outcome. One of my interesting findings is that MCMs insufficiency induces cell cycle G2/M arrest instead of S phase, suggesting S phase ATM/ATR dependent checkpoint is not responsible for repair caused by dormant helicase insufficiency. This concurs with the observation that ATM/ATR functional deficient mouse is not synthetic with *Chaos3* mutation (CH Chaung, M Wallace, *et al.* data not show). Furthermore, Kawabata *et al* showed that the *Chaos3* mutation causes stalled forks in the absence of replication stress, and a

fraction of these persist into M phase. The majority of these stalled forks are resolved by the Fanconi anemia pathway [4]. This may explain why *Mcm4*^{Chaos3} cells arrested at the G2/M phase.

My finding of the post-transcriptional *Mcm* pan-down regulation in response to helicase complex instability raises several interesting questions. First, it is not clear how cells sense the instability of the helicase complexes. The sensors might belong to DNA checkpoint mechanism because the instability of helicase complex causes DNA damage. Therefore, it would be interesting to use RNAi to knock-down different DNA checkpoint pathways and monitor which knock-down could attenuate the *Mcms* pan-down regulation. Another unsolved question is which miRNA or small RNA performs the function to decrease *Mcms* mRNA levels. RNA sequencing might answer this question.

3. The real core helicase

Biochemical fractionation of cell extracts has yielded a variety of MCMs sub-complexes, such as dimer, trimer, and tetramer [5-18], and as well as the intact MCMs hexamer containing all six subunits [6-8, 10, 12, 13, 15, 17]. Interestingly, during most purification methods, MCM4, MCM6, and MCM7 subunits were most tightly bound together to form a trimeric complex called the MCM core. MCM4/6/7 core will dimerize itself to form a double-trimer $(MCM4/6/7)_2$. In vitro result show that MCM3 and MCM5 dimerize together and bind to the MCM4/6/7 core, probably through MCM7. MCM3/5 blocks the formation of $(MCM4/6/7)_2$ and inhibits the $(MCM4/6/7)_2$ helicase activity. Interestingly, $(MCM4/6/7)_2$ retains several activities required of the DNA replicative helicase, such as DNA binding, ATP hydrolysis, and DNA unwinding. Additionally, $(MCM4/6/7)_2$ can bind and unwind circular DNA, suggesting its ability to clamp genomic DNA which does not have open end [11]. $(MCM4/6/7)_2$ via MCM7 can also bind CDC45 which links it to DNA polymerase. In vitro systems shows that of all the sub-complexes isolated, only $(MCM4/6/7)_2$ has helicase activity [9, 19]. However, in normal cell physiological situation, all of MCM

sub-complex or MCM2-7 should not have helicase activity unless bound to DNA and other preRC molecules such as CDC45. The uncertain functions of MCM sub-complex leads to the dilemma known as "MCM puzzle" [20] and has not been solved.

In *Xenopus* egg extracts and yeast cells, the major complex is a MCM2-7 hetero-hexamer, suggesting they employ MCM2-7 to be the DNA helicase. In contrast, in mammalian cells, the MCM3/5 dimer and MCM4/6/7 double trimer are the most abundant complexes [14, 21, 22]. Besides, in vitro data showed that $(MCM4/6/7)_2$ can bind and unwind DNA without ORC protein [9, 11], raising the question whether $(MCM4/6/7)_2$ substitutes for MCM2-7 as the functional helicase after S phase. In this thesis, we proved that MCM3 is a negative factor for MCMs loading into chromatin. Furthermore, MCM3/5 dimers block other MCMs from binding to chromatin, and the blocking activity is MCM3/5 interaction dependent. These discoveries are the first *in vivo* evidence to support *in vitro* results. Taken together, we propose that mammalian cells utilize the $(MCM4/6/7)_2$ as the replicative helicase and the MCM3/5 dimers are able to negatively regulate DNA replication. This assumption does not negate the existence and the function of MCM2-7 hetero-hexamer. The two forms of helicase might be employed on different occasions and/or MCM3:5 functions as the switch. To further understand the function of MCM3/5 dimer, it would be interesting to generate MCM5 gene trap animals again to answer whether MCM5 is also a negative factor similar to MCM3. We can also purify the active DNA replication folk (as know as "iPOND technique" [23]) and analyze the stoichiometry of MCM components with different MCM3:5 levels. Another approach to distinguish the function of each MCM could be through the use of inducibly degraded MCM proteins. This way we could examine different MCMs role by inducing a single MCMs to degrade at different cell cycle stages.

References

1. Wong, P.G., et al., *Cdc45 limits replicon usage from a low density of preRCs in mammalian cells.* PLoS One, 2011. **6**(3): p. e17533.
2. Woodward, A.M., et al., *Excess Mcm2-7 license dormant origins of replication that can be used under conditions of replicative stress.* J Cell Biol, 2006. **173**(5): p. 673-83.
3. Ibarra, A., E. Schwob, and J. Mendez, *Excess MCM proteins protect human cells from replicative stress by licensing backup origins of replication.* Proc Natl Acad Sci U S A, 2008. **105**(26): p. 8956-61.
4. Kawabata, T., et al., *Stalled Fork Rescue via Dormant Replication Origins in Unchallenged S Phase Promotes Proper Chromosome Segregation and Tumor Suppression.* Molecular Cell, 2011. **41**(5): p. 543-53.
5. Ricke, R.M. and A.K. Bielinsky, *Mcm10 regulates the stability and chromatin association of DNA polymerase-alpha.* Mol Cell, 2004. **16**(2): p. 173-85.
6. Madine, M.A., et al., *MCM3 complex required for cell cycle regulation of DNA replication in vertebrate cells.* Nature, 1995. **375**(6530): p. 421-4.
7. Adachi, Y., J. Usukura, and M. Yanagida, *A globular complex formation by Nda1 and the other five members of the MCM protein family in fission yeast.* Genes Cells, 1997. **2**(7): p. 467-79.
8. Davey, M.J., C. Indiani, and M. O'Donnell, *Reconstitution of the Mcm2-7p heterohexamer, subunit arrangement, and ATP site architecture.* J Biol Chem, 2003. **278**(7): p. 4491-9.
9. Ishimi, Y., *A DNA helicase activity is associated with an MCM4, -6, and -7 protein complex.* J Biol Chem, 1997. **272**(39): p. 24508-13.
10. Ishimi, Y., et al., *Binding of human minichromosome maintenance proteins with histone H3.* J Biol Chem, 1996. **271**(39): p. 24115-22.
11. Kanter, D.M., I. Bruck, and D.L. Kaplan, *Mcm subunits can assemble into two different active unwinding complexes.* J Biol Chem, 2008. **283**(45): p. 31172-82.
12. Kubota, Y., et al., *A novel ring-like complex of Xenopus proteins essential for the initiation of DNA replication.* Genes Dev, 2003. **17**(9): p. 1141-52.
13. Lee, J.K. and J. Hurwitz, *Isolation and characterization of various complexes of the minichromosome maintenance proteins of Schizosaccharomyces pombe.* J Biol Chem, 2000. **275**(25): p. 18871-8.
14. Musahl, C., et al., *A human homologue of the yeast replication protein Cdc21. Interactions with other Mcm proteins.* Eur J Biochem, 1995. **230**(3): p. 1096-101.
15. Prokhorova, T.A. and J.J. Blow, *Sequential MCM/P1 subcomplex assembly is required to form a heterohexamer with replication licensing activity.* J Biol Chem, 2000. **275**(4): p. 2491-8.
16. Schulte, D., et al., *Properties of the human nuclear protein p85Mcm. Expression, nuclear localization and interaction with other Mcm proteins.* Eur J Biochem, 1996. **235**(1-2): p. 144-51.

17. Schwacha, A. and S.P. Bell, *Interactions between two catalytically distinct MCM subgroups are essential for coordinated ATP hydrolysis and DNA replication.* Mol Cell, 2001. **8**(5): p. 1093-104.
18. Yabuta, N., et al., *Mammalian Mcm2/4/6/7 complex forms a toroidal structure.* Genes Cells, 2003. **8**(5): p. 413-21.
19. Lee, J.K. and J. Hurwitz, *Processive DNA helicase activity of the minichromosome maintenance proteins 4, 6, and 7 complex requires forked DNA structures.* Proc Natl Acad Sci U S A, 2001. **98**(1): p. 54-9.
20. Forsburg, S.L., *Eukaryotic MCM proteins: beyond replication initiation.* Microbiol Mol Biol Rev, 2004. **68**(1): p. 109-31.
21. Ritzi, M., et al., *Human minichromosome maintenance proteins and human origin recognition complex 2 protein on chromatin.* J Biol Chem, 1998. **273**(38): p. 24543-9.
22. Burkhart, R., et al., *Interactions of human nuclear proteins P1Mcm3 and P1Cdc46.* Eur J Biochem, 1995. **228**(2): p. 431-8.
23. Sirbu, B.M., et al., *Analysis of protein dynamics at active, stalled, and collapsed replication forks.* Genes Dev, 2011. **25**(12): p. 1320-7.